

# Upper Bathonian and lower Callovian ammonites from Chacay Melehué (Argentina)

HORACIO PARENT



Parent, H. 1998. Upper Bathonian and lower Callovian ammonites from Chacay Melehué (Argentina). — *Acta Palaeontologica Polonica* **43**, 1, 69–130.

Contribution to IGCP 322 (IUGS/UNESCO): 'Jurassic events in South America' and to PLPB 001/89 (IFG/UNR): 'El Jurásico Medio-Superior Andino'.

The upper Bathonian–lower Callovian ammonite fauna of Chacay Melehué was sampled through new exposures under close stratigraphic control. Two new faunal horizons are described: the *Iniskinites gulisanoi* horizon and the *Iniskinites crassus* horizon, lying in the lower and middle parts, respectively, of the Steinmanni Zone. The ammonite fauna contains some species not previously described: *Choffatia* aff. *neumayri* (Siemiradzki, 1899) [M&m], *Iniskinites evolutus* sp. n. [M], *Iniskinites* sp. A [M], *Eurycephalites* aff. *gottschei* (Tornquist, 1898) [M], *Xenocephalites* aff. *neuquensis* (Stehn, 1923) [m], and *Xenocephalites* sp. A [m]. *Oxycerites tenuistriatus* (de Grossouvre, 1888) is new for the Andean region. Several species are represented by large samples that allow descriptions and analyses to be made of the entire ontogeny and the characterization of the principal morphs within each species. It is then possible to propose sexual dimorphic correspondence between some nominal morphospecies. The successive species *Lilloettia steinmanni* (Spath, 1928), *Eurycephalites gottschei* (Tornquist, 1898), *E. rotundus* (Tornquist, 1898), and *E. extremus* (Tornquist, 1898) form a phyletic morphocline here interpreted as a mosaic heterochronocline.

**Key words:** Andes, Bathonian, Callovian, ammonites, systematics, biostratigraphy, evolution, heterochrony.

Horacio Parent [infomax@satlink.com], Laboratorio de Paleontología y Biocronología, Instituto de Fisiografía y Geología, Universidad Nacional de Rosario, Pellegrini 250, 2000 Rosario, Argentina.

## Introduction

Chacay Melehué is a classic highly fossiliferous locality in the Middle Jurassic of the Neuquén-Mendoza Basin. This back-arc basin was, during Early and Middle Jurassic times at least, bounded in the west by an active volcanic arc and in the east by the land formed by Palaeozoic and Triassic volcanics, plutonics and metamorphics (Gulisano in Riccardi *et al.* 1992) with a southeastward extension called 'engolfamiento neuquino'.

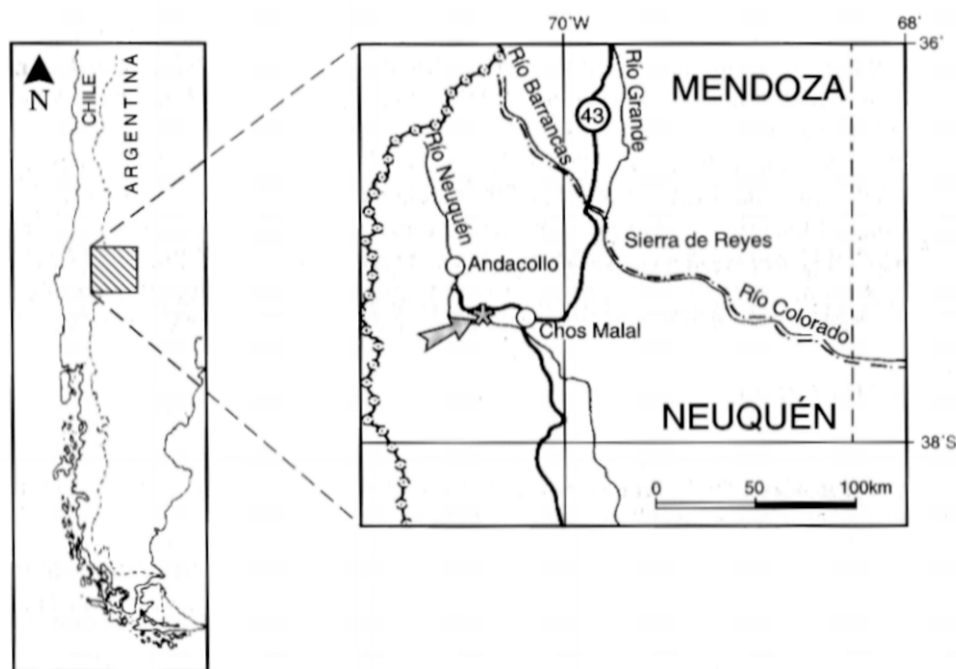


Fig. 1. Geographic location of the studied section Chacay Melehué (big arrow).

In the last two decades knowledge of the Neuquén-Mendoza Basin has grown quickly: the geodynamic and palaeogeographic patterns of the basin are summarized in Digregorio *et al.* (1984), the sequence stratigraphy was developed by Gulisano *et al.* (1984) and the Middle Jurassic biostratigraphy and standard biochronology by Westermann & Riccardi (1972, 1979), Riccardi & Westermann (1991), Riccardi (1984), and Riccardi *et al.* (1988, 1989); some additional data have been provided by Fernández-López *et al.* (1994). A complete up-to-date geologic-stratigraphic summary of the basin is given by Riccardi & Gulisano (1990). The Bathonian–Callovian ammonoid faunas have been studied by Riccardi *et al.* (1989) and Riccardi & Westermann (1991).

A Bajocian transgressive maximum was succeeded by a pronounced Bathonian regression, after which the Neuquén-Mendoza and Tarapacá (Northern Chile) basins were partially separated (Riccardi 1993: p. 19; Westermann & Riccardi 1985) and the former isolated from oceanic influences. This fact seems to be reflected in some features of the late Bathonian–early Callovian ammonoid faunas: endemic (*sensu* Callomon 1985) forms such as the species of *Stehnocephalites*; perisphinctids scarce and occurring in narrow horizons (sometimes with intrathalamic epibionts at the body chamber indicating a relatively long time of drifting after death); and the almost total absence of the 'leiostraca' (the generally smooth-walled Phylloceratidae and Lytoceratidae). Communication between these two basins was reinstated during the middle Callovian following a new transgressive episode.

The Chacay Melehué area is especially suitable for studying the Bathonian–Callovian ammonoid fauna since it exposes many richly fossiliferous, ammonite-dominated



successions, which record rhythmic deposition at the depocentre and shelf-edge to slope during late Bathonian–Callovian times. Many sections exposed in recent years during the construction of National Road 43 lie mainly in the upper Bathonian–lower Callovian interval.

This paper presents the results of the study of a new upper Bathonian–lower Callovian ammonoid fauna (more than 500 specimens) collected in one of these new sections. The material was collected in Chacay Melehué, northern Neuquén, 33.12 km northwest of Chos Malal, towards Andacollo on the above-mentioned Road 43 (Fig. 1). The collection is housed at the Laboratorio de Paleontología y Biocronología (abbreviated LPB) of the Instituto de Fisiografía y Geología, Universidad Nacional de Rosario.

## Stratigraphy

The Middle Jurassic stratigraphy of Chacay Melehué has been recently dealt with by Westermann & Riccardi (1979), Riccardi & Westermann (1991), and papers cited above, where references to earlier studies may be found.

**The section** (Fig. 2). — The studied section belongs to the Los Molles Formation and its top (bed 29) is situated at about 100–110 m below the base of the evaporitic mid-Callovian Tábanos Formation.

The succession is made up of four part-sections separated by non-exposed beds. It consists of dark grey to black shales and shaly limestones, with several thin tuffaceous beds, and is rich in finely distributed pyrite, mainly in the basal shales. Several levels of sideritic, fossiliferous concretions occur in the shales, commonly containing either well-preserved adult ammonites or monospecific assemblages of juvenile and subadult ammonites. The weathered surface of the shales, and in part that of the shaly limestones, is yellowish brown and very friable, by oxidation of  $\text{Fe}^{2+}$  to  $\text{Fe}^{3+}$  and dissolution of the calcareous cement, respectively. Erosive discontinuity surfaces occur at the top of beds 11a and 25 with ammonites in horizontal position and eroded equatorially. An horizon with crushed ammonites occurs at the base of bed 13, reflecting differential compaction. Pyritous shales of bed 3 contain poorly preserved pyritous ammonites.

Taking into account these features and the palaeogeographic data given by Gulisano (in Riccardi *et al.* 1992) and Riccardi & Gulisano (1990), the section should represent platform-edge to slope sedimentation in a confined, low-energetic, kenoxic (*sensu* Cepek & Kemper 1981) environment with stratified water column, influenced by tectonic instability and volcanic activity. Some features of the fossil content support this interpretation. There is no shell debris and the ammonites, in most cases well preserved, largely dominate the macrofauna. The benthic fauna comprises scarce, medium-sized to large adult specimens of the bivalves *Retroceramus stehni* Damborenea, 1990 and *R. patagonicus* (Philippi, 1899), which occur in shaly limestone beds, and abundant '*Bositra buchii*' clustered on the surface of ammonitiferous concretions in shaly beds. A single gastropod, *Turbo?* sp., was found in the body chamber of a specimen of *Stehnocephalites gerthi* (Spath, 1928) at the top of the Steinmanni Zone,

bed 25, and a single terebratulid brachiopod was found in the body chamber of another specimen of *S. gerthi*.

**Biostratigraphy.** — The ammonite succession (Fig. 2) may be classified as follows, in ascending order:

**Steinmanni Zone** [= upper *Retrocostatum*–*Discus* Zones of the European standard according to Riccardi *et al.* (1989)]. Based on the ammonite succession given by Riccardi & Westermann (1991: p. 11) and on that resulting from the present study (Fig. 2), three faunal horizons may be distinguished within the zone (the first two are new):

- *Iniskinites gulisanoi* horizon, lower part of the zone. It comprises the levels M252–257 of Riccardi *et al.* (1988, 1989: fig. 2), and is represented by bed 0 in the present section (Fig. 2). The base is defined by the base of the zone, the top by the base of the *Iniskinites crassus* horizon (see below). It is characterized by *Iniskinites gulisanoi* Riccardi & Westermann, 1991 [M], *Iniskinites evolutus* sp. n. [M], *Iniskinites* sp. A, *Xenocephalites* cf. *araucanus* (Burckhardt, 1903) [m], and the faunal elements listed by Riccardi & Westermann (1991: p. 11).
- *Iniskinites crassus* horizon, middle part of the zone. It comprises the levels M258–262 of Riccardi *et al.* (1988: fig. 2) and it is represented in the present section (Fig. 2) by beds 1–11a. The base is defined by the first occurrence of *Neuquenicerias* (*N.*) *steinmanni* (Stehn, 1923), above the last occurrence of *I. gulisanoi* Riccardi & Westermann, 1991; the top at the base of the *Stehnocephalites gerthi* horizon. It is characterized by *Iniskinites crassus* Riccardi & Westermann, 1991 [M], *Lilloettia steinmanni* (Spath, 1928) [M], *Xenocephalites* aff. *neuquensis* (Stehn, 1923) [m], *Choffatia* aff. *neumayri* (Siemiradzki, 1899) [M], *Ch.* cf. *transitoria* Spath, 1931 (Riccardi & Westermann 1991: p. 11), and the first *Neuquenicerias* (*N.*) *steinmanni*.
- *Stehnocephalites gerthi* horizon (Riccardi *et al.* 1988: fig. 2: levels M263–266), upper part of the zone. It comprises in the present section beds 11b–25, which yield the typical faunal association listed by Riccardi & Westermann (1991: p. 11) as well as *Eurycephalites* aff. *gottschei* (Tornquist, 1898) [M] at the top, *Choffatia* aff. *neumayri* [M&m], *Ch. subbakeriae* (d'Orbigny, 1850) [M], *Ch. suborion* (Burckhardt, 1927) [M], and *Oxycerites* (*Alcidellus*) *tenuistriatus* (De Grossouvre, 1888) [M]. This last supports the latest Bathonian age currently assigned to this horizon.

**Gottschei Zone** [= lower *Macrocephalus* Zone of the European standard according to Riccardi *et al.* (1989)], new name for the Vergarensis Zone of Riccardi *et al.* (1988), since *Eurycephalites vergarensis* (Burckhardt, 1903) [M] is here treated as a junior synonym of *Eurycephalites gottschei* (Tornquist, 1898) [M&m] following Parent (1997). This zone is represented by beds 26–28 in the present section (equivalents to levels M267–271 of Riccardi *et al.* 1988: fig. 2) which yielded macro- and microconchs of the index species (described in Parent 1997), *E. gottschei latumbilicatus* Riccardi & Westermann, 1991 [M], the last *Stehnocephalites crassicosatus* Riccardi & Westermann, 1991 [M] at the base, and *Choffatia jupiter* (Steinmann, 1881) [M].

**Bodenbenderi Zone** [= upper *Macrocephalus*–middle *Gracilis* Zones of the European standard according to Riccardi *et al.* (1989)]. This zone is represented by bed 29 of the present section (equivalent to levels M272–282 of Riccardi *et al.* 1988:

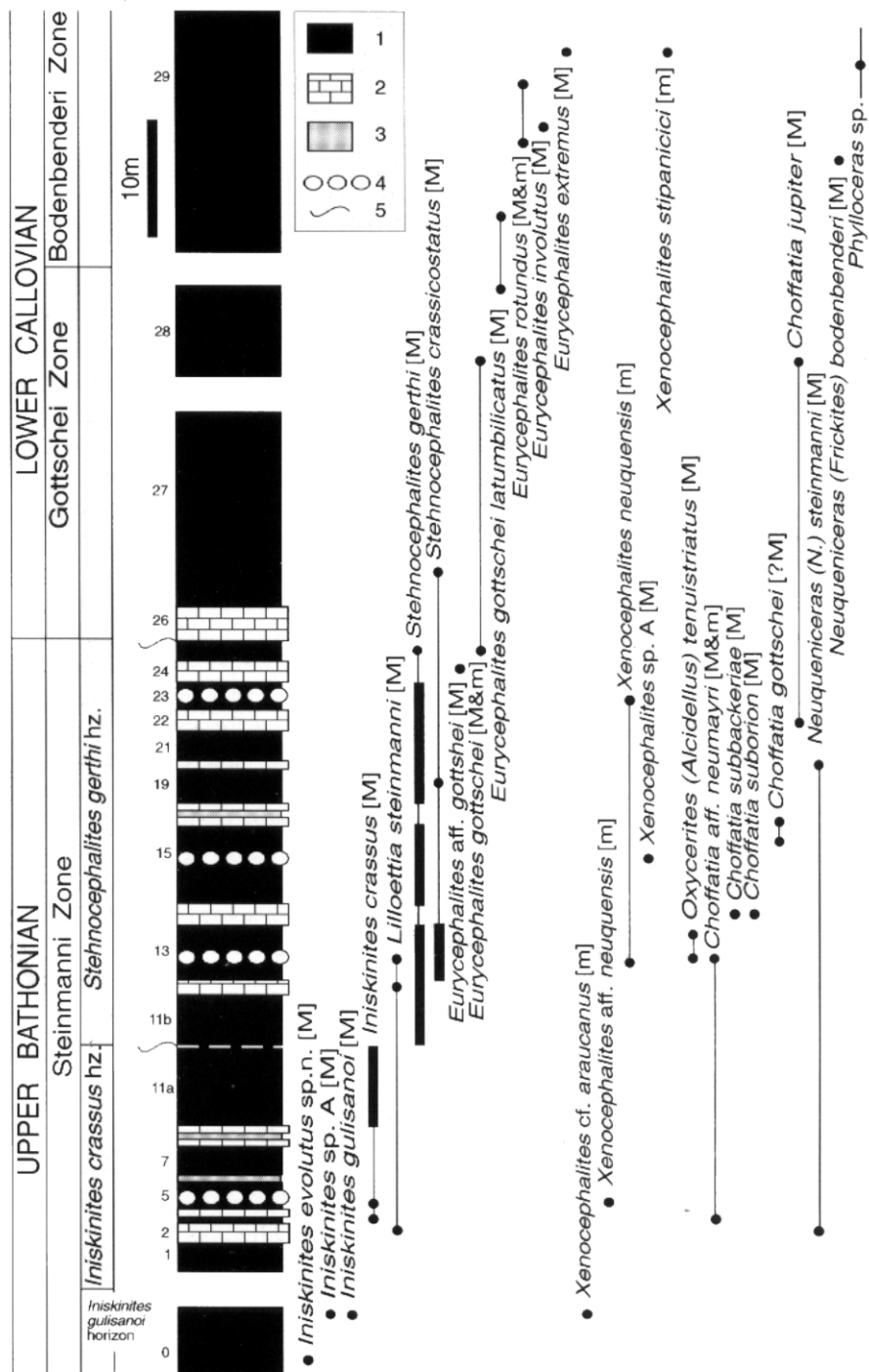


Fig. 2. Stratigraphic log and ammonoid occurrences for the studied section at Chacay Melehué. References: 1 – shale, 2 – shaly limestone, 3 – tuff, 4 – sideretic concretions, 5 – erosive discontinuity.



fig. 2) which yielded the index species (fragmentary material), the last *E. gottschei latumbilicatus* Riccardi & Westermann, 1991 [M], *E. rotundus* (Tornquist, 1898) [M&m], *E. extremus* (Tornquist, 1898) [M], *E. involutus* (Riccardi & Westermann, 1991) [M], *Xenoccephalites stipanicici* Riccardi, Westermann, & Elmi 1990 [m], and unusually large *Phylloceras* sp.

## Procedures and conventions

The new exposures have supplied abundant and sometimes exceptionally well preserved specimens, which allow the study of samples with several complete adult individuals. This material, and the close stratigraphical control under which it was obtained, make it possible to analyse what are essentially isochronous assemblages, delimiting their ranges of variation at many stages of growth and detecting biometrical discontinuities. A biological interpretation may then be attempted. The working hypothesis is that the assemblages at any faunal horizon are intragenerically monospecific whenever the frequency distributions of all the characters are unimodal (see Callomon *et al.* 1992; Thierry 1978; Tintant 1957). The hypothesis is not rejected if a bimodality is attributable to sexual dimorphism.

The range of intraspecific variability is found to be very broad within some of the species studied. Despite the quasi-continuous nature of the variation, it is often possible to distinguish a number of intergrading infrasubspecific variants which form morphologic groups, or morphotypes. These morphotypes have no formal taxonomic status but they may be distinguished and carefully described and figured in order to give a precise picture of the horizontal and vertical (phyletic) structure of the species (Cariou 1984a). The same is the case when true polymorphism (better termed *polyphenism*, in order to distinguish genetic from phenotypic discrete variation, see Stearns 1989) is recognized within an assemblage. The labelling of such morphotypes may be accommodated under the same specific name simply by addition of some further non-Linnean symbol, such as a Greek or Latin character as proposed by Callomon (1985), e.g. *Stehnocephalites gerthi* morphs  $\alpha$ ,  $\beta$ ,  $\gamma$ , and  $\delta$  or *Iniskinites crassus* transient  $\alpha$  and transient  $\beta$  (transients are morphotypes in phyletic succession). Similar solutions have been adopted by Bonnot (1993), Callomon (1985), Cariou (1984a), Thierry (1978) and Westermann (in Hillebrandt & Westermann 1985), among others.

Measured characters used as biometric variables are the following (Fig. 3): diameter ( $D$ ), diameter at the last adult septum ( $Dls$ ), final adult diameter at or near peristome ( $Dp$ ), umbilical width ( $U$ ), whorl width ( $W$ ), whorl height ( $H_1$ ), and whorl ventral height ( $H_2$ ), all given in millimetres [mm]; counts of number of primary ( $P$ ) and ventral ribs ( $V$ ) per half whorl; and length of body chamber at the base of the adult peristome ( $LBC$ ) in degrees [ $^\circ$ ]. Estimated measurements are indicated with ( $^c$ ), body chamber is abbreviated with BC and phragmocone with Ph. The sample statistical measurements used are: arithmetic mean ( $m$ ), standard deviation ( $s$ ), percentual variation coefficient ( $CV = 100s/m$ ), observed range ( $RO$ : minimum and maximum values), populational representation through sample [ $R/s = (\text{maximum value} - \text{minimum value})/s$ ;  $R/s = 4$  spreads about the 95% of the whole range of the variation of the normal parental population], correlation coefficient ( $r$ ), and sample

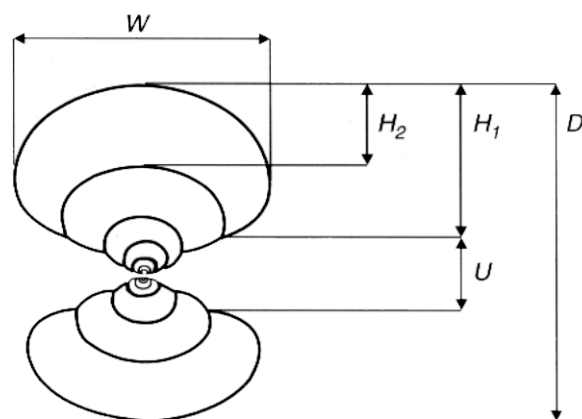


Fig. 3. Characters measured and used as biometrical variables (see text for explanations).

size ( $n$ ). Levels of significance adopted in tests are indicated as follows: *Probability*  $> 0.05$  non-significant ( $^{\circ}$ ), and *Probability*  $< 0.05$  significant ( $*$ ). Goodness of fit to theoretical gaussian distributions of samples is evaluated by the Kolmogorov-Smirnoff test ( $H_0$ ). When the samples are not adequate for statistical description (small size and/or stratigraphic heterogeneity), the individual measurements are listed in Appendix 1. References containing figures of the types are marked with ( $*$ ) in the lists of synonymy. Macroconch (= female) sexual dimorphic status noted with [M], microconch (= male) with [m].

## Descriptions

Family Phylloceratidae Zittel, 1884

Subfamily Phylloceratinae Zittel, 1884

Genus *Phylloceras* Suess, 1865

Type species: *Ammonites heterophyllus* Sowerby, 1821.

*Phylloceras* sp.

Fig. 4B–D.

**Material.** — Two incomplete phragmocones (LPB 394, 395) loose from bed 29.

**Remarks.** — The two available specimens are unusually big ?adult phragmocones (LPB 394:  $D > 300$  mm, LPB 395:  $D > 400$  mm). The suture line shows L deeper than E,  $S_1$  diphyllous,  $S_2$  triphyllous, and phylloid saddle terminal-ends (Fig. 4B). These features are characteristic of *Calliphyloceras* and *Phylloceras*, but the absence of constrictions in both specimens indicates they belong to *Phylloceras* (Joly 1976). The whorl section is ovate-compressed ( $W/H_1 = 0.57$ – $0.62$ ) with slightly convex flanks and rounded venter; umbilical shoulder is broadly rounded into an inclined wall. Poorly preserved fragments of the test (LPB 394) show dense, fine ventral ribbing as in *Phylloceras kudernatschi* (Hauer, 1854) although the size of the present specimens is

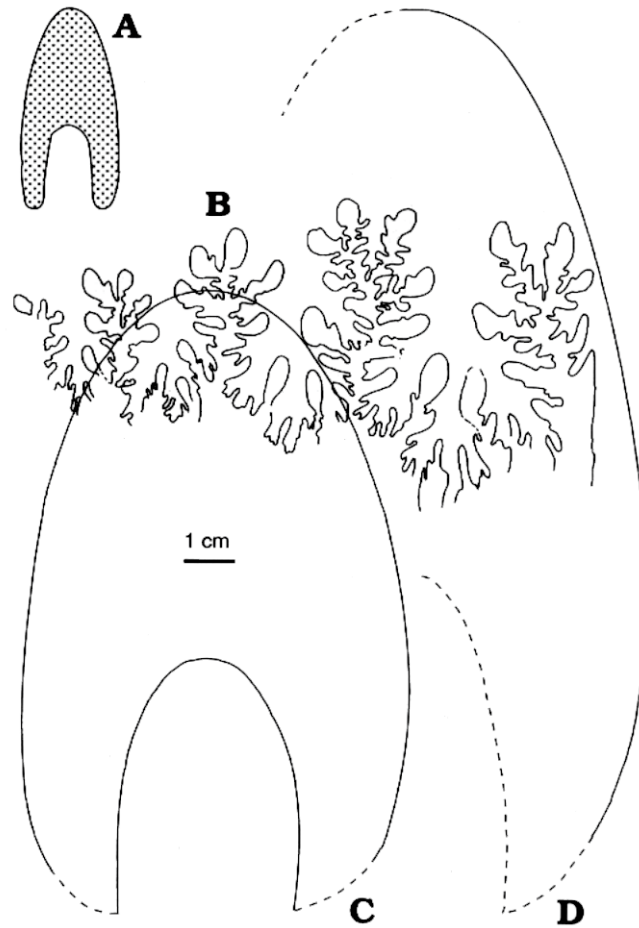


Fig. 4. Cross sections through phragmocone, body chamber (stippled) and suture line. A. *Oxycerites tenuistriatus* [M], LPB 293,  $D = 80$  mm; B–D. *Phylloceras* sp.: LPB 394,  $D = 300$  mm (B, C), LPB 395,  $D = 400$  mm (D).

larger than that of the biggest known representatives of this species (B. Joly personal communication 1995).

Family Oppeliidae Bonarelli, 1894

Subfamily Oppeliinae Bonarelli, 1894

Genus *Oxycerites* Rollier, 1909

Subgenus *Alcidellus* Westermann, 1958

Type species: *Ammonites tenuistriatus* de Grossouvre, 1888.

*Oxycerites (Alcidellus) tenuistriatus* (de Grossouvre, 1888) [M]

Figs 4A, 5A, B; App. 1.

*Alcidellus tenuistriatus* (de Grossouvre); Krystyn 1972: p. 237, pl. 3: 6, 7, pl. 4: 3, 6 [with synonymy].



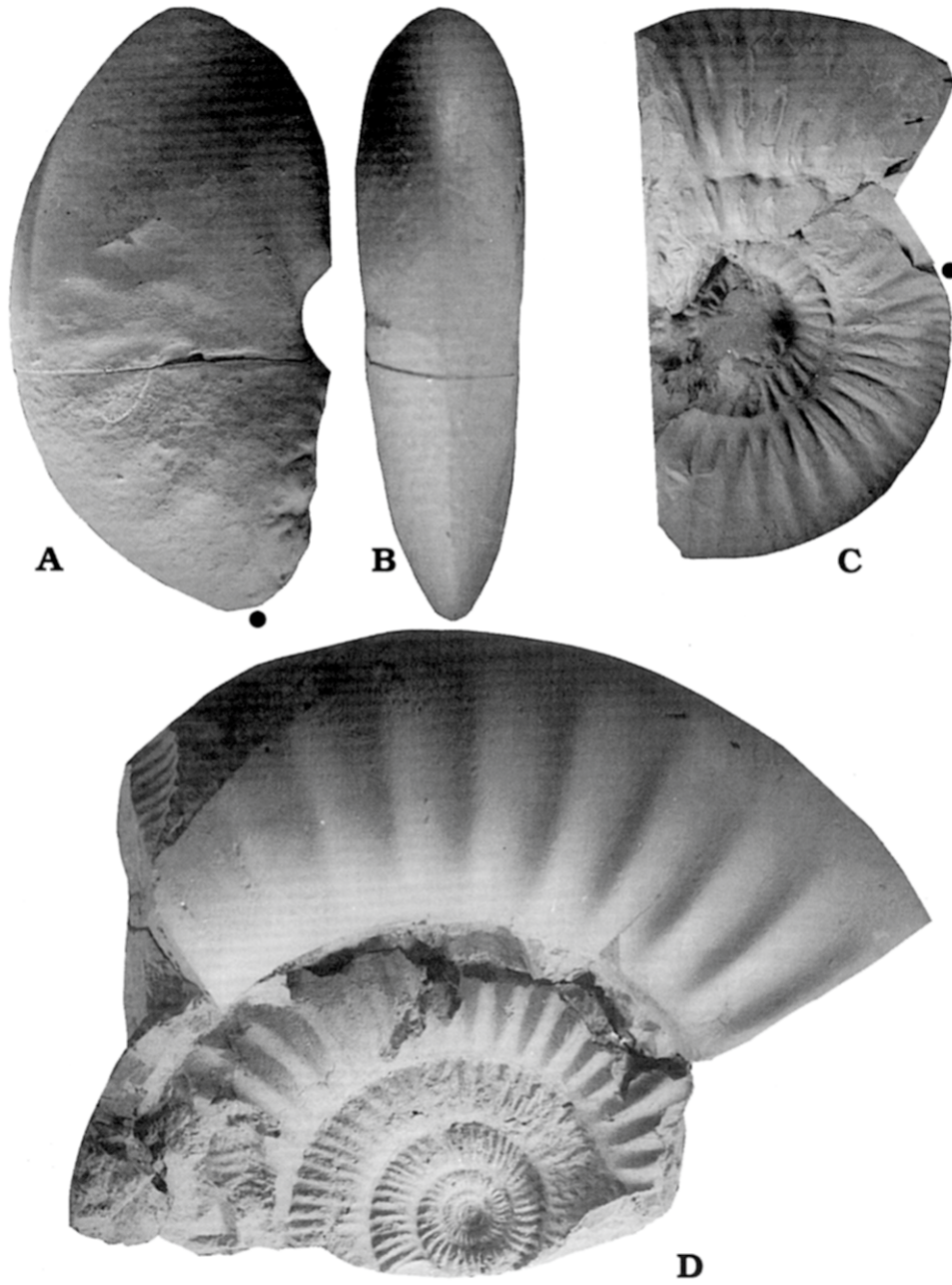


Fig. 5. **A, B.** *Oxycerites tenuistriatus*, [M], adult body chamber (LPB 293) from bed 13. **C.** *Choffatia* aff. *neumayri* [M], incomplete adult specimen (LPB 052) from bed 13. **D.** *Choffatia subbakeriae* [M], adult specimen (LPB 011) from bed 14. All natural size. Point at last septum.

**Material.** — Two almost complete adult body chambers (LPB 294 and 293, the latter with fragments of the phragmocone) from bed 13.

**Description.** — The last whorl of the phragmocone ( $Dls = 60$  mm) shows a wide, rounded-tegulate venter. The body chamber is involute ( $H_2/H_1 = 0.62$ ) with a shallow, wide umbilicus ( $U/D = 0.15\text{--}0.17$ ), with convex walls and rounded shoulder. Whorl section fusiform, widest in the lower third of the flanks which are perumbilically subparallel, passing, with no ridge, to converge to the venter. Venter fairly acute at the beginning of the body chamber and almost rounded near the end. The first half of the body chamber has, in the upper third of the flanks, 10 proversely concave (lunuloid), rather obsolete ribs. Some growth lines are visible between these ribs. The specimens must have been about 90 mm in final diameter.

**Remarks.** — Discrimination between *Oxycerites* (*Alcidellus*) and *O.* (*Paroxycerites*) is based on the absence of tertiary ribbing on the ventro-lateral shoulder of the former, a feature absent in the present specimens, which moreover, have no spiral ridge on the flanks and have a somewhat stouter and more rounded body chamber than that of the typical species of *Oxycerites* (*Paroxycerites*). *Oxycerites* (A.) *tenuistriatus* differs from *O.* (A.) *obsoletoides* Riccardi, Westermann, & Elmi, 1989 and *O.* (A.) *cualascensis* Sandoval & Westermann, 1990 in the more evolute coiling, wider umbilicus and more rounded ventral side with no ventral tegulation along the body chamber. The adult size and the stratigraphic occurrence of the present specimens are intermediate between those two species. *O.* (A.) *tenuistriatus* is very widely distributed in the European upper Bathonian, recently recorded in Spain (Sandoval 1983), and Mexico (Sandoval *et al.* 1990); here it is described for the first time in the Andean region.

Family Perisphinctidae Steinmann, 1890

Subfamily Pseudoperisphinctinae Schindewolf, 1925

**Remarks.** — The current specific and generic taxonomy of this subfamily is morpho-typical, thus the picture is one of several parallel morphospecies having vertical ranges through the Bathonian–Callovian. When large samples from single faunal horizons are not to hand, it is hard or impossible to recognize the range of variation from small samples, and they can well give the impression of being made up of several (morpho-) species. This can be seen clearly in the well documented, isochronous perisphinctid assemblage coming from a single faunal horizon studied by Dietl (1994). Several morphotypes, provisionally assigned by Dietl (1994) to 6–7 species (3 subgenera and 2 genera) occur there, intergrading from the coarsely ribbed *Homoeoplanulites* (*Parachoffatia*) *arkelli* [M] and *H.* (*H.*) *bugesiacus* [m] to the more finely ribbed *H.* (*P.*) aff. *arisphinctoides* [M] and *H.* (*H.*) *balinensis* [m]. They all resemble each other in the inner whorls, strongly suggesting that they are intimately related, and probably morphotypes of a single dimorphic biospecies. The classification of Dietl (1994) based on a vertical species concept that is purely morphologic and largely subjective (Callomon *et al.* 1992: p. 28); a picture analogous to Arkell's systematics of the Oxfordian perisphinctids (Callomon 1988; Atrops & Meléndez 1993). The Andean Bathonian and Callovian Pseudoperisphinctinae have received separate names from the European ones which they, however, commonly closely match and with which they have been compared (Riccardi *et al.* 1989; Sandoval *et al.* 1990), the Andean assemblages showing the same morpho-ornamental patterns of variation, with more or less intergrading morphotypes mainly assigned to *Subgrossouvria*, *Choffatia* and *Homoeoplanulites*. Following Westermann (in Westermann *et al.* 1984) and Sandoval *et al.* (1990:

p. 128), the genera *Choffatia*, *Subgrossouvria*, *Grossouvria* (*partim*, only the Bathonian to middle Callovian species), *Homoeoplanulites* and *Parachoffatia* are here placed into the undivided genus *Choffatia*, since the differences are not sufficient for generic distinction.

### Genus *Choffatia* Siemiradzki, 1898

Type species: *Perisphinctes cobra* (Waagen, 1875).

Age: late Bathonian–late Callovian.

**Remarks.** — The specific taxonomy adopted here within the genus is mainly morphotypic, due to the small size of the samples, the specific names selected to match as closely as possible the existing, better known morphospecies. Emphasis has been put on the relationships between the coeval and successive species.

### *Choffatia subbakeriae* (d'Orbigny, 1850) [M]

Figs 5D, 6A–D; App. 1.

\* *Choffatia subbakeriae* (d'Orbigny); Arkell 1959: p. 215, text-fig. 78 (holotype), original spelling (*lapsus calami*, Art. 32) corrected.

non *Choffatia subbakeriae* (d'Orbigny); Raileanu & Nastaseanu 1960: pp. 7, 19; pl. 11: 39 [a proplanulitid-like ammonite].

*Homoeoplanulites* (*Parachoffatia*) *subbakeriae* (d'Orbigny); Sandoval 1983: pp. 482–484, figs 131M, 132, 133G, pl. 50: 1 [with synonymy].

*Homoeoplanulites* (*Parachoffatia*) sp. cf. *H. (P.) subbakeriae* (d'Orbigny); Sandoval 1983: pp. 484, 486, figs 131L, 133H, pl. 51: 1.

**Material.** — Three almost complete regularly preserved adult body chambers (LPB 033, 035, 075) and fragments of big adult body chambers (LPB 034, 377/5) from bed 14, plus one adult specimen (LPB 011) loose from bed 14.

**Description.** — Shell evolute throughout post-embryonic ontogeny ( $H_2/H_1 = 0.80–0.94$ ). Whorl section subcircular to subrectangular in the inner whorls passing to subelliptical in the adult phragmocone, then subtrapezoidal in the adult body chamber. Very regularly and densely ribbed on inner whorls, reaching the maximum,  $P = 30$ , at  $D = 40–50$  mm, then diminishing towards adult body chamber ( $P = 18$ ). Primaries acute, radial to slightly prorsiradiate, bifurcating near ventro-lateral shoulder. About 3 feeble ventral ribs to each primary throughout last whorl of phragmocone and first half of body chamber, with no ventral interruption. Largest specimens exhibit projected primaries and smooth ventral region at the uncoiled end of the body chamber.

**Remarks.** — The present specimens are smaller at the adult stage than the European representatives of the species. After analysis of the available data of *Ch. subbakeriae* from Galacz (1980), Hahn (1969), Mangold (1970), Sandoval (1983), and Sandoval *et al.* (1990), it was found that there is a gradient, a clinal pattern of variation, of adult size measured by means of the  $Dls$ , diminishing gradually from north-central Europe (Hungary–Germany–France) towards the Andean region through south Spain and Mexico (Fig. 6D). Although this pattern should be statistically measured by means of larger and closely isochronous samples, there seems to be a very consistent intraspecific clinal paedomorphosis by progenesis. Thus, the present sample, despite the smaller adult size of its specimens, can be included into this species.

*Ch. subbakeriae* [M] and *Ch. homoeomorpha* (Buckman, 1922) [m], both of the upper Bathonian and basal Callovian of the Mediterranean Province (Hahn 1969;



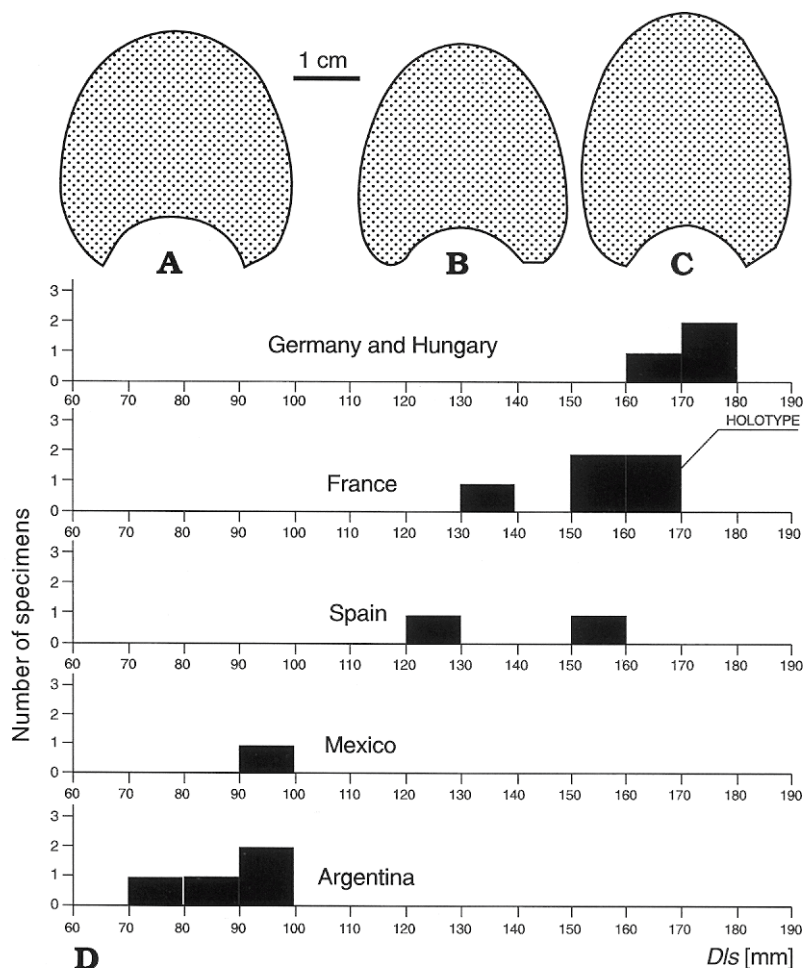


Fig. 6. A–D. *Choffatia subbakeriae* [M]. A–C. Cross sections through adult body chamber. A. LPB 011,  $D = 115$  mm. B, C. LPB 033,  $D = 146$  mm. D. Clinal gradient of phragmocone adult size (see explanation in text).

Mangold 1970), have identical phragmocones and they have been proposed as sexual dimorphs by Hahn (1969: p. 71), but from the Andean region neither *Ch. homoeomorpha* [m] nor any other species which may be considered as the microconch of *Ch. subbakeriae* [M] has yet been described.

#### *Choffatia suborion* (Burckhardt, 1927) [M]

Fig. 7A, B; App. 1.

? *Perisphinctes jupiter* Steinmann; Lóczy 1914: p. 404, pl. 24(12): 4.

\* *Perisphinctes suborion* n. sp.; Burckhardt 1927: pp. 77, 78, pl. 31: 2–4, 7.

*Perisphinctes cualacensis* n. sp.; Burckhardt 1927: pp. 78–80, pl. 30: 6–9.

*Perisphinctes* Cfr. *Gottschei* (Steinmann); Burckhardt 1927: p. 80, pl. 31: 1, 5, 6.

*Choffatia suborion* (Burckhardt); Sandoval *et al.* 1990: p. 130, pl. 10: 2, pl. 12: 1, 2.

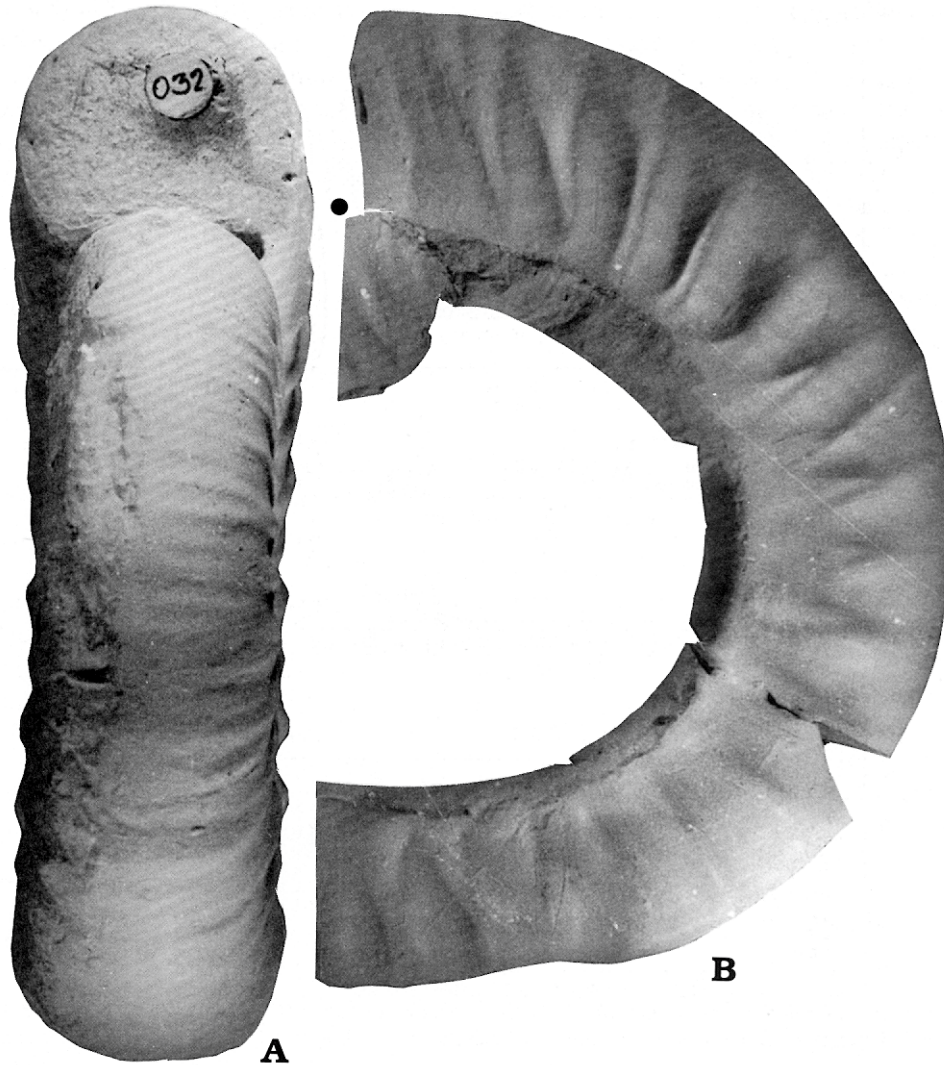


Fig. 7. A, B. *Choffatia suborion* [M], adult body chamber (LPB 032) from bed 14. Natural size. Point at last septum.

**Material.** — One complete well preserved adult body chamber (LPB 032) and 1 almost complete adult phragmocone (LPB 036) from bed 14, and 1 complete subadult body chamber (LPB 281) loose from bed 14?.

**Remarks.** — The present specimens clearly belong to this morphospecies; the body chamber, about 360°, is evolute with a very wide umbilicus and subcircular whorl section. Strong blade-like, prosocline primaries arise at the umbilical shoulder and bifurcate at the ventro-lateral shoulder. Ventral ribs are weaker and denser than primaries ( $V/P = 2-3$ ). Throughout the last half of the body chamber the primaries are

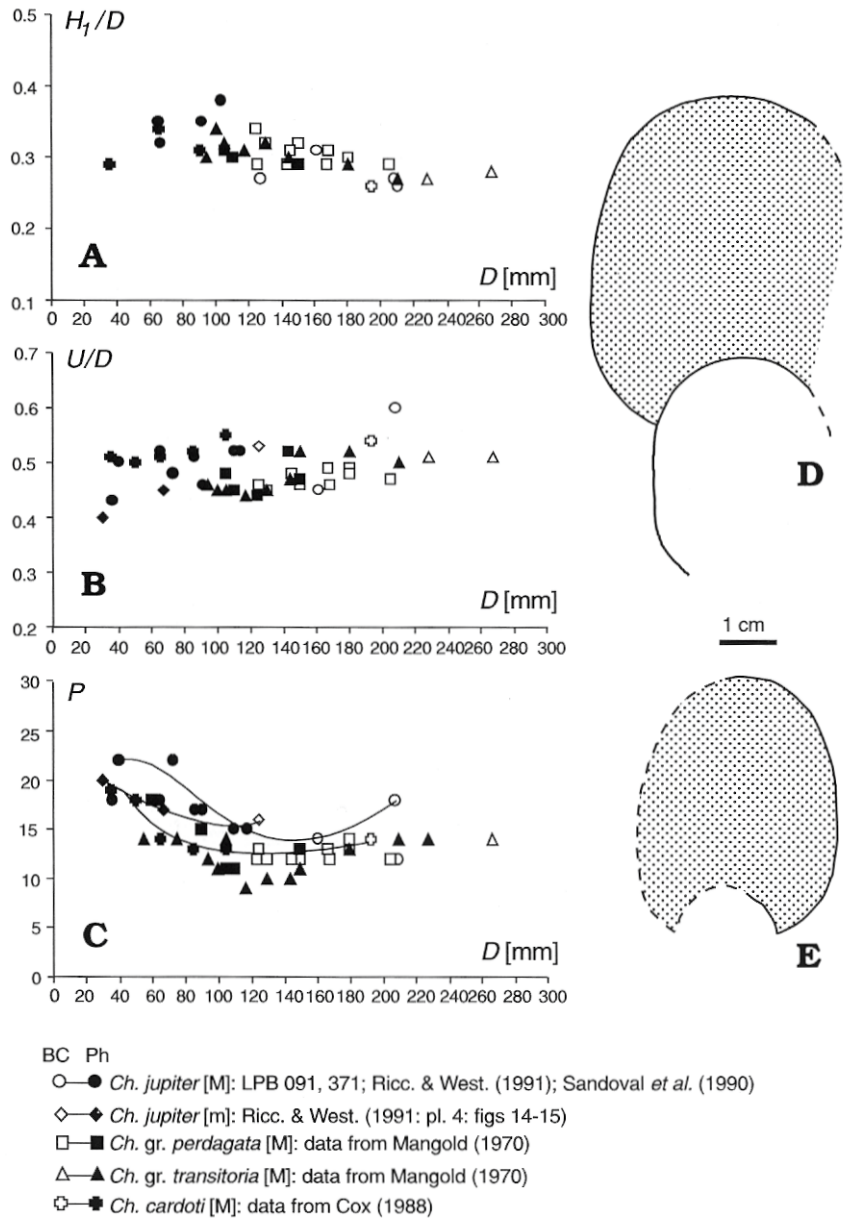


Fig. 8. A–E. *Choffatia jupiter* [M]. Scatter diagrams and cross sections through phragmocone and body chamber (stippled).  $H_1/D$ -D (A);  $U/D$ -D (B);  $P$ -D (C); LPB 091,  $D = 208$  mm (D); LPB 371,  $D = 161$  mm (E).

somewhat irregular. No ventral furrow is developed in the present specimens whereas it is present in some Mexican specimens (Sandoval *et al.* 1990).

The specimen figured by Lóczy (1915) may be assigned to this species on morphological grounds, but it seems to come from the middle-upper Callovian of Hungary.



It should be noted that the designation of the lectotype of the species was erroneously made twice, first by Westermann (in Westermann *et al.* 1984), later by Riccardi *et al.* (1989). The first designation is valid, the holotype of *Ch. suborion* being thus the specimen figured by Burckhardt (1927: pl. 31: 2–4) from Cualac, State of Guerrero (Mexico) and belonging to the *Lilloettia–Neuquenicer* Association of Sandoval *et al.* (1990).

*Choffatia jupiter* (Steinmann, 1881) [M]

Figs 8A–E, 9; App. 1.

- \* *Perisphinctes jupiter* Steinmann 1881: p. 277, pl. 9: 6 [lost].
- non *Perisphinctes jupiter* Steinmann; Lóczy 1915: p. 404, pl. 24 (12), fig. 4.
- non *Subgrossouvria* cf. *jupiter* Lóczy [recte Steinmann]; Raileanu & Nastaseanu 1960: pp. 7, 19, pl. 6: 19 [probably a *Virgatosimoceras*].
- \* *Choffatia jupiter* (Steinmann); Riccardi *et al.* 1989: p. 568, pl. 5: 1 (neotype); pl. 6: 3.
- Choffatia* cf. *jupiter* (Steinmann); Sandoval *et al.* 1990: p. 131, pl. 10: 1a, b, 3; pl. 15: 3.

**Material.** — Two almost complete adult specimens (LPB 091, 371) and body chamber fragments (LPB 375 and 377/1–3) from beds 22 and 28.

**Description.** — Last whorl of the adult phragmocone evolute, rounded subquadratic in whorl section, with strong projected primaries that arise at the umbilical shoulder. Body chamber evolute and contracted at the end, with ovate-compressed whorl section, widely spaced, bullate primaries, and very blunt to obsolete secondaries. Peristome simple, expanded, slightly projected ventrally.

**Remarks.** — The present specimens agree with the neotype and the other macroconch figured by Riccardi *et al.* (1989), differing only in the last half of the body chamber which shows subdued primaries in the present specimens (Fig. 9). *Ch. jupiter* [m], as defined by Riccardi *et al.* (1989), is known from a single specimen with the peristome not preserved; differences between dimorphs are in the more compressed and densely ribbed body chamber and the smaller adult size of the microconch.

The Mexican specimens figured by Sandoval *et al.* (1990) as *Ch. cf. jupiter* have more prominent primaries than the Andean morphotypes, but do not differ in other aspects of morphology and involution, and certainly fit into the variability range of the species. Of these specimens, that figured by Sandoval *et al.* (1990: pl. 15: 3) stands very close to *Ch. suborion* (Burckhardt, 1927) [M]. Main differences between these two species lie in the more rounded and more prominent primaries of *Ch. suborion*, and although this last tends to be more evolute, the inner whorls of both species strongly resemble each other in whorl section and ribbing. The two species seem to be very closely related.

The poorly known *Ch. praecursor* Mangold, 1970 and *Ch. vicenti* Mangold, 1970, both of the *blanazense* horizon of the upper Bathonian (Mangold 1970) and probably variants of a single species, are the late Bathonian European species closest to *Ch. jupiter*. Differences lie in the slightly more evolute and widely umbilicate body chamber and in the denser and radial ribbing of the inner whorls of *Ch. jupiter*.

The early Callovian macroconchiate species *Ch. gr. perdagata* (Waagen, 1875) (*sensu* Mangold 1970), *Choffatia transitoria* (Spath, 1931), and *Ch. cardoti* (Peticlerc, 1915) strongly resemble *Ch. jupiter* [M], and comprise a rather homogeneous group intergrading in morphology and ribbing which cluster tightly around common trends



Fig. 9. *Choffatia jupiter* [M], incomplete adult specimen (LPB 091) from bed 28. Natural size.

in scatter diagrams (Fig. 8A–C). The biggest specimen (LPB 091), from the *S. gerthi* horizon, differs from *Ch. gr. perdagata* in the smoother body chamber; the other specimen (Fig. 9), from the Gottschei Zone, is almost identical with *Ch. transitoria* as



figured by Mangold (1970: pl. 8: 1), and differs from *Ch. gr. perdagata* in the lower density of the primaries throughout the inner whorls (between diameters of 30–80 mm). *Ch. jupiter* differs from *Ch. cardoti*, as figured by Cox (1988: pl. 10), in that the latter has a more compressed adult body chamber. Thus, within the known material of *Ch. jupiter*, it seems possible to distinguish two temporal succeeding morphotypes, or transients, ranging between extreme morphotypes comparable to *Ch. transitoria* and *Ch. gr. perdagata* respectively. The resemblance between all of them throughout ontogeny, with intergrading morphotypes, and the narrow chronostratigraphic interval in which these morphospecies occur, together with the known biogeographical connections between the Pacific and the Tethys during Jurassic times, strongly suggest their close genetic relationships. The differences between these Andean and European forms could thus be attributed to geographic and phyletic variation within a single chronospecies.

*Choffatia* aff. *neumayri* (Siemiradzki, 1899) [M&m]

Figs 5C, 10A–D, 11A–F; Table 1.

**Material.** — ?One almost complete adult macroconch specimen (LPB 070) from bed 3; several well preserved, complete or almost complete, adult macroconch specimens (LPB 037, 051, 052, 054–057, 073), and 1 incomplete adult microconch (LPB 088) from bed 13.

**Description.** — The sample is very homogeneous and of low variability, comprising adult macroconchs and one microconch, mostly restricted to a single level (Fig. 2).

Macroconch: Mean adult size  $D = 68.2$  mm ( $n = 7$ ,  $CV = 10.8\%$ , some specimens with peristome not fully preserved), mean adult phragmocone size  $Dls = 51.9$  mm. Evolute ( $H_2/H_1 = 0.90$ – $0.70$ ;  $U/D = 0.50$ – $0.40$ ) and non-constricted throughout ontogeny. At diameters of less than 4 mm (3–4 first whorls) the whorl section is ovate, very depressed; there is no ribbing, only feeble prorsiradiate growth lines. Between 4 and 10 mm diameter the whorl section is ovate with broad, smooth venter; there appear 2 or 3 fat primary ribs per half whorl, followed by a short stage of fine, prosocline primary ribs ( $P = 12$ – $15$ ) which do not pass across the venter, each third rib bearing a ventro-lateral parabolic node. Between 10 and 45–60 mm (end of the phragmocone) diameter the whorl section is subcircular, slightly wider than high ( $W/H_1 = 1.10$ – $1.30$ ). At a diameter of about 10 mm appears a very characteristic, mostly irregular ornamental stage, composed of prominent pairs of fused primary ribs bearing a ventro-lateral parabolic node. There is a pair of fused-primaries to each 1 or 2 normal primaries at the beginning, but frequency of fused-primaries decreases towards the end of phragmocone. Normal primaries are sharp and rectiradiate to slightly prosocline and bifurcate at the ventro-lateral shoulder into 3 feeble, very regularly spaced secondaries which pass transversely across the rounded venter with some intercalatories. Adult body chamber, about  $360^\circ$ , evolute and ovate in whorl section, with umbilical seam slightly uncoiled; ribbing remains unchanged. Some specimens retain 1 to 3 fused pairs of primaries with parabolic nodes at the beginning of body chamber. The peristome is simple, slightly expanded and preceded by a shallow constriction in some of the specimens.

**Microconch:** A single adult specimen ( $D = 57$  mm) with incompletely preserved ventro-lateral lappets is available. It differs from the macroconch in the presence of lappets and the slightly smaller final adult size.

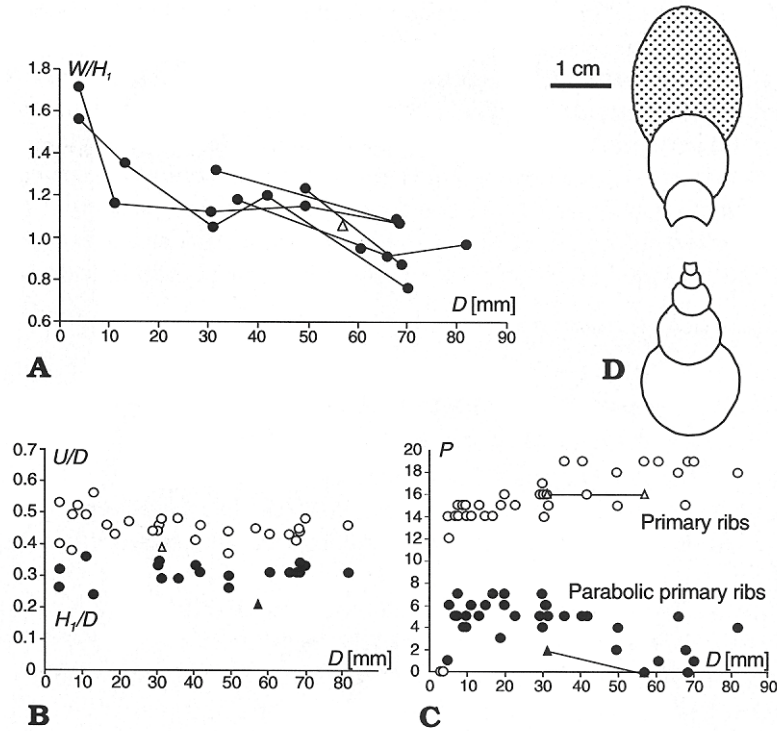


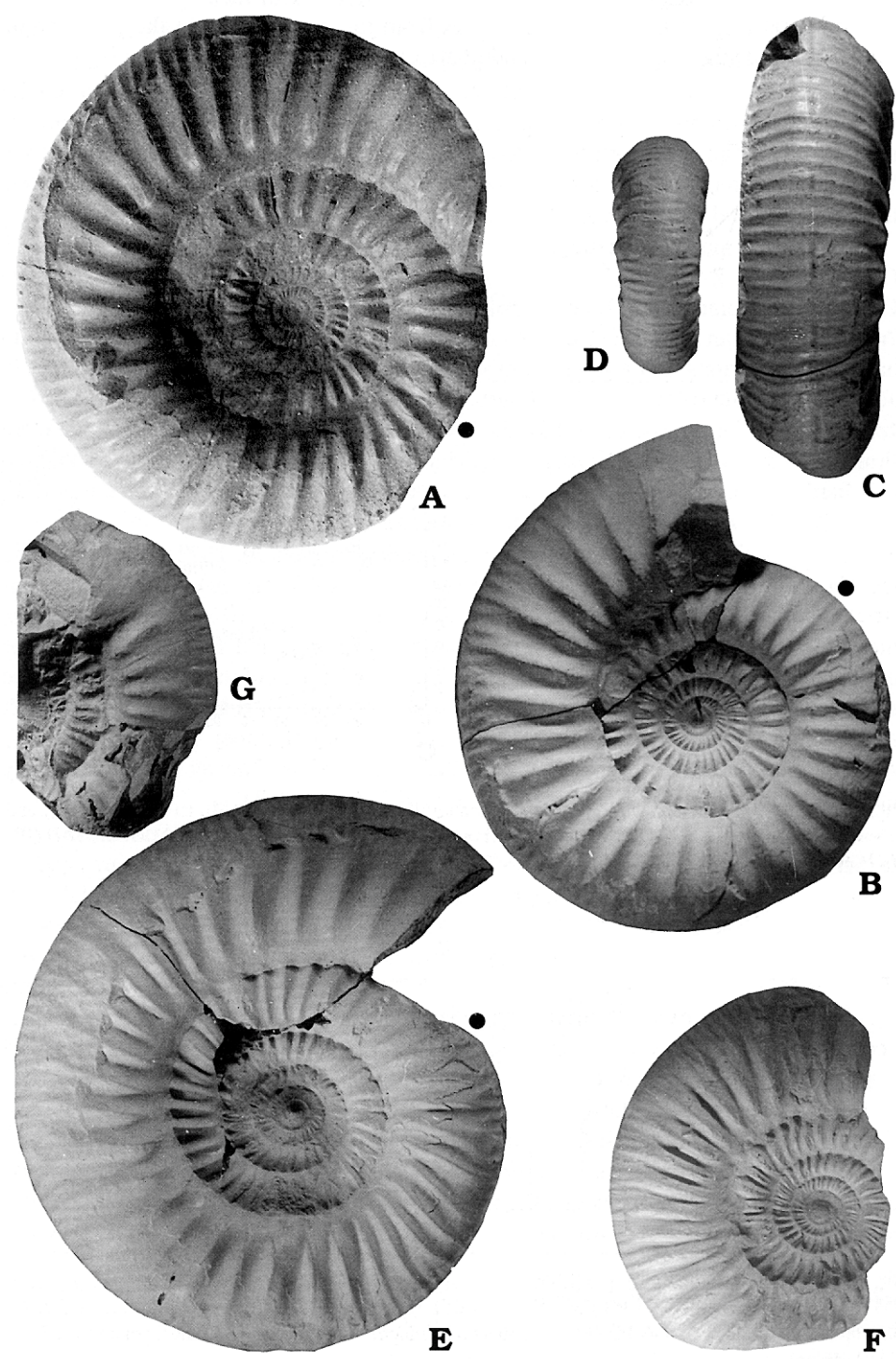
Fig. 10. A–D. *Choffatia* aff. *neumayri* [M&m]. Scatter diagrams (circles for [M], triangles for [m]) and cross sections through phragmocone and body chamber (stippled).  $W/H_1$ - $D$  (A);  $U/D$ - $D$  and  $H_1/D$ - $D$  (B);  $P$ - $D$  and parabolic fused  $P$ - $D$  (C); complete adult macroconch specimen LPB 055 (D).

Table 1. *Choffatia* aff. *neumayri*: statistical measurements at or near peristome for the sample of adult macroconch specimens. For abbreviations see pp. 74–75.

	<i>n</i>	<i>m</i>	<i>CV</i>	<i>RO</i>	<i>R/s</i>	<i>Ho</i>
$Dp$ [mm]	7	68.23	10.8	57.00–81.95	3.4	0.131(°)
$Dls$ [mm]	6	51.92	6.7	47.80–57.00	2.6	0.226(°)
$W/D$	7	0.31	10.6	0.25–0.36	3.3	0.107(°)
$H_1/D$	6	0.32	3.8	0.31–0.34	2.5	0.392(°)
$U/D$	7	0.45	4.6	0.41–0.48	3.4	0.096(°)
$H_2/D$	4	0.24	9.8	0.21–0.27	2.5	–

Fig. 11. A–G. *Choffatia* aff. *neumayri* [M&m]. A–F. Complete adult macroconchs  $\times 1$ , LPB 055 (A), LPB 054 (B–D), inner whorl (D), LPB 056 (E), LPB 051 small sized and densely ribbed variant (F). G. Incomplete adult microconch (LPB 088) with incomplete lappets. All specimens come from bed 13. Point at last septum.





**Remarks.** — The variation is the highest for macroconch adult size,  $D = 57\text{--}82$  mm near the peristome. The characteristic parabolic-fused primaries (pairs of fused primaries bearing a moderately prominent ventro-lateral parabolic node) and the striking complete lack of constrictions throughout ontogeny make this form unique within the Andean upper Bathonian–lower Callovian perisphinctid assemblages. The development of this ornamental pattern could be interpreted as a neotenuous expression of the ‘Siemiradzka-stage’ as defined by Mangold (1970), reaching more external whorls than in the typical ‘*Siemiradzka*’ and in any other species of *Choffatia*.

The present material most closely resembles the specimen figured by Kopik *et al.* (1980: pl. 57: 3) as *Ch. neumayri* (Siemiradzki, 1899) from the lower–?middle Callovian of Poland. The holotype of *Ch. neumayri*, a specimen from the lower–?middle Callovian of Lvov (Ukraine) figured by Mangold (1970: fig. 114), differs in having constrictions and a lower number of parabolic-fused primaries, but agrees in adult size, involution, and whorl section. Cariou (1984b) cited *Ch. neumayri* and *Ch. kontkiewiczzi* (Siemiradzki, 1894) for the lower Baylei Subzone, Coronatum Zone from France. *Ch. kontkiewiczzi* as illustrated by Mangold (1970), another species from which it is hard to separate *Ch. aff. neumayri* as described above, differs little or not at all from *Ch. neumayri*, and they could be conspecific.

The European lower Callovian *Ch. recuperoi* (Gemmellaro, 1872) is very close to the *Ch. neumayri*–*kontkiewiczzi* group, differing from *Ch. aff. neumayri* in the constricted whorls throughout ontogeny, with few or no parabolic ribs (Cox 1988), and in the somewhat stouter whorl section; however, involution and ribbing do not differ between macroconchs. At diameters larger than 30 mm the number of primaries is the same for both, although some specimens of Gemmellaro’s species attain bigger adult size and are more coarsely ribbed throughout the body chamber. Some fragmentary specimens (unpublished) from the Bodenbenderi Zone at Chacay Melehué closely match the morphotype figured by Mangold (1970: pl. 10: 2, 3).

*Choffatia gottschei* (Steinmann, 1881) is the most closely allied Andean species. It differs from *Ch. aff. neumayri* in having constrictions and a lower number of fused-primaries although it shows great resemblance in morphology and modal adult size and also in stratigraphic occurrence. In Chacay Melehué *Choffatia aff. neumayri* appears as an intermediate form between *Ch. gottschei* and *Choffatia aff. aequalis* (Roemer in Riccardi *et al.* 1989: pl. 2: 6, 7). This last occurs at the *Iniskinites gulisanoi* horizon (lower Steinmanni Zone) and differs from *Ch. aff. neumayri* in the occurrence of shallow constrictions, absence of parabolic-fused primaries and higher density of primaries. *Ch. cf. gottschei* has been cited from the lower Callovian of Poland (Dayczak-Calikowska & Kopik 1976), which suggests the presence in Europe of the same or a similar group of more or less successive morphotypes, i.e., *Ch. aequalis*–*gottschei*–*recuperoi*–*neumayri*–*kontkiewiczzi*, in comparable chronostratigraphic succession to that of the Andean group. Recognition of direct phyletic relationships must await better data.

Family Sphaeroceratidae Buckman, 1920

Subfamily Eurycephalitinae Thierry, 1978 (1976)

[incl. Paracephalitinae Tintant & Mouterde, 1981]

# Genus *Iniskinites* Imlay, 1975

Type species: *Kheraicerus magniforme* Imlay, 1953 by original designation.

Age: (?late Bajocian) early Bathonian–late Bathonian.

## *Iniskinites crassus* Riccardi & Westermann, 1991 [M]

Figs 12A–I, 13A–E; Table 2.

\* *Iniskinites crassus* sp. nov., [M]; Riccardi & Westermann 1991: pp. 63–66, pl. 12: 2 (holotype)–4, pl. 13: 1–4.

? *Stehnocephalites gerthi* (Spath); Riccardi & Westermann 1991: p. 11.

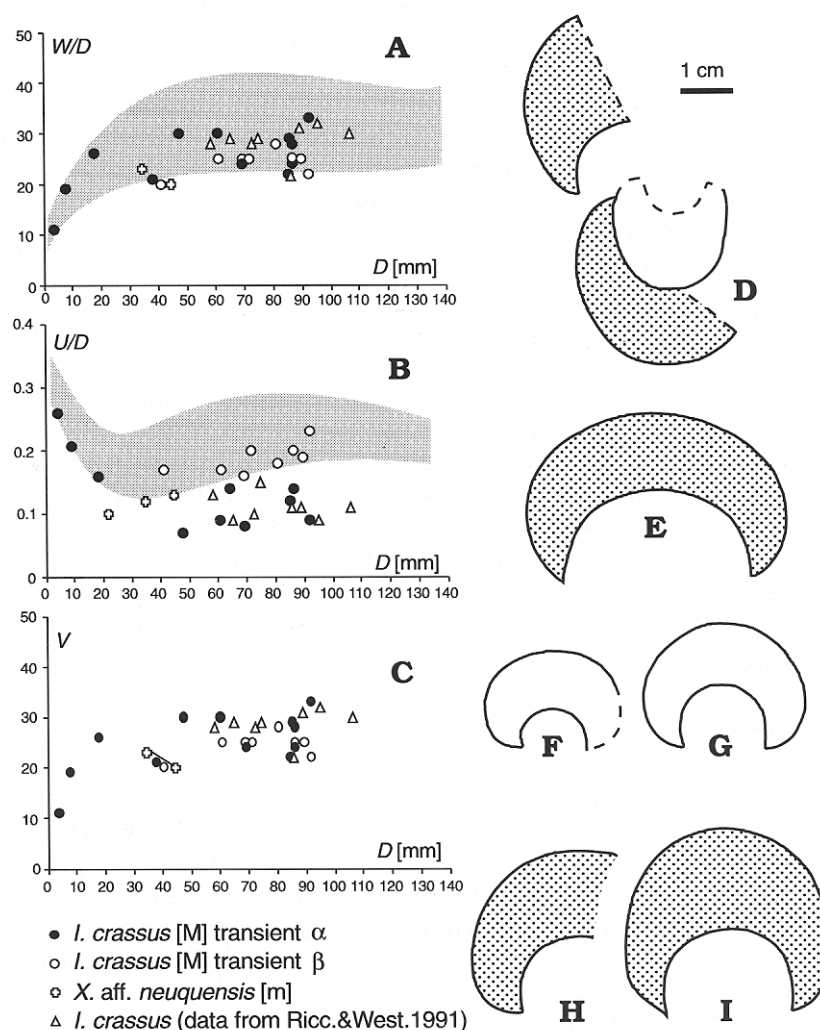


Fig. 12. A–I. *Iniskinites crassus* [M] and *Xenocephalites* aff. *neuquensis* [m]. Scatter diagrams (with shaded areas indicating the ranges of variability of *Stehnocephalites gerthi* for comparison) and cross sections through phragmocone and body chamber (stippled). W/D–D (A); U/D–D (B); V–D (C); LPB 072, transient  $\alpha$  (D); LPB 022, morph  $\alpha$  ( $D \approx 60$  mm) (E); LPB 289, transient  $\beta$  (I at  $D \approx 83$  mm) (F–I).



**Material.** — One complete adult (LPB 072) from bed 3; 2 juvenile specimens (LPB 023, 083/2) in the body chamber of an almost complete adult specimen (LPB 022) from bed 5; 7 more or less complete adult specimens (LPB 010, 288–292, 411) from bed 11a.

**Description.** — Two transients (morphotypes in phyletic succession) may be distinguished within this species throughout its vertical range (cf. Riccardi & Westermann 1991: p. 64):

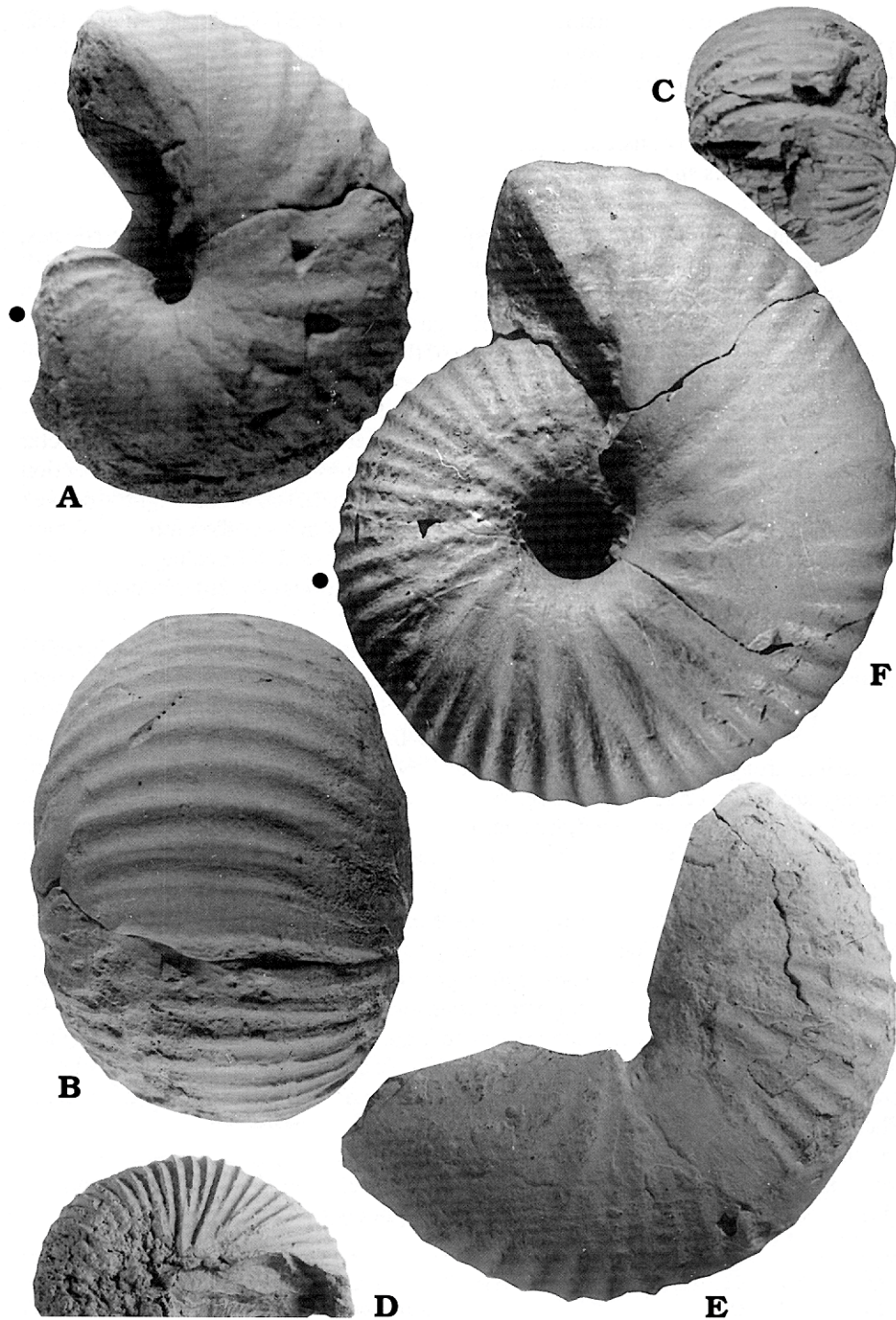
Transient  $\alpha$  (Fig. 13A–E). — It corresponds to the original concept of the species, i.e., to the type transient, as described by Riccardi & Westermann (1991); it is well characterized by the holotype and predominates in the samples (populations) which occur in the lower and middle parts of the range of the species. Two juvenile specimens (LPB 023, 083/2) allow the characterization of the juvenile whorls. At diameter of 3–5 mm the shell is very depressed and moderately evolute with a wide umbilicus ( $U/D = 0.26$ ) and convex flanks. Ten to twelve wide rounded, straight primaries pass transversely across the venter with neither furcation nor intercalatories. At 10–18 mm diameter the umbilicus is much more closed ( $U/D = 0.16$ ) with rounded shoulder; whorl section subrectangular ( $W/H_l = 1.27$ ) with parallel, almost flat flanks and slightly convex venter; ribbing is much more acute, about 11 primaries arise at the umbilical suture, bend backward at the umbilical shoulder and project forward, bifurcating at mid-flank and passing across the venter together with the intercalatories ( $V = 26$ ). At about 30 mm diameter the umbilicus is very closed,  $U/D = 0.09$ .

Transient  $\beta$  (Fig. 13F). — It includes specimens with morphology and stratigraphic occurrence intermediate between *I. crassus* transient  $\alpha$  and *Stehnocephalites gerthi* (Spath, 1928). Transient  $\beta$  differs from transient  $\alpha$  in the body chamber, which is more compressed and widely umbilicate ( $U/D = 0.18$ – $0.23$ ), particularly near the peristome, where it is strongly egressive and shows a shallow lateral constriction. The numbers of primary and ventral ribs do not differ from those of transient  $\alpha$ , but the primaries are more flexuous and not projected, resembling the adult ribbing of *S. gerthi*. Inner whorls like transient  $\alpha$ , involute with narrow umbilicus, whorl section subrectangular with slightly convex to subplanar flanks and venter.

**Remarks.** — The involute, narrow umbilicate phragmocone and the almost flat flanks and venter determine the inclusion of the last group of specimens described (transient  $\beta$ ) in *I. crassus* rather than in *Stehnocephalites gerthi*, whose septate whorls at comparable diameters are more depressed and wider, with more open umbilicus and higher wall, passing to inflated flanks and a convex venter. *I. crassus* transient  $\beta$  includes the highest occurrences of the species in Chacay Melehué (Fig. 2: bed 11a). One of the two specimens cited as ?*Stehnocephalites gerthi* by Riccardi & Westermann [1991: p. 11 (Museo de La Plata 23898)], close to the top of the *Iniskinites crassus* horizon, belongs to *I. crassus* transient  $\beta$ ; the other specimen (Museo de La Plata 23897), from the same horizon, matches *I. crassus* transient  $\alpha$ , showing the persistence of the older of the two morphotypes after the temporal shifting of the modal morphology.

Fig. 13. A–F. *Iniskinites crassus* [M] transients  $\alpha$  and  $\beta$ . A, B. Transient  $\alpha$ , complete adult specimen (LPB 022) from bed 5. C. Same specimen at last whorl of phragmocone. D. Transient  $\alpha$ , incomplete adult specimen (LPB 072) from bed 3. E. Same specimen at last whorl of phragmocone. F. Transient  $\beta$ , complete adult specimen (LPB 289) from bed 11a. All natural size. Point at last septum.





The microconch of the present species could be represented by the form described below as *Xenocephalites* aff. *neuquensis* (Stehn, 1923) [m].

The Canadian assemblage described by Frebold (1978), and dated by Callomon (1984) as middle–late Bathonian, comprises a group of the morphospecies *Iniskinites tenasensis*, *I. robustus*, *I. yukonensis* Frebold, 1978 spp. and *I. cf. abruptus* (Imlay, 1953) which encompasses the range and pattern of variation here assigned to *I. crassus*. This assemblage comprises evolute-compressed morphotypes such as *I. robustus*, which is comparable with *I. crassus* transient  $\beta$ , and involute-depressed morphotypes such as *I. yukonensis* and *I. tenasensis*, which are comparable with *I. crassus* transient  $\alpha$ . Full comparison was made by Riccardi & Westermann (1991) who, moreover, stressed the stratigraphical and morphological proximity between *I. crassus* Riccardi & Westermann, 1991 and *I. yukonensis* Frebold, 1978. The greatest morphological differences between the Andean and the Canadian forms are those pointed out by Riccardi & Westermann (1991: p. 66) and the bigger adult size of the Canadian assemblage, about 100–130 mm in mean diameter vs. 70–100 mm in *I. crassus*. These differences may be merely continuous intraspecific variation, and, although there is no known record in Mexico, the Canadian assemblage and *I. crassus* seem to belong to a single species, the Andean form representing perhaps late populations radiating from the main Canadian stock.

Table 2. *Iniskinites crassus*: statistical measurements at or near peristome for the samples of adult macroconch specimens transients  $\alpha$  and  $\beta$ . For abbreviations see pp. 74–75.

	<i>n</i>	<i>m</i>	<i>CV</i>	<i>RO</i>	<i>R/s</i>	<i>Ho</i>
Transient $\alpha$						
<i>Dp</i> [mm]	5	81.99	8.1	68.80–85.94	2.6	0.418(°)
<i>U/D</i>	5	0.11	20.2	0.08–0.14	2.7	0.218(°)
<i>W/D</i>	5	0.61	19.1	0.45–0.73	2.4	0.226(°)
<i>H<sub>1</sub>/D</i>	5	0.49	6.1	0.44–0.53	3.0	0.118(°)
<i>H<sub>2</sub>/D</i>	5	0.28	11.4	0.25–0.33	2.5	0.216(°)
<i>P</i>	5	10	11.5	9–12	2.6	0.216(°)
<i>V</i>	5	27	13.6	22–33	3.0	0.226(°)
Transient $\beta$						
<i>Dp</i> [mm]	5	82.45	7.7	71.02–89.10	2.8	0.218(°)
<i>U/D</i>	5	0.20	8.3	0.18–0.23	3.0	0.300(°)
<i>W/D</i>	5	0.54	11.1	0.45–0.63	3.0	0.133(°)
<i>H<sub>1</sub>/D</i>	4	0.46	4.5	0.44–0.49	2.4	–
<i>H<sub>2</sub>/D</i>	3	0.26	1.8	0.25–0.26	2.1	–
<i>P</i>	5	11	6.7	10–12	2.7	0.216(°)

### *Iniskinites evolutus* sp. n. [M]

Figs 14A, 15A, B; App. 1.

*Iniskinites* sp. nov. C; Riccardi & Westermann 1991: pp. 70, 71, pl. 16: 3a, b.

non *Iniskinites* sp. nov. C in Riccardi & Westermann, 1991 (M); Fernandez-López *et al.* 1994: p. 192, pl. 1: 5.



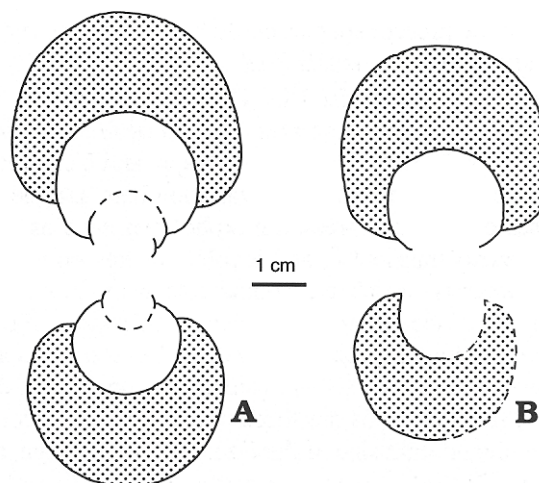


Fig. 14. Cross sections through phragmocone and body chamber (stippled). A. *Iniskinites evolutus* sp. n. [M], holotype (LPB 229). B. *Iniskinites* sp. A [M] (LPB 021).

Holotype: the complete adult specimen (LPB 229), illustrated in Fig. 15A, B, from bed 0 of the Chacay Melechué section, *Iniskinites gulisanoi* horizon, lower Steinmanni Zone of Chacay Melehué. Derivation of the name: Latin for evolute, referring to evolute coiling and wide umbilicus through ontogenetic development.

**Diagnosis.** — Evolute *Iniskinites* with subrounded whorl section and prominent, projected primaries through the juvenile and adult ontogeny.

**Material.** — The holotype.

**Description.** — Adult shell,  $Dp = 94$  mm. The two last whorls of the phragmocone (between diameters of 30 and 60–70 mm) and body chamber evolute, moderately to widely umbilicate ( $U/D = 0.16–0.23$ ). Deep umbilicus, with subvertical wall and rounded shoulder. Whorl section subrounded, slightly wider than high ( $W/H_l = 1.05–1.20$ ) with maximum width on inner third of the flanks, which are convex and converge to the rounded venter. There are 12–13 prominent, projected primaries per half whorl which arise at the umbilical shoulder (at the base of the umbilical wall where the test is preserved), bend backward, curve forward on the inner third of the flank, and become projected towards the venter. They bifurcate on the upper half of the flanks throughout the body chamber, and with 1 intercalatory per 4 secondaries, pass transversely across the venter.

Body chamber about  $300^\circ$ , peristome simple and ribbing slightly prorsiradiate and blade-like. Septal sutures not preserved.

**Remarks.** — Two specimens from Chile, Antofagasta, Quebrada San Pedro (TUB 790321/5) and Quebrada el Profeta (TUB 7-080672), described by Riccardi & Westermann (1991) as *Iniskinites* sp. n. C, match the holotype and are included in the present species, representing a distinctive morphology within *Iniskinites*. The stratigraphic position of the holotype seems to be the same as that of the Chilean specimens as indicated by the faunal association, *Iniskinites gulisanoi* horizon, lower Steinmanni Zone. *Iniskinites evolutus* sp. n. [M] resembles the upper Bathonian *Iniskinites abruptus* (Imlay, 1953) [M] at the level of the adult body chamber, but Imlay's species is



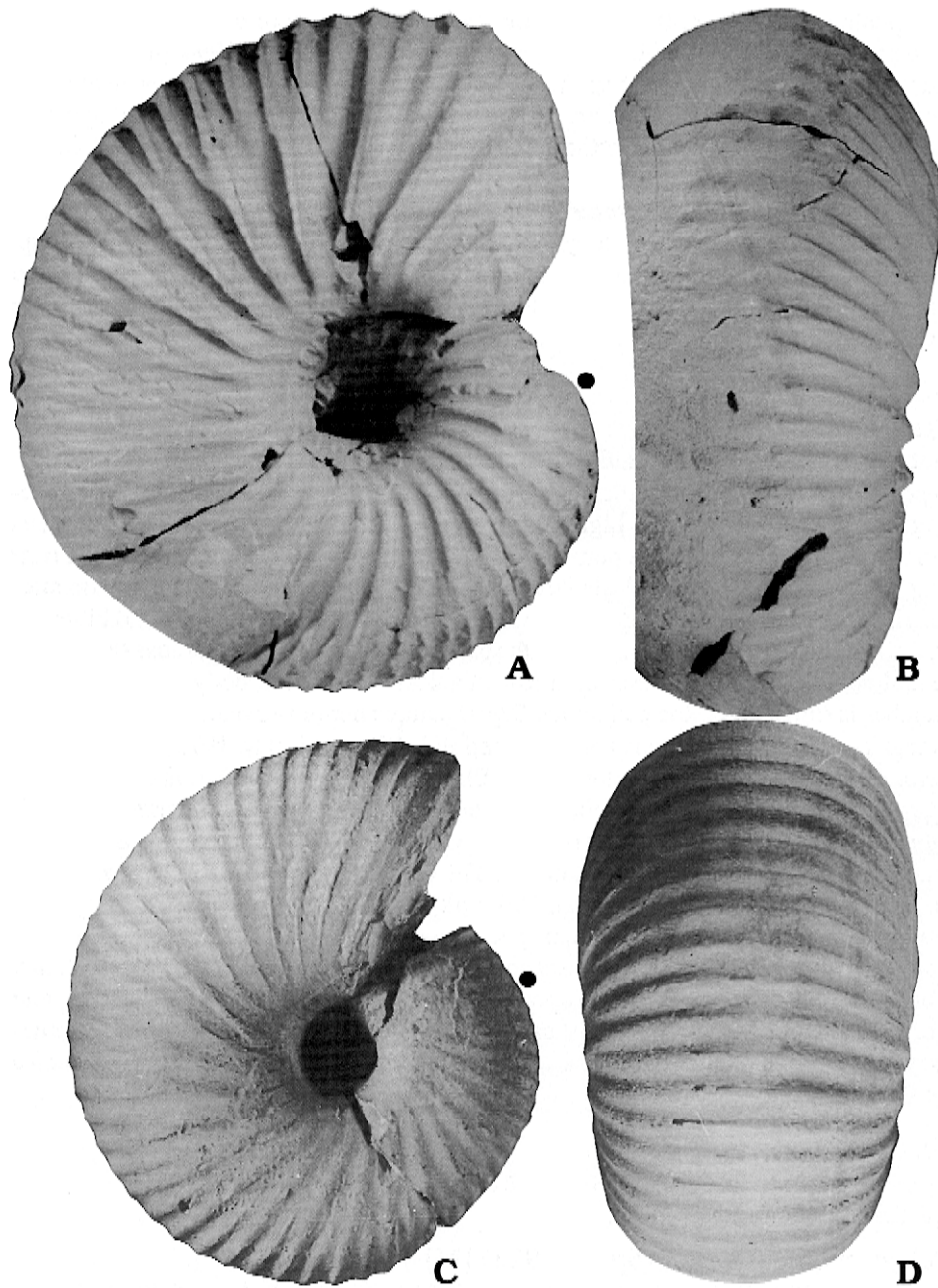


Fig. 15. **A, B.** *Iniskinites evolutus* sp. n. [M], holotype, complete adult specimen (I.PB 229) from bed 0. **C, D.** *Iniskinites* sp. A [M] complete adult specimen (LPB 021) from bed 0. All natural size. Point at last septum.

much more involute throughout and its phragmocone is more densely and more finely ribbed. *I. crassus* Riccardi & Westermann, 1991 is more involute and narrowly

umbilicate from at least 30 mm diameter, and commonly more depressed with fewer primary ribs. The specimen illustrated by Fernandez-López *et al.* (1994: pl. 1: 5) stands apart from *Iniskinites evolutus* sp. n. [M]: adult size is smaller, primaries swollen on the lower third of the flanks, and the umbilical width seems to be smaller at comparable diameter. This specimen shows the diagnostic features of the morphogenus *Xenocephalites* Spath, 1928.

*Stehnocephalites crassicostratus* Riccardi & Westermann, 1991 [M] and *I. evolutus* sp. n. [M] resemble each other in general morphology and ribbing, but *I. evolutus* sp. n. is more involute and compressed and its adult body chamber is less egressive and longer than that of *S. crassicostratus*, whose primary ribs on the adult body chamber are broader at the base and stronger.

### *Iniskinites* sp. A [M]

Figs 14B, 15C, D; App. 1.

**Material.** — One complete adult specimen (LPB 021) loose from bed 0.

**Description.** — Complete adult shell about 76 mm in diameter. Whorl section subrectangular, slightly wider than high ( $W/H_1 = 1.10$  behind the peristome). Umbilicus narrow at the last whorl of the phragmocone ( $U/D = 0.12$ ) then slightly egressive near the peristome ( $U/D = 0.16$ ). A shallow lateral, pre-peristomatic depression (constriction) is preserved. 15 prosocline primaries arise on the umbilical shoulder and bifurcate on the upper half of the flanks, then, with sparse intercalatories, pass across the venter; ventral ribs are wide and describe a low adapical arch on the body chamber. Body chamber is ribbed up to the peristome. Septal sutures not preserved.

**Remarks.** — The specimen is here included in *Iniskinites* Imlay, 1975, rather than in *Stehnocephalites* Riccardi, Westermann & Elmi, 1989, because of the small umbilicus, subrectangular whorl section, ribbed peristome and prorsiradiate primaries, a combination which does not occur in the highly variable *S. gerthi*; *S. crassicostratus* has coarser primary ribs and wider umbilicus. The closest resemblance is with *Iniskinites* sp. indet. (in Riccardi & Westermann 1991: pl. 16: 4a, b) and '*Sphaeroceras subtransiens*' Tornquist, 1898 but the present specimen is wider in whorl section, bigger, and more narrowly umbilicate. The present specimen differs from *Eurycephalites gottschei* (Tornquist, 1898) [M] in the more open umbilicus, subrectangular whorl section, and prorsiradiate primaries which persist on the body chamber up to the peristome, whereas *Eurycephalites gottschei* (Tornquist, 1898) is smooth perumbilically, and the primaries are flexuous.

### Genus *Stehnocephalites* Riccardi, Westermann & Elmi, 1989

Type species: *Indocephalites gerthi* Spath, 1928 by original designation.

Age: late Bathonian–early Callovian.

### *Stehnocephalites gerthi* (Spath, 1928) [M]

Figs 16A–E, 17A–E, 18A–H, 19A–G, 20A–E, 21A–D, 22A, B, 23A–E; Table 3.

\* *Stehnocephalites gerthi* (Spath, 1928) (?M&?m); Riccardi & Westermann 1991: p. 83, pls 20–25 [for synonymy].

*Stehnocephalites* sp. A; Riccardi & Westermann 1991: p. 89, pl. 26: 3–5.

**Material.** — 139 subadult and adult specimens (LPB 1, 2, 5, 9/1, 20, 24, 25, 38, 39, 43–48, 50, 58–64, 66, 71, 76, 89, 92–97, 107–109, 207–210, 218, 219, 222–226,



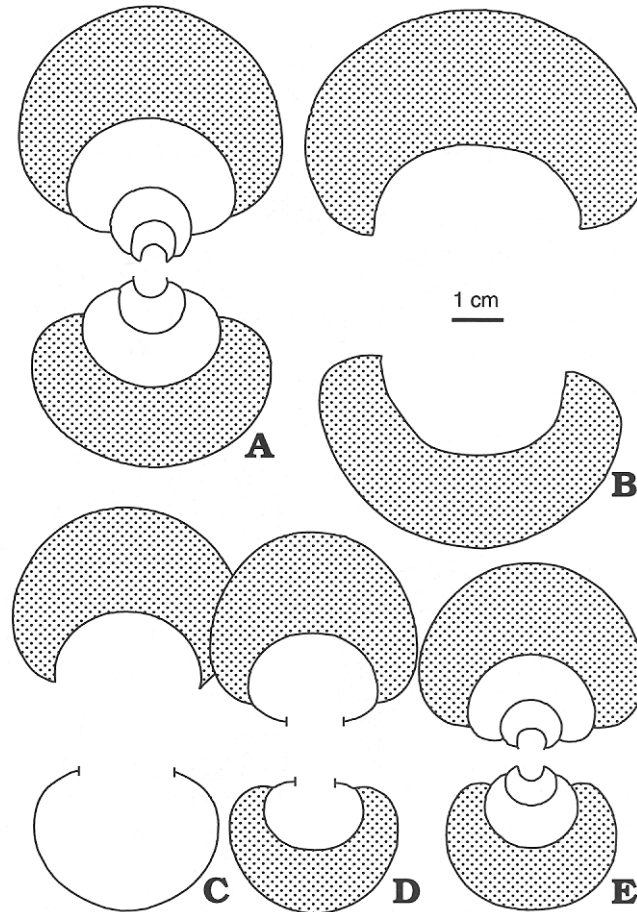


Fig. 16. A–E. *Stehnocephalites gerthi* [M]. Cross sections through phragmocone and body chamber (stippled); morph  $\beta$  (LPB 222) (A); morph  $\alpha$  (LPB 273) (B); morph  $\alpha$  (LPB 058) (C); morph  $\alpha$  (LPB 305) (D); morph  $\beta$  (LPB 257) (E).

230–258, 265–273, 275–280, 283, 295, 296, 301–305, 307, 312–319, 322, 327, 330, 336, 338–341, 344–348, 354, 357–359, 362–370, 372, 373, 387, 388, 396–398, 429, 434, and 8 unnumbered specimens) from beds 11b–13, 15, 19–23 and 25; plus about 50 well to badly preserved specimens coming from the same stratigraphic interval.

**Description.** — At diameters of less than 4 mm shell globose, evolute and widely umbilicate, with suboval depressed whorl section; flanks smooth, somewhat convex continuing to a broad rounded umbilical shoulder and smooth, broadly convex venter. From 4–8 mm diameter whorl section subcircular, as wide as high; evolute ( $U/D > 0.20$ ); at 4–5 mm diameter there are about 12 wide, rounded primaries which do not divide, and pass across the rounded venter without weakening. Between 8 and 15–20 mm diameter, whorl section becomes compressed, slightly higher than wide in some specimens, with subplanar to slightly convex flanks; umbilicus becomes narrower ( $U/D = 0.13$ ), with subvertical walls and more or less abrupt shoulder; 10–15



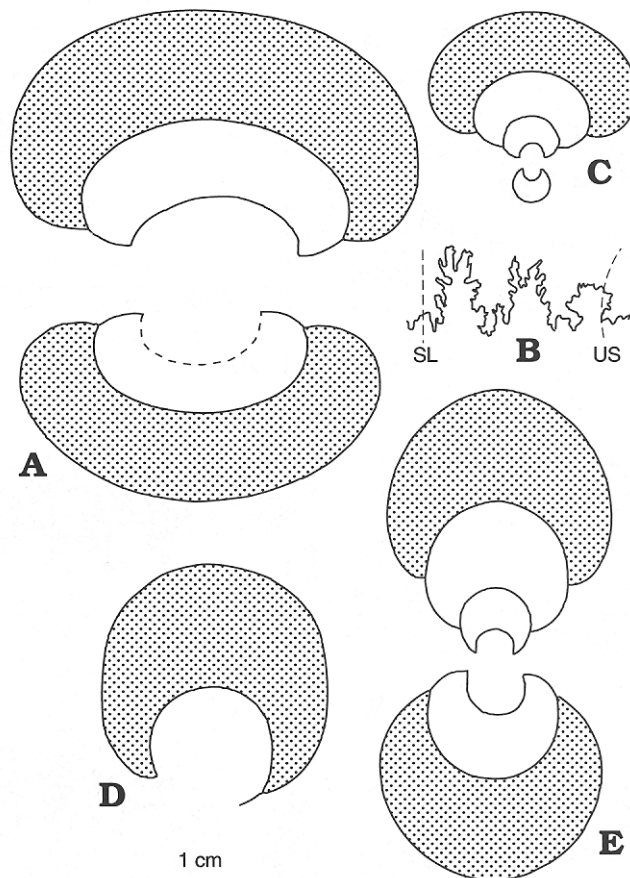


Fig. 17. **A–E.** *Stehnocephalites gerthi* [M]. Cross sections through phragmocone and body chamber (stippled), and suture line. **A, B.** Morph  $\alpha$  (LPB 258), last adult septum at  $D = 63$  mm (**B**). **C.** Morph  $\beta$  (LPB 021). **D.** Morph  $\gamma$  (LPB 001) at  $D = 91$  mm. **E.** Morph  $\delta$  (LPB 071). Abbreviations: SL – siphonal line, US – umbilical seam.

flexuous, fine primaries divide (fasciculated) on the inner half of the flanks, and, together with some intercalatories, pass across the rounded-narrow venter without weakening. At 20–25 mm diameter, in most specimens, the shell suddenly becomes expanded and depressed in whorl section, widening the umbilicus and making the ribs stronger. After these changes several morphogenetic patterns are developed. Adult size and morphology are extremely variable within the species, with globose to compressed ( $W/D = 0.94$  to  $0.44$ ), medium to wide umbilicate ( $U/D = 0.13$  to  $0.30$ ), adult individuals with subcircular (in the most compressed individuals) to subovate-depressed whorl section and fine to coarse ribbing.  $LBC$  averages  $261^\circ$ , the extremes of the range are some moderately compressed specimens with only  $205^\circ$  and other extremely depressed ones with  $360$ – $390^\circ$ , but correlation between  $W/D$  and  $LBC$  seems to be very low:  $r(LBC-W/D) = 0.251(*)$ ,  $n = 89$ .

Four main adult morphotypes may be distinguished within the species, all of them intergrading in final size, shell proportions, and ornamentation:

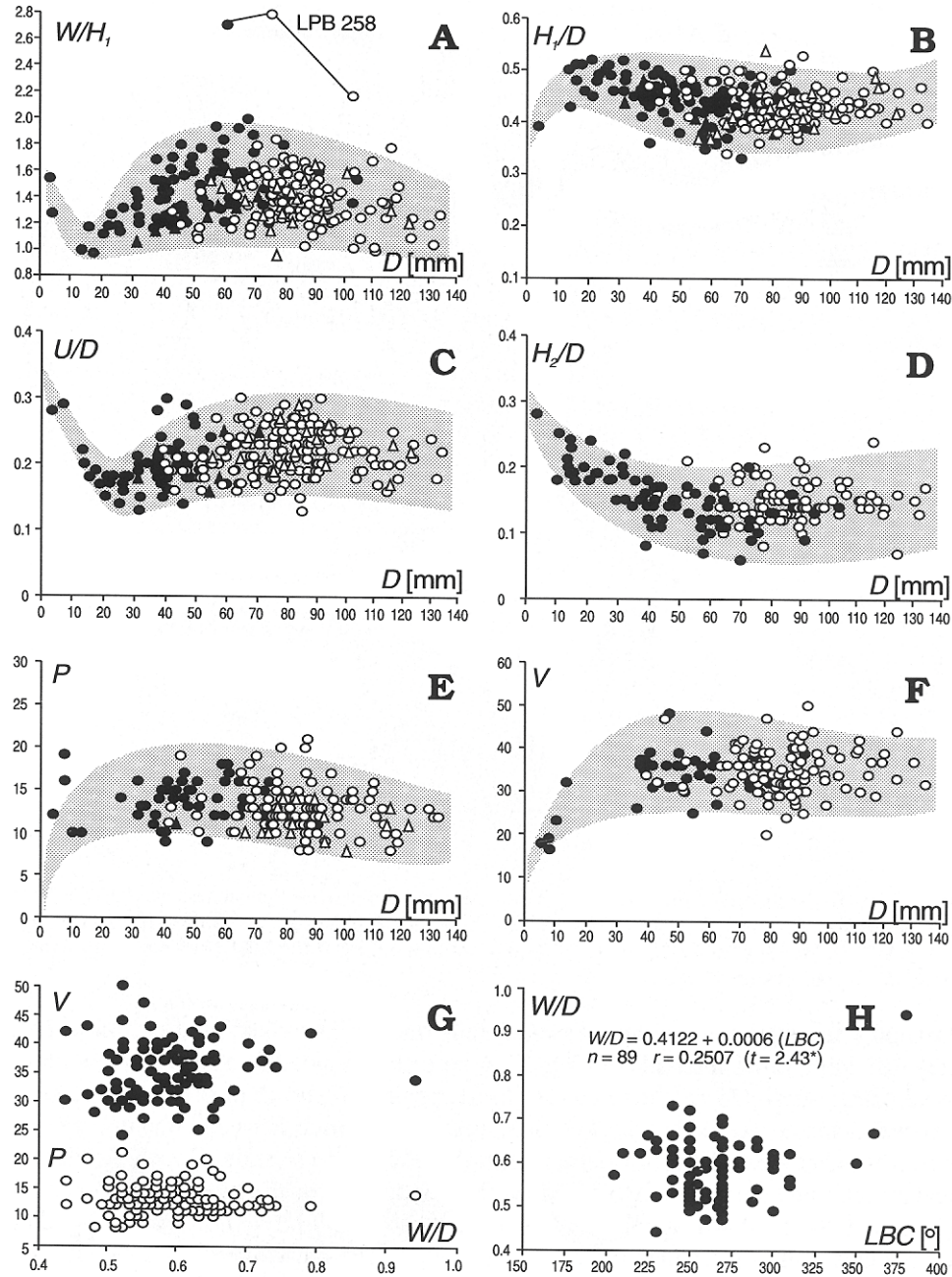


Fig. 18. A–H. *Stehnocephalites gerthi* [M]. Scatter diagrams for all the studied specimens, several measurements through ontogeny for each specimen (A–F); only for adults or near peristome (G–H).  $W/H_1$ - $D$  (A);  $H_1/D$ - $D$  (B);  $U/D$ - $D$  (C);  $H_2/D$ - $D$  (D);  $P$ - $D$  (E);  $V$ - $D$  (F);  $V$ - $W/D$  and  $P$ - $W/D$  (G); and  $W/D$ - $LBC$  (H) (lineal regression parameters and correlation indicated). In all figures (except G and H) black symbols for phragmocone, white for body chamber. Circles for present specimens, triangles for data of Riccardi & Westermann (1991).



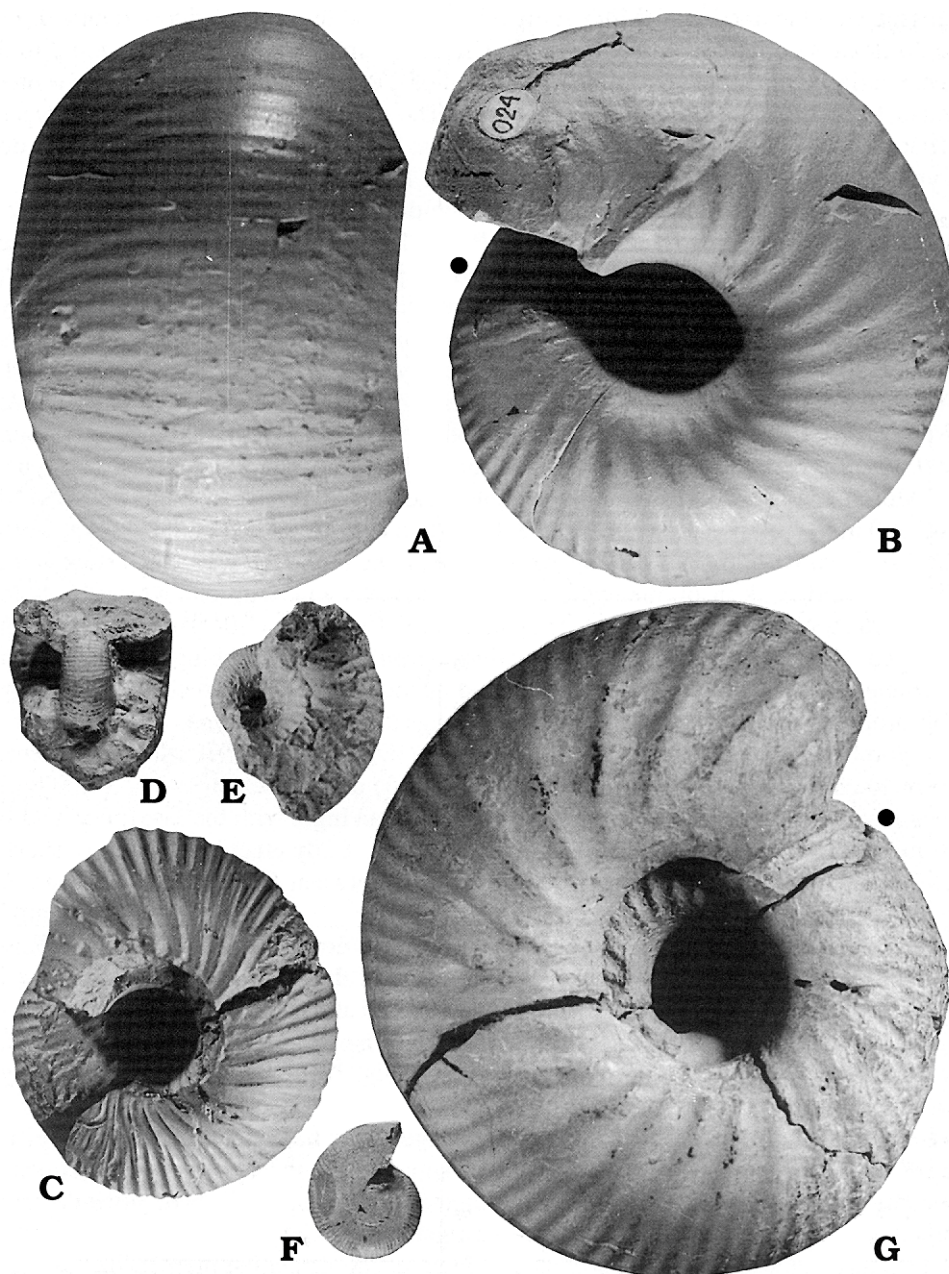


Fig. 19. A–G. *Stehnocephalites gerthi* [M]. A, B. Morph  $\beta$ , complete adult specimen (LPB 024) from bed 15. C. Same specimen at last whorl of phragmocone. D, E. Inner whorls of the same specimen. F. Morph  $\beta$ , inner whorls of a complete adult specimen (LPB 222) from bed 15. G. Morph  $\alpha$ , almost complete adult specimen (LPB 062) from bed 19. All natural size. Point at last septum.

Morph  $\alpha$ . — Medium to large adult specimens, involute and globose ( $W/D = 0.56–0.94$ ) with moderately deep, narrow umbilicus. The whorl section is subelliptical-de-



pressed with the maximum width at the mid-flank, and the venter widely rounded. 13 to 20 flexuose primaries per half-whorl arise at the umbilical wall, divide into 2 to 3 secondaries at mid-flank or on the upper third of the flank, and pass across the venter either transversely or describing a low arch. The holotype and one of the paratypes (Riccardi & Westermann 1991: pl. 20: 1a, b, 2a, b) belong to this morphotype, as do some other specimens (Riccardi & Westermann 1991: pl. 26: 3a, b, 5a, b).

**Morph  $\beta$ .** — Specimens grouped here, including the biggest adults of the sample, are more coarsely ribbed, the primaries ( $P = 8-13$ ) are more distant, swollen on the lower half of the flank or at mid-flank, and projected from the umbilical shoulder; ventrals ( $V = 25-36$ ) are also coarser. Whorl section, umbilicus and involution display the same ranges as in morph  $\alpha$ . Some specimens show the shortest body chambers ( $LBC = 205-260^\circ$ ) in the sample, and are ventrally smooth in the last quarter of whorl. Within the material figured by Riccardi & Westermann (1991), a paratype (Riccardi & Westermann 1991: pl. 21: 1a, b) and some other specimens (Riccardi & Westermann 1991: pl. 22: 1a, b, pl. 23: 3a, b, pl. 25: 1a, b, pl. 26: 4a, b), belong to this morphotype.

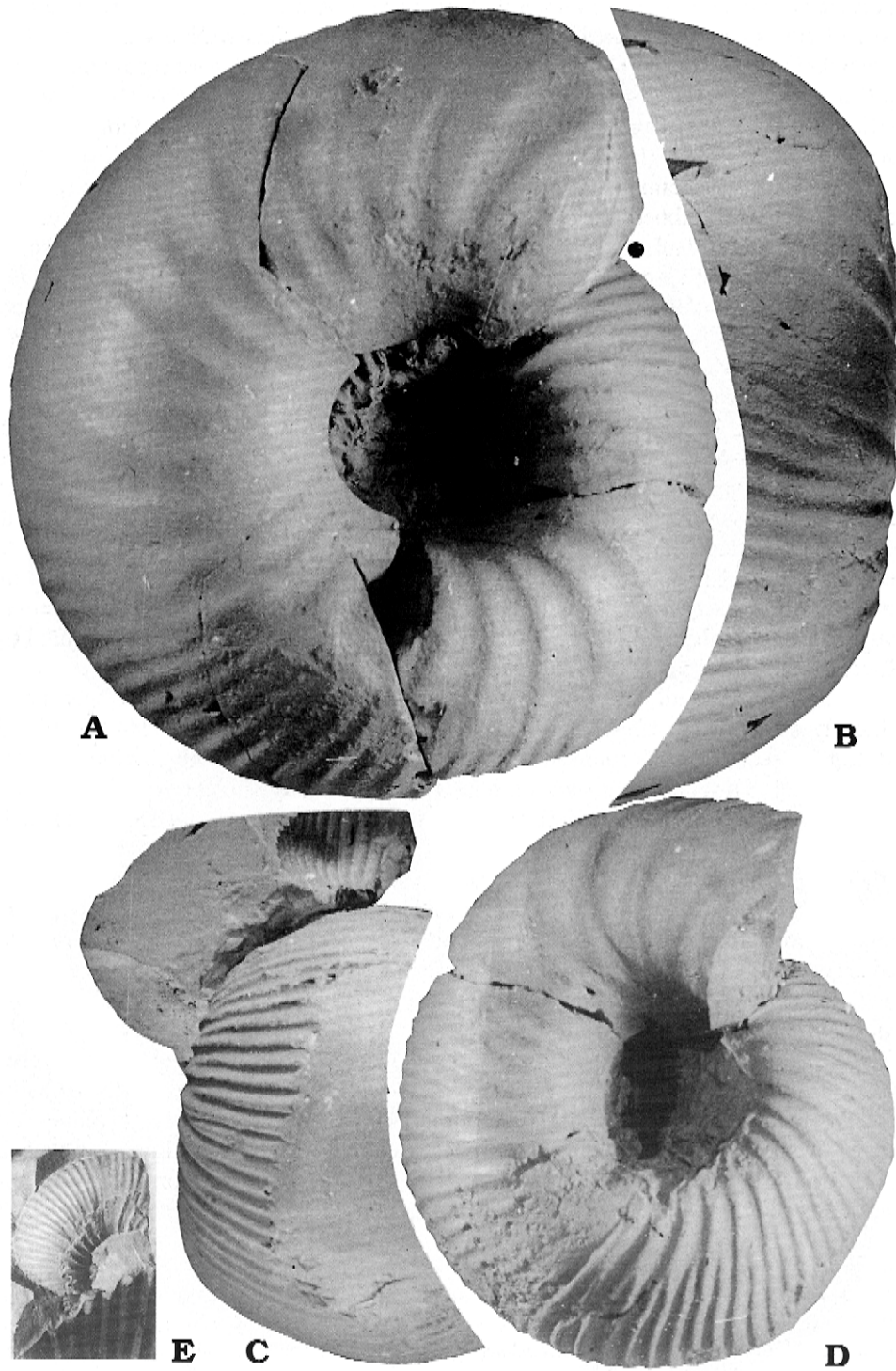
**Morph  $\gamma$ .** — Specimens strongly variable in adult size (diameters range between 40 and 120 mm), compressed ( $W/D = 0.43-0.56$ ) and densely ribbed on the flanks; 13 to 22 fine, flexuose primaries per half whorl arise on the umbilical wall, bend backward, divide at mid-flank or on the upper third of the flanks and, with one intercalatory to each two secondaries, pass transversely across the venter ( $V = 30-50$ ). Whorl section rounded, slightly wider than high. Relative morphology and ribbing remain almost unchanged from about  $D = 8$  mm up to the adult body chamber. A specimen figured by Riccardi & Westermann (1991: pl. 24: 1) belongs to this morphotype.

**Morph  $\delta$ .** — Medium to large, compressed ( $W/D = 0.43-0.56$ ) adult specimens, coarsely and sparsely ribbed on flanks ( $P = 7-13$ ) and venter ( $V = 24-36$ ). Whorl section subrectangular to rounded, slightly wider than high, with the maximum width at mid-flank. Umbilicus narrow to moderately wide. Body chamber relatively short,  $LBC$  about  $230-270^\circ$ . Some specimens intergrade between *S. gerthi* morph  $\gamma$  and *S. crassicosatus*.

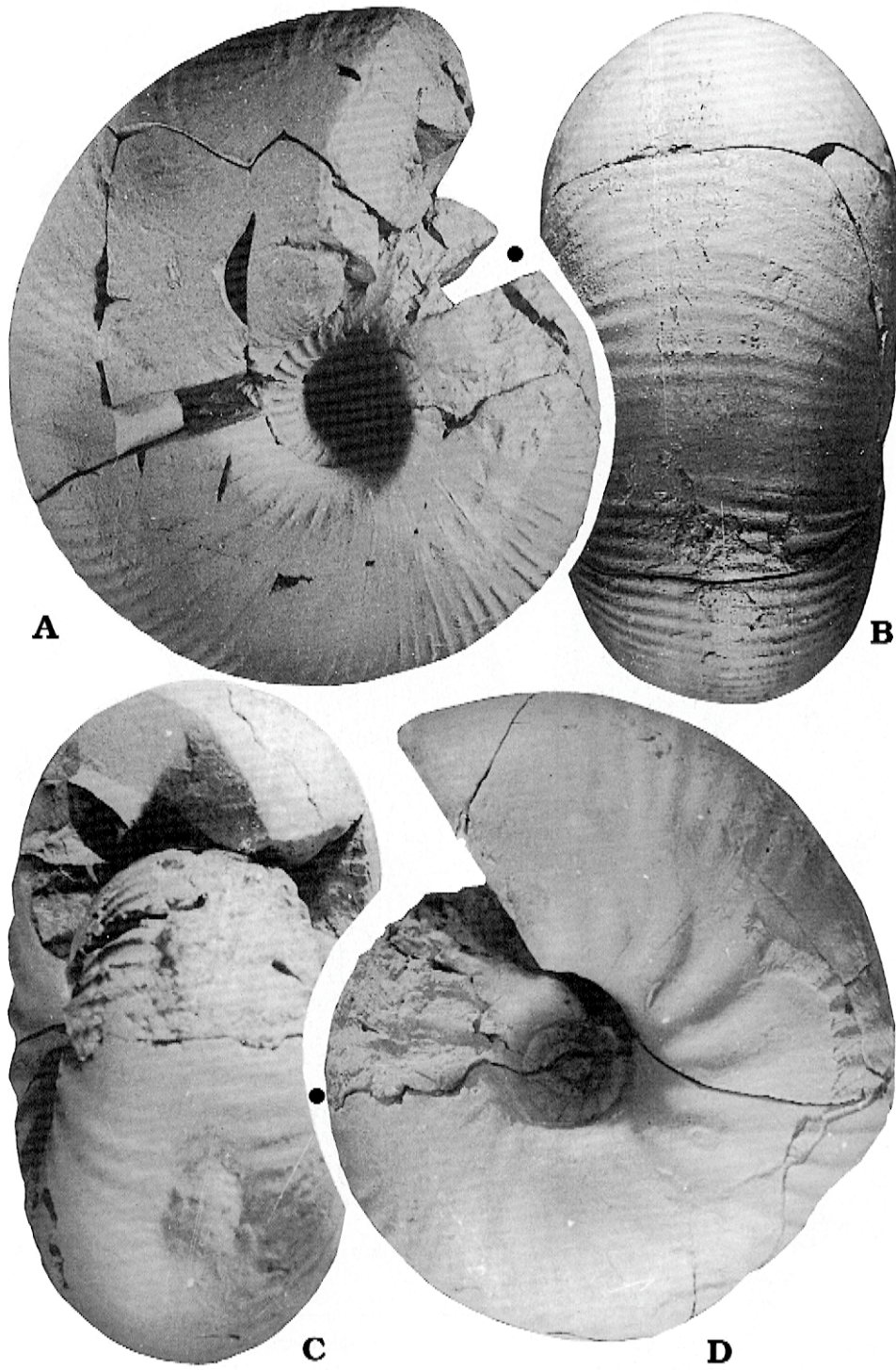
Some of the features that characterise the species dominate the strong individual variability (cf. Riccardi & Westermann 1991: p. 86): the widest and most depressed whorl section and the strongest involution are reached at the end of the adult phragmocone (Fig. 18A–D); the adult body chamber tends to be more compressed and evolute, with primary ribbing tending to become sparser (Fig. 18E) and coarser, fading away on the umbilical shoulder.

**Remarks.** — No significant morphologic changes have been detected in the investigated sampling interval (Fig. 2). Moreover, some of the most depressed specimens contain in their body chambers very compressed and finely ribbed, juvenile and subadult specimens (Fig. 20E). The investigated material is stratigraphically and statistically homogenous, with size and all parameters of relative morphology, involution and ribbing normally distributed (within confidence-limits of 95%) at the adult

Fig. 20. A–E. *Stehnocephalites gerthi* [M]. A, B. Morph  $\alpha$ , complete adult specimen (LPB 258) from bed 25. C, D. Same specimen at last whorl of phragmocone and beginning of body chamber. E. Inner whorl of a compressed and finely ribbed specimen belonging to morph  $\delta$  incorporated in the body chamber of the same specimen. All natural size. Point at the last septum.









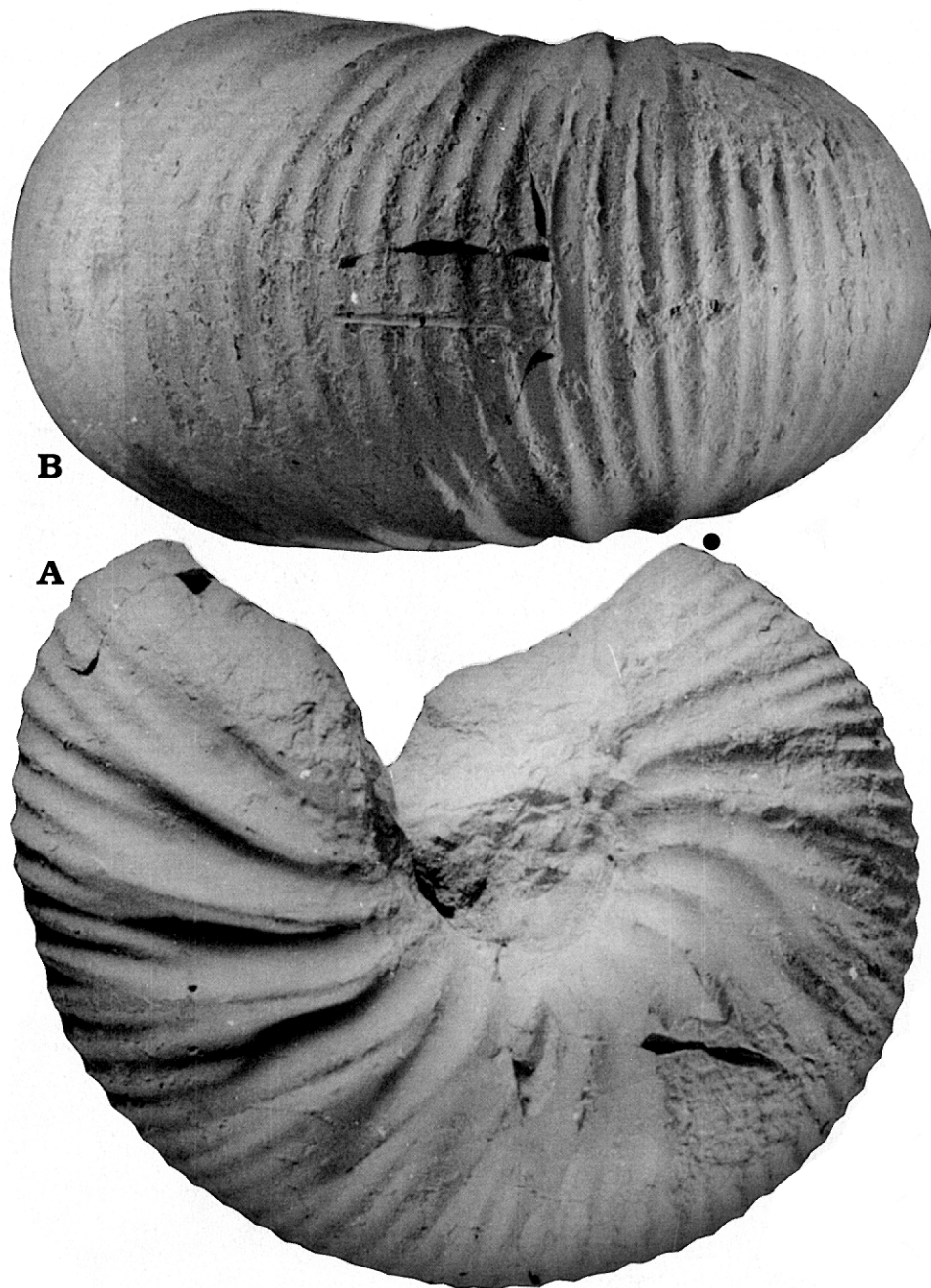


Fig. 22. A, B. *Stehnocephalites gerthi* [M]. Morph  $\alpha$ , complete adult body chamber (LPB 076) from bed 21. All natural size. Point at last septum.

Fig. 21. A–D. *Stehnocephalites gerthi* [M]. A, B. Morph  $\delta$ , complete adult specimen (LPB 226) from bed 22. C, D. Morph  $\gamma$ , complete adult specimen (LPB 363) from bed 11b. All natural size. Point at last septum.

stage, and ranging throughout the inferred range of variation of the species (Table 3:  $R/s = 4.9\text{--}6.8$ ). Thus, the broad range of variation described is considered to represent continuous intraspecific variability within a single species (cf. Riccardi & Westermann 1991), not *polyphenic* (see Procedures and conventions) in the strict sense of the term, covering the reaction norm of the species (*sensu* Stearns 1989: p. 436).  $Dls$  and  $Dp$  are the most variable features (Table 3) in the investigated material; on the contrary, and like in most Eurycephalitinae, variation of  $H_1/D$  between adult individuals and throughout ontogeny is the lowest (Table 3, Fig. 17), suggesting that development of this character is highly canalized (Dommergues *et al.* 1989; Zakharov 1992). Two main sources of variation may be distinguished: (1) individual differences controlled by differential rates of germinal and somatic development (developmental heterochronies) which produce the extremely variable adult size, the juvenile aspect of the compressed finely ribbed specimens (morph  $\gamma$ ) and the high variation of the ontogenetic trajectories of umbilical width (Fig. 18C) and other characters (Fig. 18A–F); and (2) differences related to independence or very low correlation between some characters at the adult stage:  $r(P-V) = 0.580(^*)$ ,  $n = 65$ ;  $r(W/D-V) = 0.117(^{\circ})$ ,  $n = 102$ ;  $r(W-P) = -0.175(^*)$ ,  $n = 120$ ;  $r(W/D-P) = -0.016(^{\circ})$ ,  $n = 120$ ;  $r(W-U) = 0.637(^*)$ ,  $n = 118$ . These two sources of individual variation act in combination, resulting in high levels of developmental plasticity (*sensu* Zakharov 1992), which, in small samples of adult individuals, is seen as a mosaic of morphotypes.

Table 3. *Stehnocephalites gerthi*: statistical measurements at or near peristome for the sample of adult macroconch specimens morphs  $\alpha$ ,  $\beta$ ,  $\gamma$ , and  $\delta$ . For abbreviations see pp. 74–75.

	<i>n</i>	<i>m</i>	<i>CV</i>	<i>RO</i>	<i>R/s</i>	<i>Ho</i>
<i>Dp</i> [mm]	125	87.98	19.9	36.99–134.48	5.6	0.094(^)
<i>Dls</i> [mm]	65	64.84	24.1	27.00–106.50	5.1	0.044(^)
<i>W/D</i>	125	0.59	12.4	0.44–0.94	6.8	0.054(^)
<i>H<sub>1</sub>/D</i>	119	0.43	7.3	0.37–0.53	5.1	0.071(^)
<i>U/D</i>	125	0.22	15.9	0.13–0.30	4.9	0.058(^)
<i>H<sub>2</sub>/D</i>	91	0.25	11.1	0.17–0.33	5.8	0.101(^)
<i>W/H<sub>1</sub></i>	116	1.38	14.1	0.95–2.17	6.3	0.216(^)
<i>H<sub>2</sub>/H<sub>1</sub></i>	91	0.58	12.3	0.38–0.79	5.8	0.052(^)
<i>P</i>	123	13	19.0	8–21	5.3	0.073(^)
<i>V</i>	102	35	14.2	24–50	5.2	0.046(^)
<i>LBC</i> [°]	90	262	9.5	205–385	7.2	0.118(^)

Compressed specimens (morphs  $\gamma$  and  $\delta$ ) largely predominate in shaly limestones, whilst the more globose and depressed ones (morphs  $\alpha$  and  $\beta$ ) predominate in shales. The ontogeny of several specimens, especially the more globose and depressed ones, shows strong morphological changes, perhaps related to shifts in the mode of life into different niches in the course of development (cf. Donovan 1987; Landman 1987).



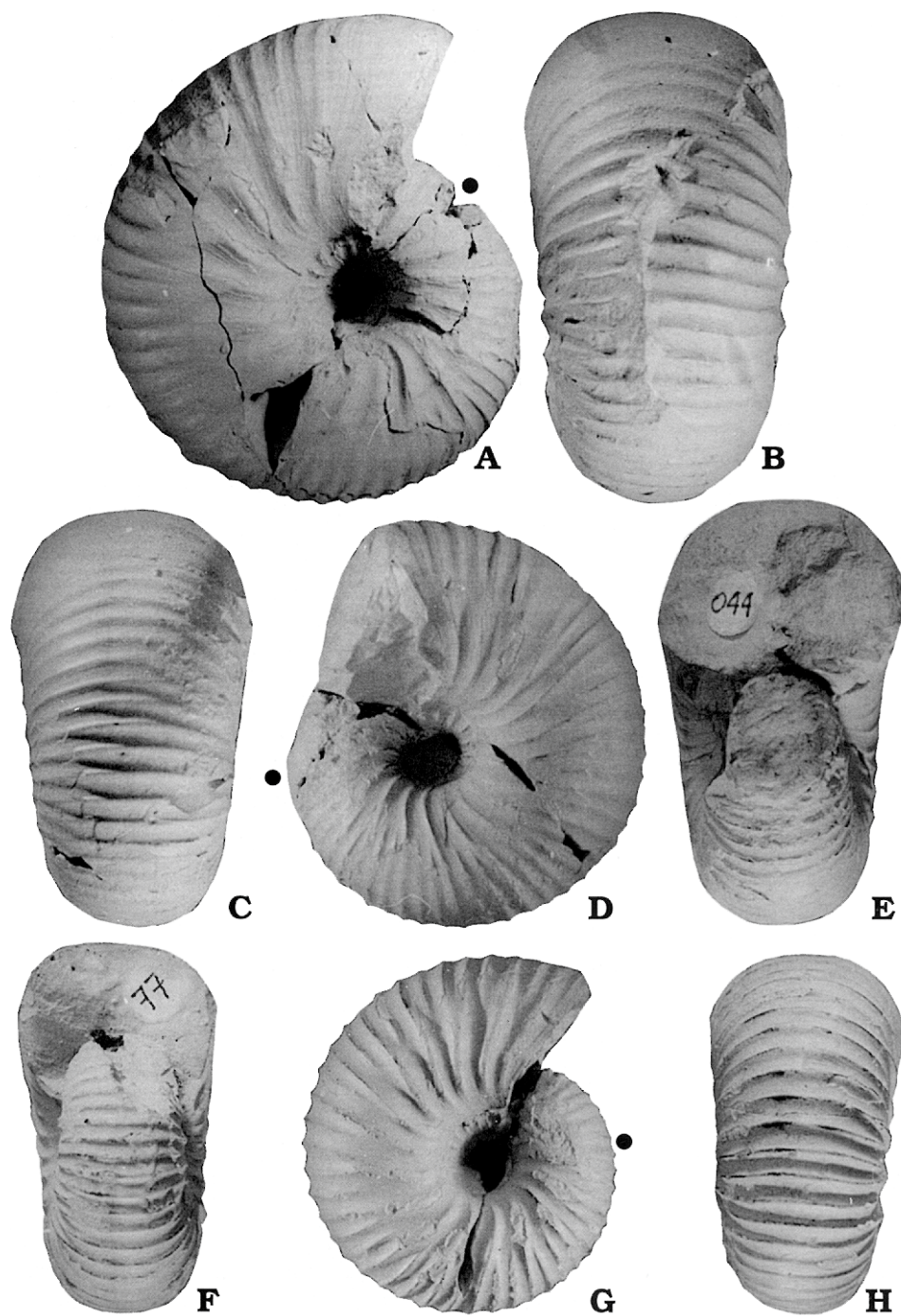


Fig. 23. A–E. *Stehnocephalites gerthi* [M] morph  $\delta$ , complete adult specimens; LPB 336 (A, B), LPB 044 (C–E) from bed 15. F–H. *Xenocephalites* sp. A [m], complete adult specimen (LPB 077) from bed 15. All natural size. Point at last septum.



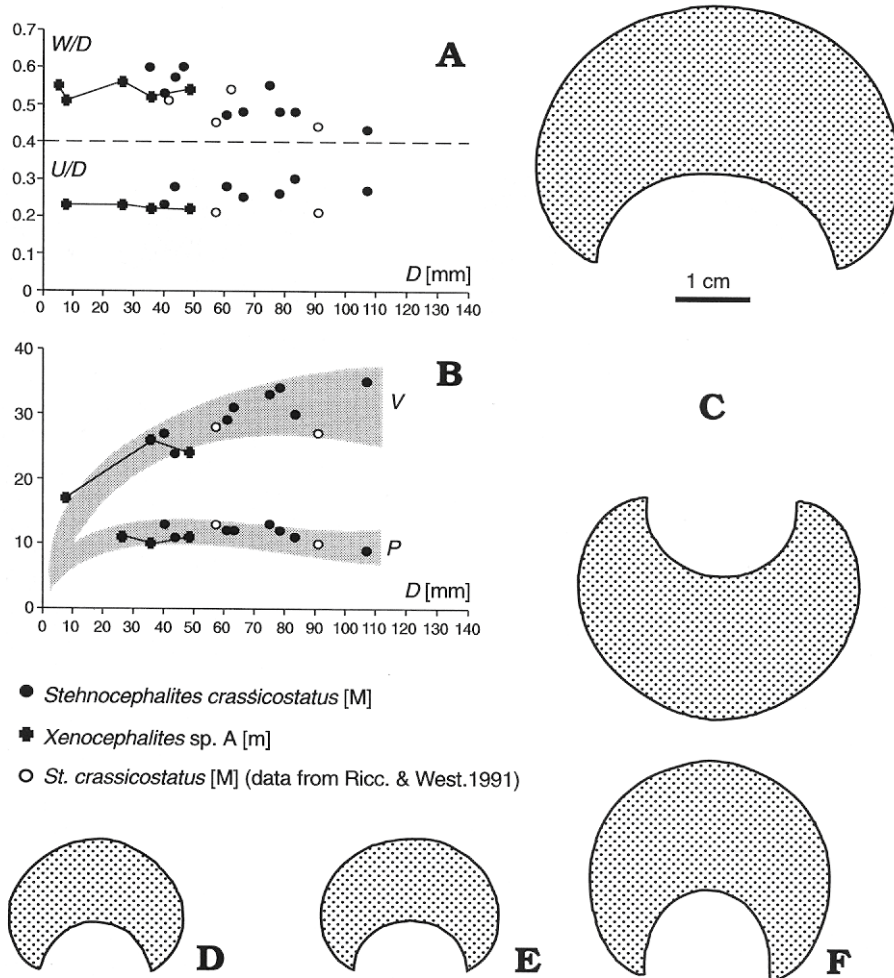


Fig. 24. *Stehnocephalites crassicosatus* [M] and *Xenocephalites* sp. A [m]. Scatter diagrams and cross sections through phragmocone and body chamber (stippled).  $W/D$ - $D$  and  $U/D$ - $D$  (A);  $P$ - $D$  and  $V$ - $D$  (B); LPB 007 (C); LPB 333 at  $D = 40$  mm (D); LPB 006 at  $D = 67$  mm (E, F).

The specimens described by Riccardi & Westermann (1991) as *Stehnocephalites* sp. A fall into the range of variability here assigned to *S. gerthi*; inner whorls of comparable specimens are those of morph  $\beta$  in the present sample.

Sexual dimorphism remains problematic. The smallest adult individuals included in morph  $\gamma$  could be considered progenetic microconchs, but there is no morphological discontinuity between them and the bigger specimens, and they do not exhibit the standard microconch adult characters. On the contrary, ribbing at the end of their shells tends to fade away or remains unchanged. Thus, they may be interpreted as progenetic macroconch variants. The most depressed specimens of *Xenocephalites neuquensis*, morph  $\alpha$  here below, which occur at the *S. gerthi* horizon (uppermost Steinmanni

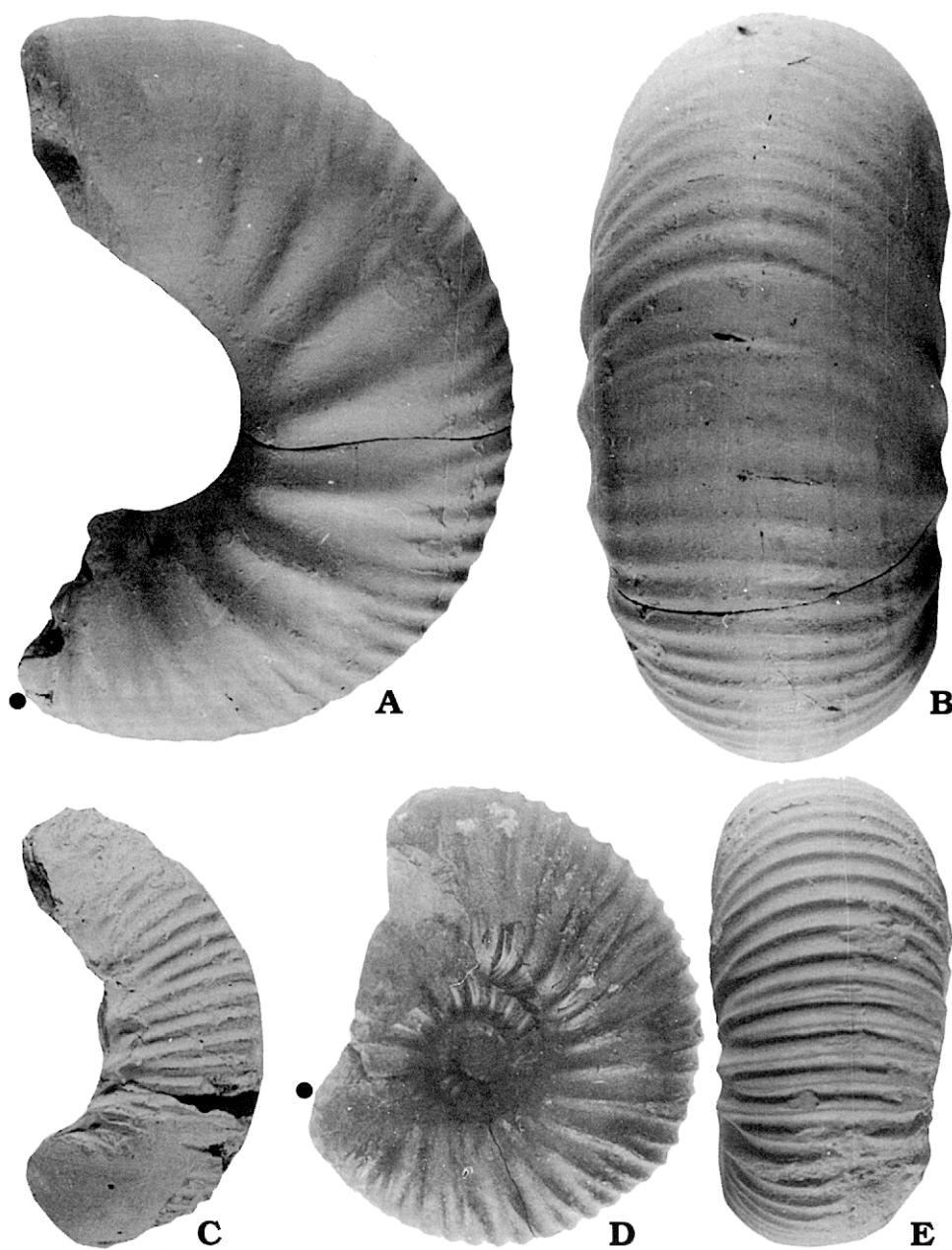


Fig. 25. A–E. *Stehnocephalites crassicosatus* [M]. A, B. Complete adult body chamber (LPB 007) from bed 13. C. Same specimen remains of last whorl of the phragmocone. D, E. Complete adult specimen (LPB 006) loose from bed 19. All natural size. Point at last septum.

Zone), and stand closest to the lectotype, could be microconchs of *S. gerthi* morphs  $\alpha$  and  $\beta$ , whereas the specimen described below as *Xenocephalites* sp. A could represent

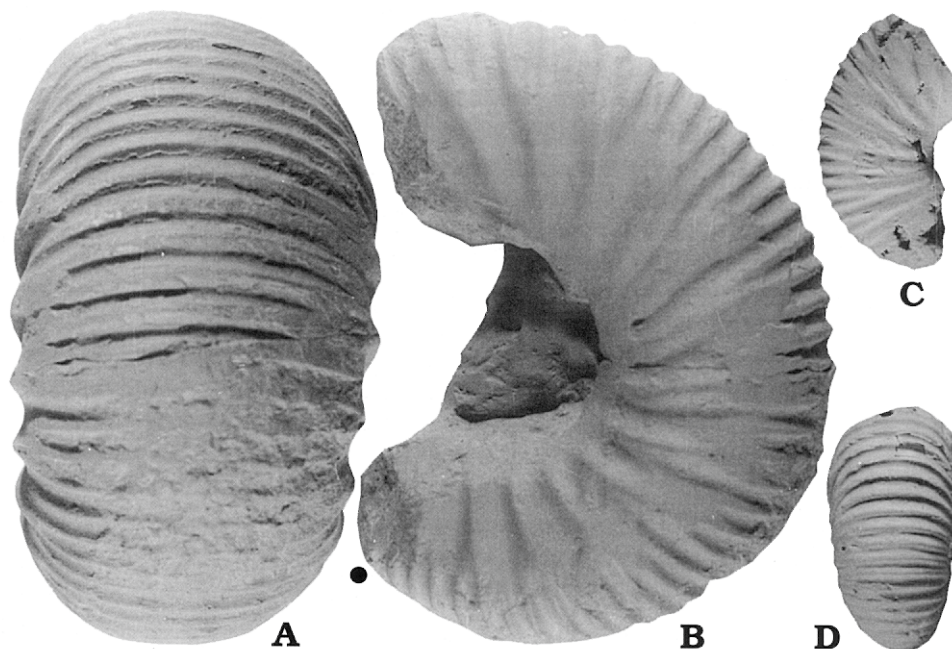


Fig. 26. A–D. *Stehnocephalites crassicosatus* [M]. A, B. Complete adult body chamber (LPB 004) from bed 13. C, D. Incomplete juvenile body chamber (LPB 333/1) loose from bed 19. All natural size. Point at last septum.

microconch of morphs  $\gamma$  and  $\delta$ , taking into account the morphologic similarity of the inner whorls and the stratigraphic position of the samples.

*Stehnocephalites crassicosatus* Riccardi & Westermann, 1991 [M]

Figs 24A–F, 25A–E, 26A–D; App. 1.

**Material.** — Three adult body chambers (LPB 004, 007, 331) from bed 13, 1 complete adult specimen (LPB 006) loose from bed 19, 1 adult and 1 juvenile body chambers (LPB 333/1, 333/2) loose from bed 19 and 2 incomplete adult body chambers (LPB 008, 009) from the base of bed 27.

**Description.** — Phragmocone at  $D = 8$ – $10$  mm shows rounded whorl section and dense, fine, transverse ventral ribbing. Septate whorls from  $10$ – $70$  mm diameter evolute ( $H_2/H_1 = 0.55$ – $0.70$ ) with moderately open umbilicus ( $U/D = 0.23$ – $0.28$ ); whorl section rounded to subrectangular-depressed ( $W/H_1 = 1.17$ – $1.38$ ) with rounded umbilical shoulder, flattish to convex flanks and slightly rounded venter. Eleven to thirteen primary ribs arise at the umbilical seam, describe a backward bend on the umbilical shoulder up to about the lower half of the flank, where they bifurcate or more rarely trifurcate, curve backward and, with sparse intercalatories, pass transversely across the venter. Adult phragmocone reaches  $45$  to  $75$  mm in diameter.

Adult body chamber  $200$ – $220^\circ$ , slightly uncoiled ( $U/D = 0.25$ – $0.30$ ) and compressed towards the peristome. Whorl section depressed, subelliptical to subrounded, with flanks slightly convex and venter rounded. Nine to twelve prominent blade-like,



projected to slightly flexuous primaries arise on the umbilical shoulder and bifurcate (rarely trifurcate) on the upper third of the flank; secondaries and 1 intercalatory to each 3–4 secondaries pass across the venter describing a convex arch. Ribbing reaches the peristome, which is simple and slightly contracted. Septal sutures are not preserved.

**Remarks.** — Variation in the present sample is broad, encompassing morphologies and adult sizes intermediate between the two extreme morphotypes figured by Riccardi & Westermann (1991: pl. 26: 1a–2b). The phragmocone does not seem to differ from that of the most compressed specimens of *S. gerthi*. All of the present specimens seem to be macroconchs of a single species, in some cases hard to separate from the most compressed and coarsely ribbed *Stehnocephalites gerthi* [M], morph  $\delta$ . The systematic relationships and taxonomy of two lineages (*S. gerthi* and *S. crassicosatus*) evolving during almost the same interval in the same area is open to discussion; most probably they belong to a single, highly variable species. The specimen described below as *Xenocephalites* sp. A could be the associated microconch; it shows inner whorls almost identical with those of *S. crassicosatus* at comparable diameters (see Remarks under *S. gerthi*).

Should these presumptions be proven by comparisons between the known material and new well preserved microconchs, the genus *Stehnocephalites* Riccardi, Westermann, & Elmi, 1989 would comprise a single species, *S. gerthi* (Spath, 1928) [M&m], the macroconch including *S. crassicosatus* [M] as an extreme variant, and the microconch including some forms here provisionally assigned to *Xenocephalites neuquensis* [m] morph  $\alpha$  and X. sp. A [m].

### Genus *Lilloettia* Crickmay, 1930

Type species: *Lilloettia lilloettensis* Crickmay, 1930 by original designation.

Age: late Bathonian–early Callovian.

#### *Lilloettia steinmanni* (Spath, 1928) [M]

Figs 27A, B, 28F, 33A–D; App. 1.

\* *Lilloettia steinmanni* (Spath, 1928); Riccardi & Westermann 1991: p. 52, pl. 9: 1 (lectotype)–4; pl. 10: 1–3; pl. 11: 1. [for synonymy].

**Material.** — One almost complete adult specimen (LPB 085) and 1 juvenile (LPB 085/1) from bed 2; three almost complete adult specimens (LPB 040, 082, 084) from bed 12, one juvenile body chamber (LPB 263) from bed 12; one complete adult specimen (LPB 220) loose from bed 12?, and one complete adult (LPB 074) from bed 13.

**Remarks.** — The present specimens are typical representatives of the species; they clearly match the morphotypes from Chacay Melehué and Lonquimay figured by Riccardi & Westermann (1991: pl. 9: 3, 4a, b). The specimen LPB 085 shows globose, smooth innermost whorls ( $D = 2.90$  mm) with subcircular whorl section and a broad convex venter; umbilicus wide ( $U/D = 0.26$ ) and deep with subvertical walls and rounded shoulder.

Despite the strong differences that exist between the subadult and adult whorls of *L. steinmanni* (Spath, 1928), *S. gerthi* (Spath, 1928), and *Eurycephalites gottschei* (Tornquist, 1898), the inner whorls of these three species are almost indistinguishable at diameters of 15–20 mm.

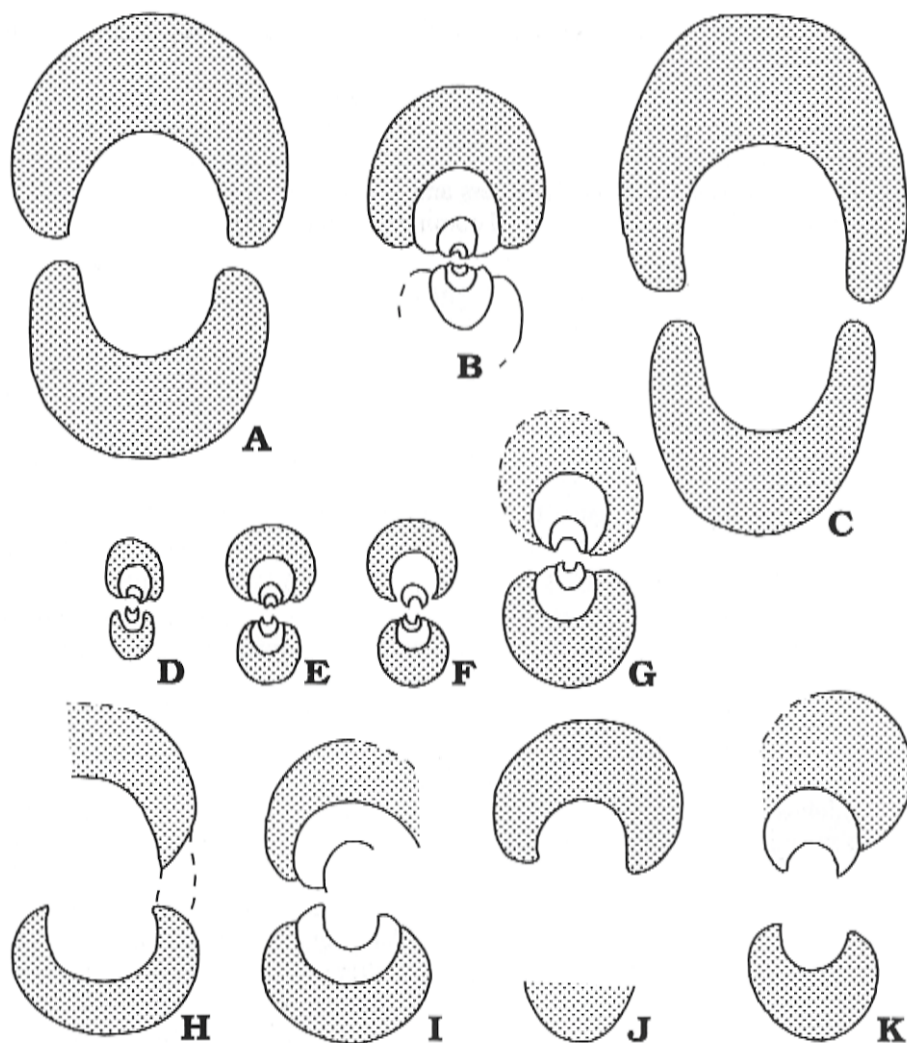


Fig. 27. Cross sections through phragmocone and body chamber (stippled),  $\times 1$  unless otherwise indicated. **A, B.** *Lilloettia steinmanni* [M], complete adult specimens: LPB 040 (**A**), LPB 074 (**B**). **C.** *Eurycephalites* aff. *gottschei* [M], adult specimen (LPB 261). **D–G.** *Eurycephalites rotundus* [M&m]. **D, F–G.** Complete juvenile macroconchs: LPB 090/3 (**D**), LPB 090/4 (**F**);  $\times 2$ , LPB 090/1 (**G**). **E.** Complete adult microconch (LPB 090/9,  $\times 2$ ). **H.** *Xenocephalites neuquensis* [m] morph  $\alpha$  (LPB 081). **I.** *X.* aff. *neuquensis* [m] (LPB 078). **J.** *X.* cf. *araucaus* [m] (LPB 069). **K.** *Xenocephalites* sp. A [m] (LPB 077).

### Genus *Eurycephalites* Spath, 1928

Type species: *Macrocephalites vergarensis* Burckhardt, 1903, by original designation (= *M. gottschei* Tornquist, 1898, subj.: Parent 1997).

**Diagnosis.** — Dimorphic. Shell globose, slightly compressed to depressed with sub-quadratic to ovate whorl section; involute to occluded umbilicus with rounded slope and shoulder. Slightly flexuous projected primaries dividing on flanks into 2 or 3 secondaries which pass across the venter without interruption. In the macroconchs ribbing

fading away progressively from the inner flanks to the venter on body chamber; in the microconchs becoming sparse and prominent.

**Remarks.** — Some of the microconchs are retained for the time being in the genus *Xenocephalites* Spath, 1928. These two genera were defined at the same time, so if they are to be united, the choice of senior synonym is arbitrary. The macroconch is preferable because it is richer in characters and is hence more precisely interpretable chronologically (J.H. Callomon personal communication 1995).

Age: early Callovian–early (middle?) Oxfordian.

*Eurycephalites gottschei* (Tornquist, 1898) [M&m]

Figs 28A–D, 29A–D, 33A–D.

? *Imlayoceras? extremum* (Tornquist, 1898); Sandoval *et al.* 1990: p. 127, pl. 8: 1.

*Eurycephalites vergarensis* (Burckhardt, 1903) [M]; Riccardi & Westermann 1991: pp. 36–43, pls 1, 2. [for synonymy].

\* *Xenocephalites gottschei* (Tornquist, 1898) [m]; Riccardi & Westermann 1991: pp. 76–78, pl. 17: 3–6. [for synonymy].

*Eurycephalites gottschei* (Tornquist, 1898) [M&m]; Parent 1997: p. 416, fig. 6.

**Material.** — ?one almost complete adult macroconch (LPB 274) from bed 28; and 2 complete adult microconchs (LPB 013, 014) from bed 25.

**Remarks.** — The species was extensively described and discussed by Riccardi & Westermann (1991) and Parent (1997); here only new specimens which add some information on the species are described.

A big adult macroconch (Fig. 28A–D) is tentatively included in this species by the style of the ventral ribbing and incipient perumbilical fading of the primary ribs throughout the last half of the body chamber, but differs from typical *E. gottschei* [M] in the more globose and involute phragmocone and larger final adult size. Four morphological stages may be distinguished during ontogeny: From 10–25 mm diameter the shell is globose, involute with narrow umbilicus and depressed, rounded whorl section; ribbing fine and dense. At diameters of 30–50 mm the shell becomes somewhat more compressed and the primary ribs stronger. From about 50 mm diameter and up to the end of the adult phragmocone, about  $Dls = 90$  mm, the shell is extremely inflated with very narrow umbilicus and circular whorl section; the primary ribs are flexuous on the inner half of the flanks and bifurcate at the middle, passing transversely across the venter. Adult body chamber ( $D = 90$ –114 mm,  $LBC = 300$ –360°) extremely involute and closely umbilicate ( $U/D = 0.04$ ) egressing slightly at the peristome; it shows a wide, shallow pre-peristomatic constriction. It differs from *E. extremus* (Tornquist, 1898) [M] only in the body chamber, which is, in the present specimen, more compressed, narrowly umbilicate and sparsely ribbed. Moreover, it comes from beds of the Gottschei Zone, and *E. extremus* (Tornquist, 1898) occurs at the upper part of the Bodenbenderi Zone. The macroconch specimen figured by Sandoval *et al.* (1990: pl. 8: 1) as *Imlayoceras? extremum* (Tornquist, 1898), has characters in common with the present specimen, and may be closely compared with it.

The two microconchs (Fig. 29A–D) are compressed evolute variants; they have been extracted from the body chamber of an adult *S. gerthi* morph  $\beta$  (LPB 258) from bed 25, at the top of the *S. gerthi* horizon, upper Steinmanni Zone, which suggests that they could represent the microconchs of an early transient of *E. gottschei* such as *E. aff. gottschei* [M] as described below.



*Eurycephalites* aff. *gottschei* (Tornquist, 1898) [M]

Figs 27C, 28E; App. 1.

**Material.** — Four adult body chambers with incomplete phragmocone (LPB 260–262, 284), and 3 minute, well preserved juveniles (LPB 284/1–3) from bed 24.

**Description.** — The 3 juveniles, extracted from the body chamber of an adult (LPB 284) and ranging from 7–20 mm in diameter, are involute, with subcircular to depressed ovate whorl section; the umbilicus is narrow with rounded shoulder and vertical wall. Ten fine, flexuous primaries arise at the umbilical wall and bifurcate at mid-flank; about 20 secondaries and a few intercalatories pass across the venter unchanged.

Adult body chambers involute, with subrectangular to ovate whorl section, slightly convex flanks, and broadly convex venter. Umbilicus narrow with rounded shoulder and subvertical walls. Primary ribs flexuous and more or less prominent and acute on the phragmocone, with the point of bifurcation at mid-flank; throughout the last half of the body chamber there are about 14 primaries which fade away perumbilically, and 33–35 blunt ventrals which become coarser on the venter. Two specimens (LPB 220, 261) show very fine pre-peristomatic growth lines and a shallow lateral constriction followed by a slightly expanded peristome.

**Remarks.** — Adult size and ribbing of the 4 adult body chambers are intermediate between *L. steinmanni* and *E. gottschei*, but whorl section and umbilicus best match the latter. However, the stratigraphic position of the present specimens is immediately below beds containing undoubted *E. gottschei* [M&m] and above the uppermost occurrence of *L. steinmanni*; they should thus represent an intermediate form (transient) between these two species. Moreover, the present specimens show the ontogenetic pattern of migration of the point of bifurcation of the primaries, from the lower to the mid-third of the flanks, that in *E. gottschei* [M&m] is associated with expansion of the width of whorl section from about diameters of 12 mm. This pattern has been observed in *Stehnocephalites gerthi*, but not in *Lilloettia*.

*Eurycephalites rotundus* (Tornquist, 1898) [M&m]

Figs 27D–G, 28E–K, 33A–D.

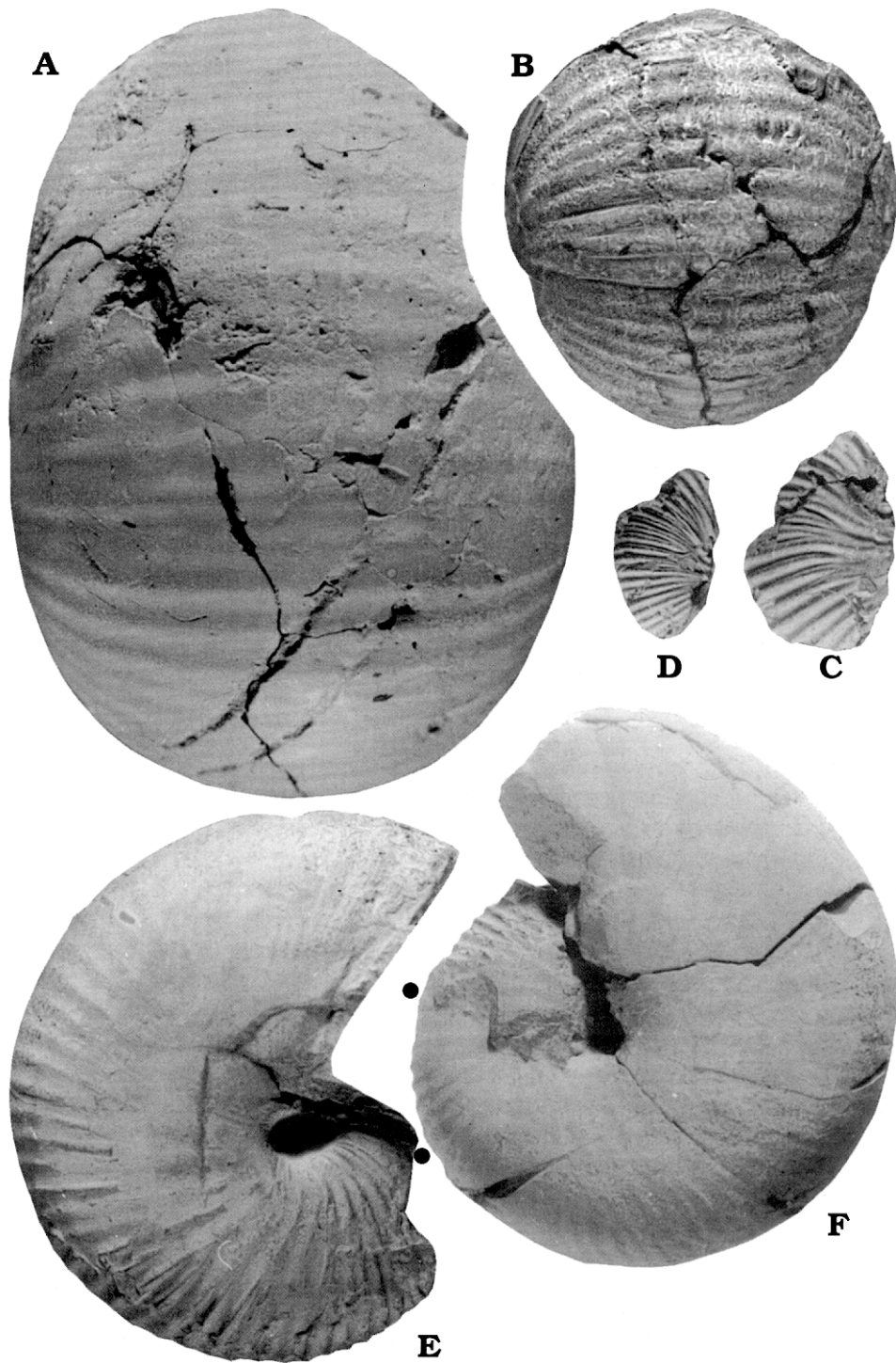
\* *Sphaeroceras rotundum* Tornquist 1898: p. 49(181), pl. 6: 1 (lectotype)–4.

\* *Eurycephalites rotundus* (Tornquist, 1898); Riccardi & Westermann 1991: p. 43, pl. 4: 2 (lectotype)–4; pl. 5: 1, 2; pl. 6: 1–4; pl. 7: 1, 2. [for synonymy].

**Material.** — Three samples extracted from concretions containing several juvenile and subadult macroconchs and 2 adult microconchs (LPB 090/1–11, LPB 386/1–8 and LPB 212–217) from bed 29; 1 subadult body chamber (LPB 337) loose from bed 29.

**Description.** — Macroconch: At about 2 mm in diameter shell is smooth, evolute ( $H_2/H_1 = 0.72$ ), and widely umbilicate ( $U/D = 0.28$ ). Whorl section ovate-depressed ( $W/H_1 = 1.80$ ) with the maximum width at mid-flank; venter broad and convex; umbilical shoulder rounded, passing into inclined umbilical wall. At 2–10 mm

Fig. 28. **A.** *Eurycephalites gottschei*? [M], body chamber of an almost complete adult specimen (LPB 274) from bed 28. **B–D.** Successive inner whorls of the same specimen. **E.** *Eurycephalites* aff. *gottschei* [M], complete adult specimen (LPB 260) from bed 24. **F.** *Lilloettia steinmanni* [M], complete adult specimen (LPB 220) loose from bed 12. All natural size. Point at last septum.





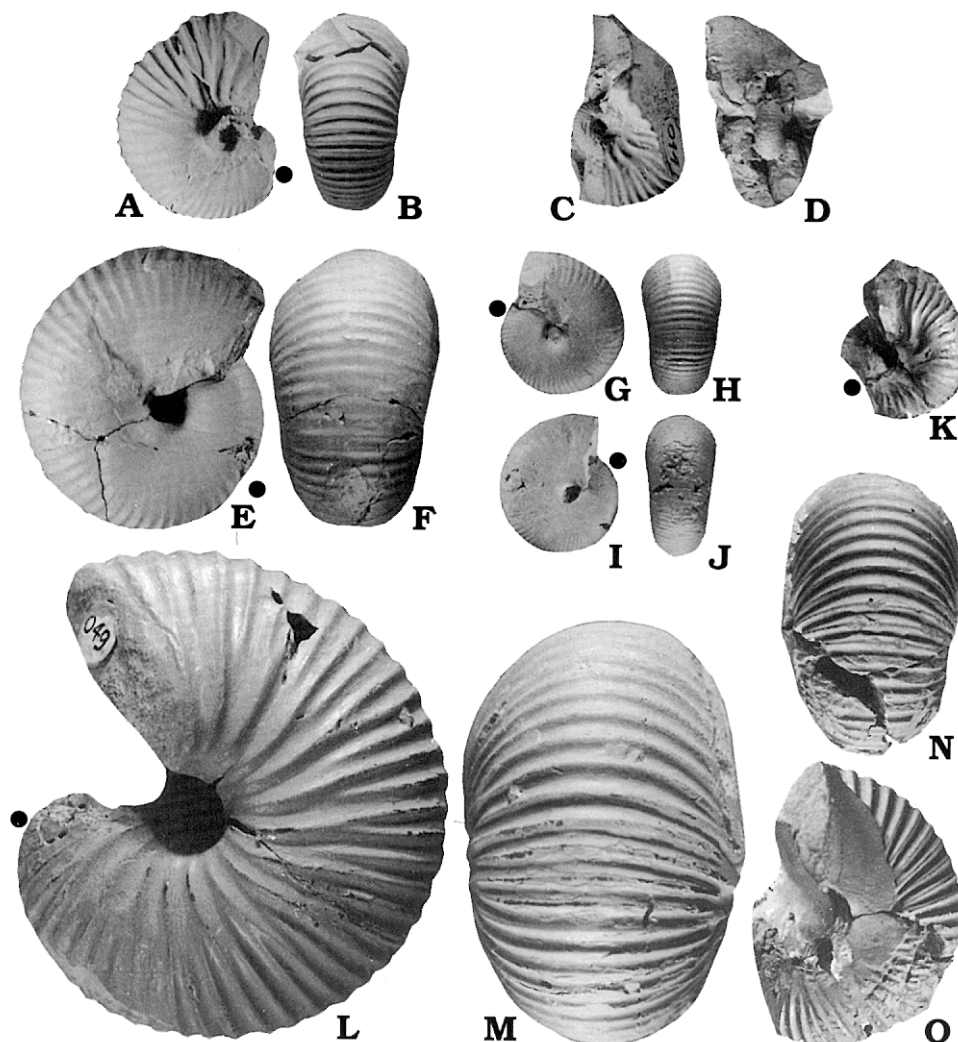


Fig. 29. A–D. *Eurycephalites gottschei* [m], complete adult specimens from bed 25: LPB 013 (A, B), LPB 014 showing inner whorls (C, D). E–J. *Eurycephalites rotundus* [M], complete juvenile macroconchs from bed 29 LPB 090/1 (E, F), LPB 090/3 (G, H), LPB 090/4 (I, J). K. *Eurycephalites rotundus* [m], adult specimen (LPB 090/9) from bed 29. L, M. *Eurycephalites involutus* [M], body chamber of an adult specimen (LPB 049) from bed 29. N, O. Last whorl of phragmocone of the same specimen. All natural size. Point at last septum.

diameter shell becomes much more compressed ( $W/H_1 = 1.06–1.16$ ) and involute ( $U/D = 0.15–0.20$ ), whorl section subovate-compressed with high, almost flat to slightly convex flanks, and rounded, somewhat narrow venter. At about 6 mm diameter some specimens are completely smooth, other show 6–10 irregular feeble primaries which bifurcate or trifurcate at mid-flank with a backward bend; ventral ribs pass transversely across the venter, being stronger than the primaries. From 10–12 mm diameter shell



becomes progressively more inflated ( $W/H_l = 1.17\text{--}1.30$ ) with subovate to subcircular whorl section. The umbilicus progressively decreases in width towards the adult stage ( $U/D = 0.13\text{--}0.10$ ). Some specimens are very faintly ribbed at this size, others have flanks almost smooth and venter showing dense, fine secondaries. At 30 mm diameter shell moderately globose and involute, flanks smooth or with fine growth lines, and venter regularly ribbed with 35–40 ventrals per half whorl. The adult morphology and ribbing are fully described in Riccardi & Westermann (1991: pp. 44–48).

**Microconch:** Adult size  $D = 22\text{--}24$  mm. Phragmocone identical to that of the macroconch at comparable diameters. Adult body chamber shows typical microconch features, fully ribbed with 5–6 strong, flexuous primaries which bifurcate on the lower third of the flank or at mid-flank, 18–20 ventral ribs pass transversely across the venter, and the umbilicus enlarges slightly ( $U/D = 0.15$ ) in the last half of adult body chamber. Adult body chamber about  $360^\circ$ .

**Remarks.** — The juvenile phragmocone of *E. rotundus* (Tornquist, 1898) differs at diameters of less than 15 mm from those of *E. gottschei* (Tornquist, 1898) and *E. extremus* (Tornquist, 1898), the ancestral and descendant species, respectively (Riccardi & Westermann 1991), only in having smooth or very feebly ribbed flanks, whereas the other two species always develop fine flexuous primaries. The whorl section and umbilicus of these three species, although variable throughout ontogeny, are almost indistinguishable, following the same ontogenetic trajectories (Fig. 33). Both sexual dimorphs of *E. rotundus* show identical phragmocones, but strongly differ in the smaller adult size and stronger lateral costation of the microconch compared to the macroconch; the microconch, treated in isolation, should be included in the morphogenus *Xenocephalites* Spath, 1928. *E. rotundus* [m] is smaller and more involute than *E. gottschei* [m].

*Eurycephalites involutus* (Riccardi & Westermann, 1991) [M]

Figs 29L–O, 30A–C, F; App. 1.

\* *Xenocephalites?* *involutus* nov. sp.; Riccardi & Westermann 1991: pp. 81, 82, pl. 19: 3a, b, 4a, b.

**Material.** — One complete adult specimen (LPB 049) from bed 29.

**Description.** — Adult size, morphology and ribbing of the body chamber fall into the ranges of the sample of Riccardi & Westermann (1991: p. 82, pl. 19: 3a, b, 4a, b), including the holotype, with which it shows the closest resemblance. Phragmocone involute with high-ovate, ventrally narrow whorl section with maximum width on lower third of flank. Ten high, flexuous primaries bifurcate on the inner third of the flank; coarse secondaries with 1 intercalatory to each pair, pass across the venter describing an adapical arch; ventral ribs are more prominent than primaries.

**Remarks.** — The dense, flexuous primaries which do not become modified on the adult body chamber, the narrow umbilicus, and the very tight coiling up to the aperture determine the inclusion of this species in *Eurycephalites* Spath, 1928 rather than in *Xenocephalites* Spath, 1928, which groups forms that are strongly variocostate (densicostate on the phragmocone, crassicostate on the body chamber) and egressive at the end of the body chamber. The best resemblance is with the septate whorls of *E. extremus* (Tornquist, 1898) [M] from which it differs significantly only in the smaller adult size and, at comparable diameters, in the more compressed whorl section (Fig. 30A, D–F). *E. involutus* [M] could be an early transient or a small, compressed variant

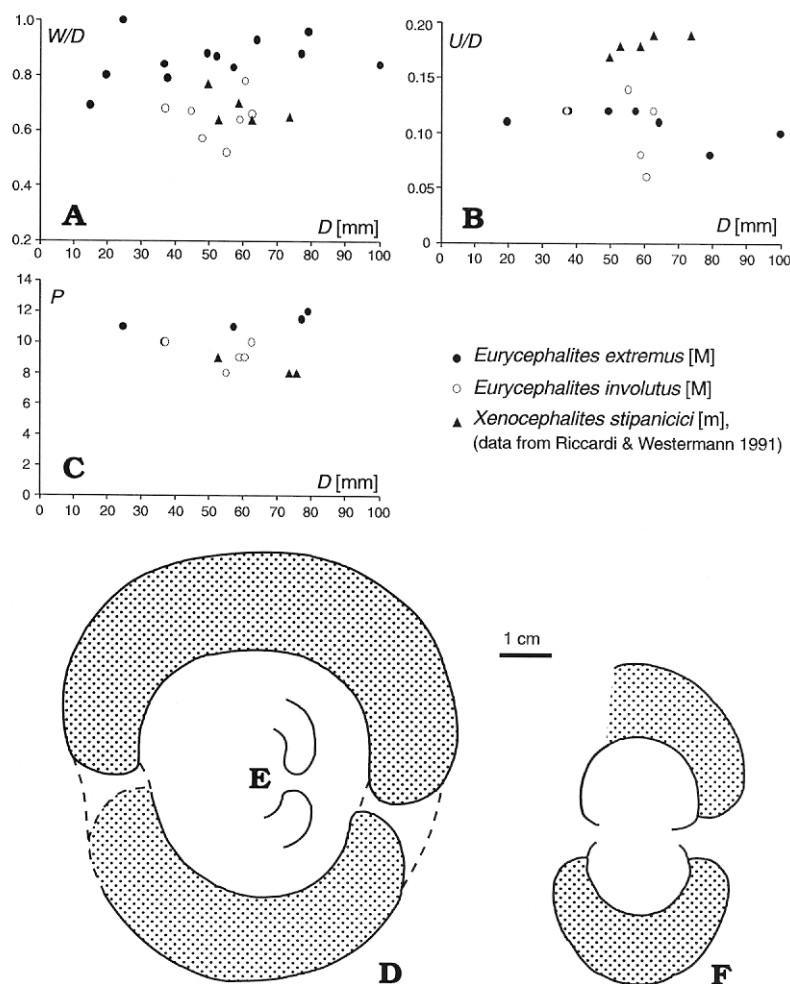


Fig. 30. Scatter diagrams and cross sections through phragmocone and body chamber (stippled): W/D-D (A), U/D-D (B), P-D (C). D, E. *Eurycephalites extremus* [M] (LPB 098, adult; LPB 297, juvenile body chamber). F. *Eurycephalites involutus* [M] (LPB 049, adult).

of *E. extremus* [M] since they occur associated in the same beds at Chacay Melehué (Fig. 2) and Vega de la Veranada (Riccardi & Westermann 1991: p. 13).

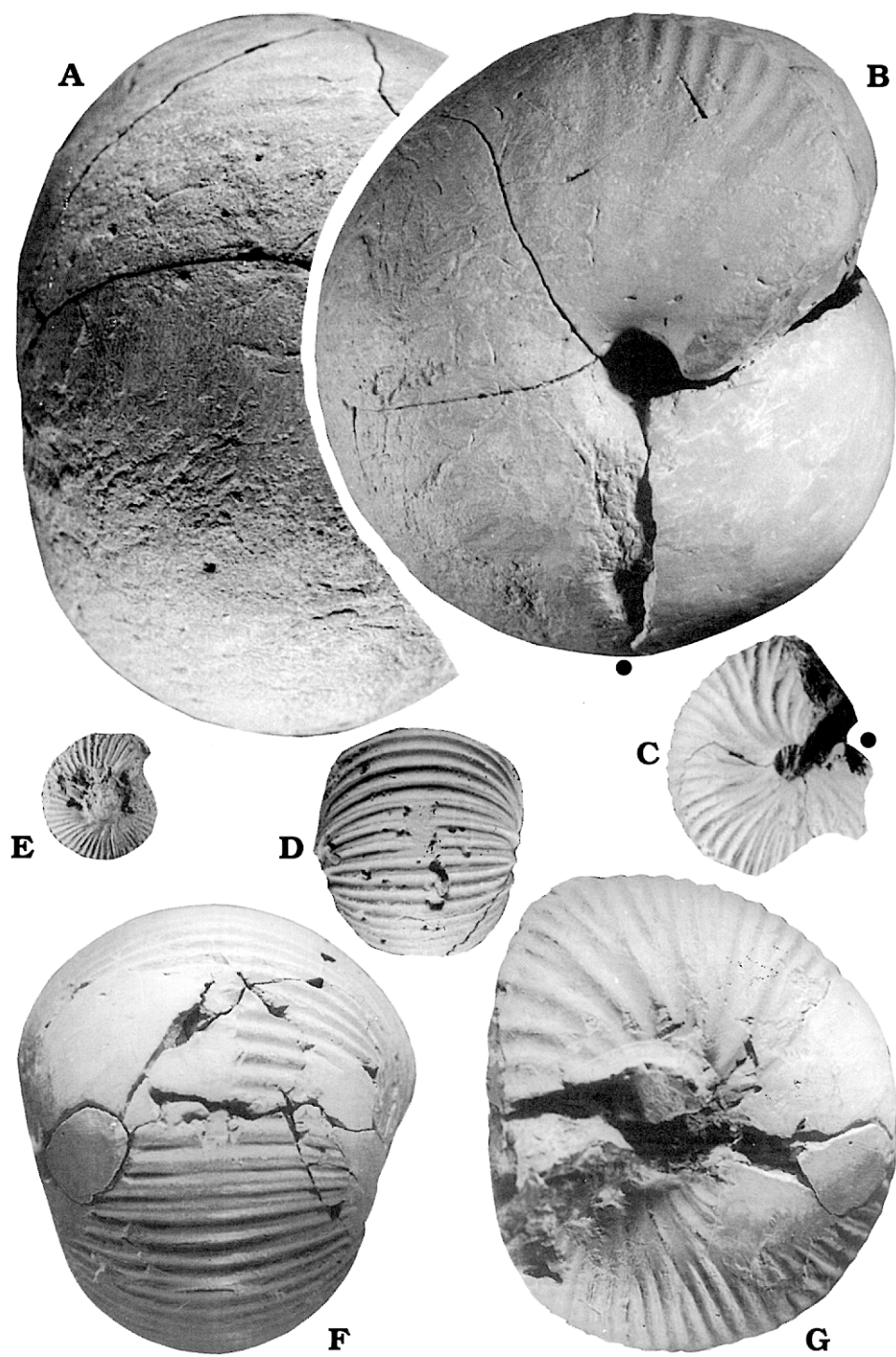
### *Eurycephalites extremus* (Tornquist, 1898) [M]

Figs 30A–E, 31A–G, 33A–D; App. 1.

\* *Sphaeroceras extremum* n. sp.; Tornquist 1898: p. 47; pl. 6 (20): 5 (lectotype), ?6.

\* *Eurycephalites extremus* (Tornquist, 1898); Riccardi & Westermann 1991: p. 48; pl. 7: 3a–c (lectotype); pl. 8: 1a–3. [for synonymy].

Fig. 31. *Eurycephalites extremus* [M]. A, B. Almost complete body chamber of an adult specimen (LPB 098) from bed 29. F, G. Last whorl of phragmocone of the same specimen. C–E. Phragmocone and body chamber of a juvenile specimen (LPB 297) from bed 29. All natural size. Point at last septum.





**Material.** — One almost complete adult specimen (LPB 098) and 1 complete juvenile specimen (LPB 297) from bed 29; 1 complete juvenile specimen (LPB 259) loose from bed 29.

**Description.** — Phragmocone ( $D = 15\text{--}60$  mm) globose and very involute ( $H_2/H_1 = 0.60$ ). Whorl section very broad ( $W/H_1 = 1.80\text{--}2.00$ ) and depressed, maximum width near the umbilical shoulder; flanks inflated, passing gradually into the broadly convex venter. Umbilicus narrow ( $U/D = 0.09\text{--}0.12$ ) with high vertical wall and rounded shoulder. Ten to eleven acute primaries arise at the umbilical seam, cross the inner third of the flank describing an adoral arch and bifurcate on the inner half; 2 secondaries with 1 intercalatory to each primary pass across the venter describing a low arch. In a complete juvenile specimen (Fig. 31C–E),  $D \approx 36$  mm, the body chamber is about  $310^\circ$ .

Adult body chamber begins at  $D = 70\text{--}80$  mm and extends through at least  $300^\circ$ . The point of furcation is on the undifferentiated ventro-lateral shoulder. Peristome and septal sutures are not preserved.

**Remarks.** — *E. extremus* (Tornquist, 1898) [M] and *Xenocephalites stipanicici* Riccardi, Westermann, & Elmi, 1990 [m], the largest species within the respective genera, co-occur in beds of the Bodenbenderi Zone at Chacay Melehué (Fig. 2) and Vega de la Veranada (Riccardi & Westermann 1991: p. 13). Their phragmocones are identical through from 30 to 50–60 mm diameter and strongly differ from about 60 mm diameter; this juvenile resemblance and stratigraphical co-occurrence strongly suggest sexual dimorphic correspondence between these two nominal species, but well preserved adult specimens are needed to compare the inner whorls of the microconch at diameters of less than 30 mm.

### Genus *Xenocephalites* Spath, 1928

Type species: *Macrocephalites neuquensis* Stehn, 1923.

Age: middle Bathonian–early (middle?) Oxfordian.

**Remarks.** — This morphogenus encompasses the microconchs of all the known mid-Jurassic Andean eurycephalitines (Callomon 1984: pp. 147–148; Riccardi & Westermann 1991; Parent 1997), including those Chilean Callovian–Oxfordian representatives described by Hillebrandt & Gröschke (1995) within which may be differentiated typical macroconchs with bigger adult size and denser ribbing than the associated typically small, coarsely ribbed *Xenocephalites*-like microconchs.

### *Xenocephalites neuquensis* (Stehn, 1923) [m]

Figs 27H, 32A–D; App. 1.

\* *Macrocephalites neuquensis* Stehn 1923: p. 86, pl. 1: 3 (lectotype).

\* *Xenocephalites neuquensis* (Stehn, 1923); Riccardi & Westermann 1991: p. 73, pl. 16: 6 (lectotype)–10. [for synonymy].

**Material.** — One almost complete adult specimen (LPB 081) from bed 23, and 3 adult specimens (LPB 065, 079, 264) from bed 13.

**Description.** — Two morphs may be distinguished within this species (cf. Riccardi & Westermann 1991):

Morph  $\alpha$  (Fig. 32A–D). — At  $D = 15\text{--}30$  mm shell depressed and involute; whorl section subovate depressed with the maximum width at the middle of the convex flanks; umbilical shoulder rounded and wall subvertical. Nine to ten acute primaries per half whorl arise on the umbilical wall, bend backward on the umbilical shoulder, bifurcate

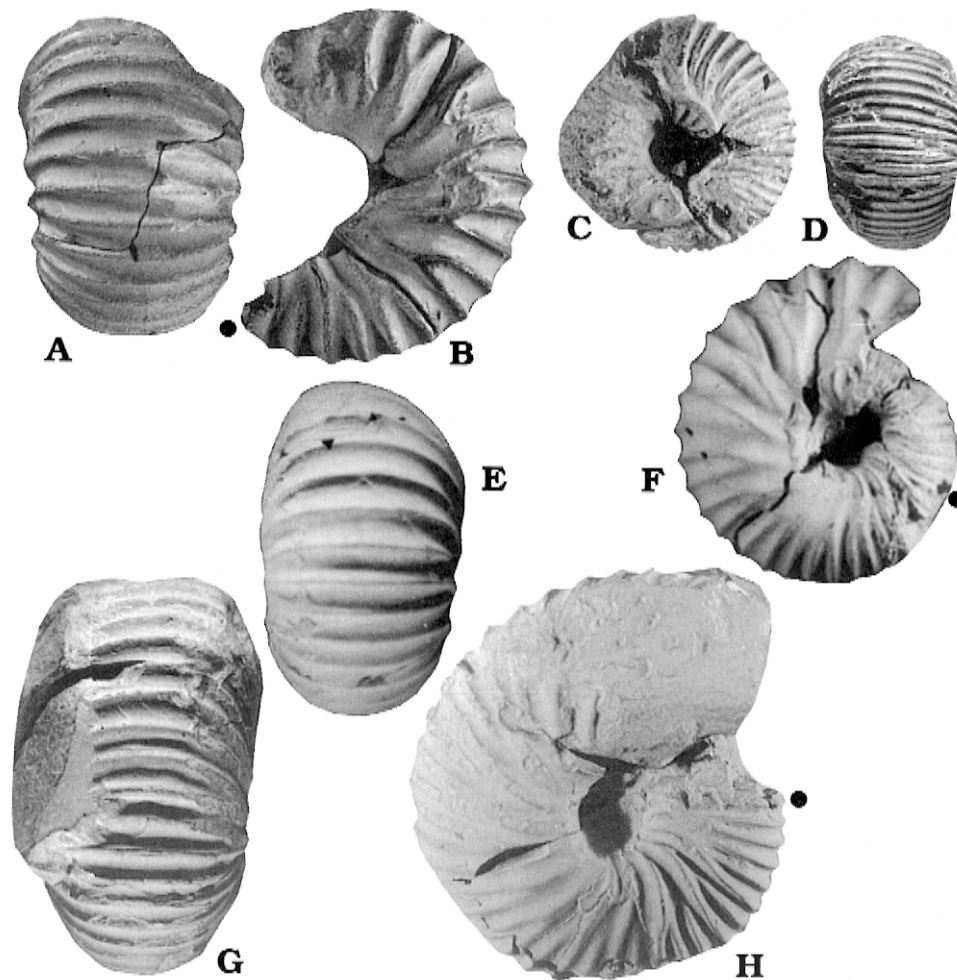


Fig. 32. **A, B.** *Xenocephalites neuquensis* [m] morph  $\alpha$ , almost complete body chamber of an adult specimen (LPB 081) from bed 23. **C, D.** Last whorl of phragmocone of the same specimen. **E, F.** *Xenocephalites* aff. *neuquensis* [m], complete adult specimen (LPB 078) from bed 5. **G, H.** *Xenocephalites* cf. *araucanus* [m], complete adult specimen (LPB 069) from bed 0. All natural size. Point at last septum.

on the upper third of the flank and, with one intercalatory ( $V = 30$ ), pass transversely across the broad, slightly arched venter. Body chamber ( $D > 30-36$  mm) strongly egressive, very depressed and ribbed with very prominent primaries ( $P = 8$ ) which bifurcate at the ventro-lateral shoulder; 16 prominent secondaries per half whorl pass transversely across the venter, intercalatory ribs are absent.

Morph  $\beta$ . — These specimens differ from morph  $\alpha$  in the more compressed section of the adult body chamber. Innermost whorls ( $D = 5-10$  mm) moderately evolute with rounded whorl section; primaries ( $P = 8$ ) radial and rounded with the point of furcation at mid-flank, ventrals ( $V = 20-21$ ) pass across the venter describing a very low arch without changes in strength.

**Remarks.** — As pointed out by Riccardi & Westermann (1991), samples assigned to this morphospecies comprise a very depressed morph and a more compressed one which occurs in beds here included in the *Iniskinites gulisanoi* and *I. crassus* horizons, lower-middle Steinmanni Zone, below beds in which occur the most depressed specimens, closest to the lectotype. *X. neuquensis* (Stehn, 1928) [m] morph  $\alpha$  shows the last whorl ( $D = 15\text{--}30$  mm) of the phragmocone identical with the inner whorls of the co-occurring *S. gerthi* [M] morphs  $\alpha$  and  $\beta$  at comparable diameters. Differences between these two species, other than differential adult size, arise at the level of the body chamber. That of *X. neuquensis* shows more prominent and sparser ribs and more pronounced uncoiling, differences that may be ascribed to microconch sexual differentiation (Parent 1997).

The compressed whorl section of *X. neuquensis* morph  $\beta$  (see Riccardi & Westermann 1991: pl. 16: 9a, b, 10) and the very similar innermost whorls suggest dimorphic correspondence with *Lilloettia steinmanni* [M], but confirmation of this will have to await better data.

The single specimen figured as *X. hebetus* Imlay, 1953 by Frebold (1978: pl. 7: 9, 10) agrees in size, morphology and ribbing with *X. neuquensis* morph  $\alpha$ .

*Xenocephalites* aff. *neuquensis* (Stehn, 1923) [m]

Figs 27I, 32E, F; App. 1.

**Material.** — One complete adult specimen (LPB 078) from bed 5.

**Description.** — Phragmocone globose involute at diameters of 20–30 mm, whorl section subcircular-depressed ( $W/H_1 = 1.22$ ) with maximum width at the middle of the convex flanks which converge to the broadly arched venter. Umbilicus narrow ( $U/D = 0.11$ ) with deep, subvertical wall and rounded shoulder. Ribbing dense ( $P = 9\text{--}10$ ,  $V = 34$ ), fine, flexuous primaries arise on the umbilical wall, bifurcate about mid-flank; secondaries pass transversely across the venter with some intercalatories. Body chamber (about 30–44 mm diameter) remains tightly coiled and only slightly egressive near the end ( $U/D = 0.13$ ). Whorl section subovate-depressed with low flanks. Ribs become progressively stronger and prominent; costal interspaces about twice as wide as ribs. Primaries flexuous, bifurcating on the upper middle of the flank, passing transversely across the venter with few intercalatories.

**Remarks.** — The present specimen differs from *X. neuquensis* [m] morph  $\alpha$  in the narrower umbilicus and the more involute and tighter coiling throughout ontogeny. *Eurycephalites gottschei* [m] is smaller and its umbilicus tends to be wider.

The phragmocone whorl section, coiling and ribbing, at comparable diameters, resemble those of *I. crassus* [M] transient  $\alpha$ , differing in the morphology and ribbing of the adult body chamber and the adult size, the macroconch being about twice the size of *X. aff. neuquensis* [m]. The specimen comes from bed 5, where *I. crassus* [M] transient  $\alpha$  also occur, and their sexual dimorphic correspondence may be tentatively proposed.

The Canadian *Iniskinites*-Assemblage described by Frebold (1978) (see remarks under *I. crassus*) most probably includes *Xenocephalites vicarius* Imlay, 1953 as an associated microconch. The present specimen most closely resembles that figured as *X. vicarius* by Frebold (1978: pl. 7: 7, 8), from which it differs only in the more flexuous and regularly bifurcated primaries.



*Xenocephalites* cf. *araucanus* (Burckhardt, 1903) [m]

Figs 27J, 32G, H.

**Material.** — One complete adult specimen (LPB 069) from bed 0.**Remarks.** — This single specimen fully agrees in size, morphology and ribbing with the morph illustrated by Riccardi & Westermann (1991: pl. 17: 10a, b) from the base of the Steinmanni Zone at Chacay Melehué. Whorl section, involution and ribbing of the last whorl of the phragmocone do not differ from those of *Iniskinites gulisanoi* [M] and the association of these two species in bed 0 (Fig. 2), suggests that they could be a sexual dimorphic pair.*Xenocephalites* sp. A [m]

Figs 23F–H, 27K; App. 1.

**Material.** — A single complete adult specimen (LPB 077) from bed 15.**Description.** — At diameters of 5–8 mm phragmocone moderately involute with slightly depressed, subovate whorl section ( $W/H_l = 1.07$  to  $1.21$ ) with maximum width at middle of the slightly convex flanks, which converge to the rounded venter. Umbilicus wide ( $U/D = 0.20$ ) with rounded shoulder. Seventeen slightly flexuous primary ribs arise at the umbilical shoulder, cross the flanks becoming coarser and rounded at the ventro-lateral shoulder, with no furcation, and pass transversely across the venter. From 26–36 mm diameter phragmocone fairly involute ( $H_2/H_l = 0.57$  to  $0.60$ ), whorl section subcircular, slightly depressed ( $W/H_l = 1.11$ – $1.18$ ) with rounded flanks which converge to the convex venter. Ten to eleven primary ribs arise at the umbilical wall, bifurcate on the upper third of flanks; 26 ventral ribs, one intercalatory for each two secondaries, pass transversely across the venter. Body chamber ( $D = 36$ – $50$  mm,  $LBC = 270^\circ$ ) moderately involute with subrectangular-depressed whorl section ( $W/H_l = 1.21$ ), maximum width at mid-flank; umbilicus wide ( $U/D = 0.22$ ) with rounded shoulder and moderately high, subvertical wall; 11 moderately prominent, acute and flexuous primaries arise at the umbilical shoulder with a backward bend and bifurcate on the upper third of flank; 24 ventrals pass across the venter describing a convex arch; fine growth lines are preserved near the simple peristome, which is incompletely preserved.**Remarks.** — The best resemblance of *Xenocephalites* sp. A is to the compressed *X. neuquensis* [m] morph  $\beta$ , differing in the somewhat wider umbilicus, more rounded whorl section throughout later ontogenetic stages and in the less prominent primaries. The modal adult diameter of *X. cf. araucanus* (in Riccardi & Westermann 1991) is greater than that of *Xenocephalites* sp. A which, moreover, is more compressed and involute with stronger primaries. *Eurycephalites gottschei* [m] is smaller in adult size and more involute than *Xenocephalites* sp. A. The phragmocone of the present specimen strongly resembles the inner whorls of the most compressed specimens of *Stehnocephalites gerthi* [M] and *S. crassicostratus* [M] (see Remarks under these species).The evolute, rounded whorl section of the nuclei ( $D = 5$ – $8$  mm), with rounded ribs, is common to *Eurycephalites gottschei* [M&m], *Lilloettia steinmanni* [M], *Stehnocephalites gerthi* [M], *S. crassicostratus* [M], *Xenocephalites neuquensis* [m] and *Xenocephalites* sp. A [m].

### **Patterns and processes in the evolution of the Andean Eurycephalitinae: developmental heterochronies with no innovations**

The (genetically determined) morphological evolution in ammonoids may be explained by means of two kinds of (genetically controlled) processes, which may occur and operate simultaneously or not: (1) relative acceleration or retardation between somatic and germinal development, heterochrony, and (2) innovations. The last involves the acquisition of novel structures (tubercles, keels, parabolae, ?constrictions) and other features absent in the ancestry (Dommergues 1987: p. 77); its expression may be modulated by the heterochronic context in which the introduction occurs; moreover, innovations can arise because of heterochrony (McNamara personal communication 1996). These two processes seem sufficient to account for the morphological patterns of evolution observed in the fossil record of ammonoids. The genetic regulation of ontogeny underlying these processes has been extensively analyzed by Raff & Kaufman (1983) and Wray & Raff (1990 and references therein). It must be kept in mind that morphological innovations may appear as a result of reactivation of suppressed ancestral developmental genetic systems (Alberch *et al.* 1979) in new positions or at a different stage in development (see Raff & Kaufman 1983: p. 165), which could be interpreted as innovation induced by heterochrony.

The temporally succeeding taxa *Lilloettia steinmanni*, *Eurycephalites gottschei*, and *Eurycephalites rotundus* clearly conform to a phyletic morphocline (Riccardi 1985), and *Eurycephalites extremus* may be considered as a terminal species immediately succeeding *E. rotundus* at the Bodenbenderi Zone.

Adult size remains almost unchanged from *Lilloettia steinmanni* to *E. rotundus* but increases in *E. extremus* (Fig. 33A), a peramorph by hypermorphosis (*sensu* Gould 1977, see also Dommergues 1987; McNamara 1982, 1986). Three stages of lateral ribbing through ontogeny of these species in terms of the progressive fading away of the primaries from the umbilical to the ventro-lateral shoulder may be distinguished (see Fig. 33A): the general trend from *L. steinmanni* to *E. rotundus* is a peramorphic pattern by acceleration, i.e., primaries fade away progressively toward the innermost whorls along the morphocline; the trend reverts with *E. extremus* which shows the phragmocone fully ribbed up to at least 60–70 mm diameter – a complex heterochronic pattern produced by association of neoteny for this feature with global hypermorphosis. Standard, complex ontogenetic paths are followed by *U/D*, *W/D* and *H<sub>1</sub>/D* through the morphocline including *E. extremus*. The umbilical width, for all these species, decreases throughout post-embryonic ontogeny, but a slight neotenuous enlargement for *D* > 20 mm is noted from *E. gottschei* towards *E. extremus* in a consistent trend (Fig. 33B). Evolution of the whorl section through the morphocline is more complex (Fig. 32C, D); the shells of all the species exhibit a marked inflection at diameters of 8–12 mm, which corresponds to the ontogenetic stage where they are most compressed. Then the whorl section inflates towards the adult stage in all species of the morphocline, with a gradual tendency to develop a less and less marked final compression of the body chamber, beginning with the compressed *L. steinmanni* and ending with *E. extremus*, which is the most inflated species from at least 10 mm diameter. Whorl height, too, follows a trend resulting from gradual neoteny throughout

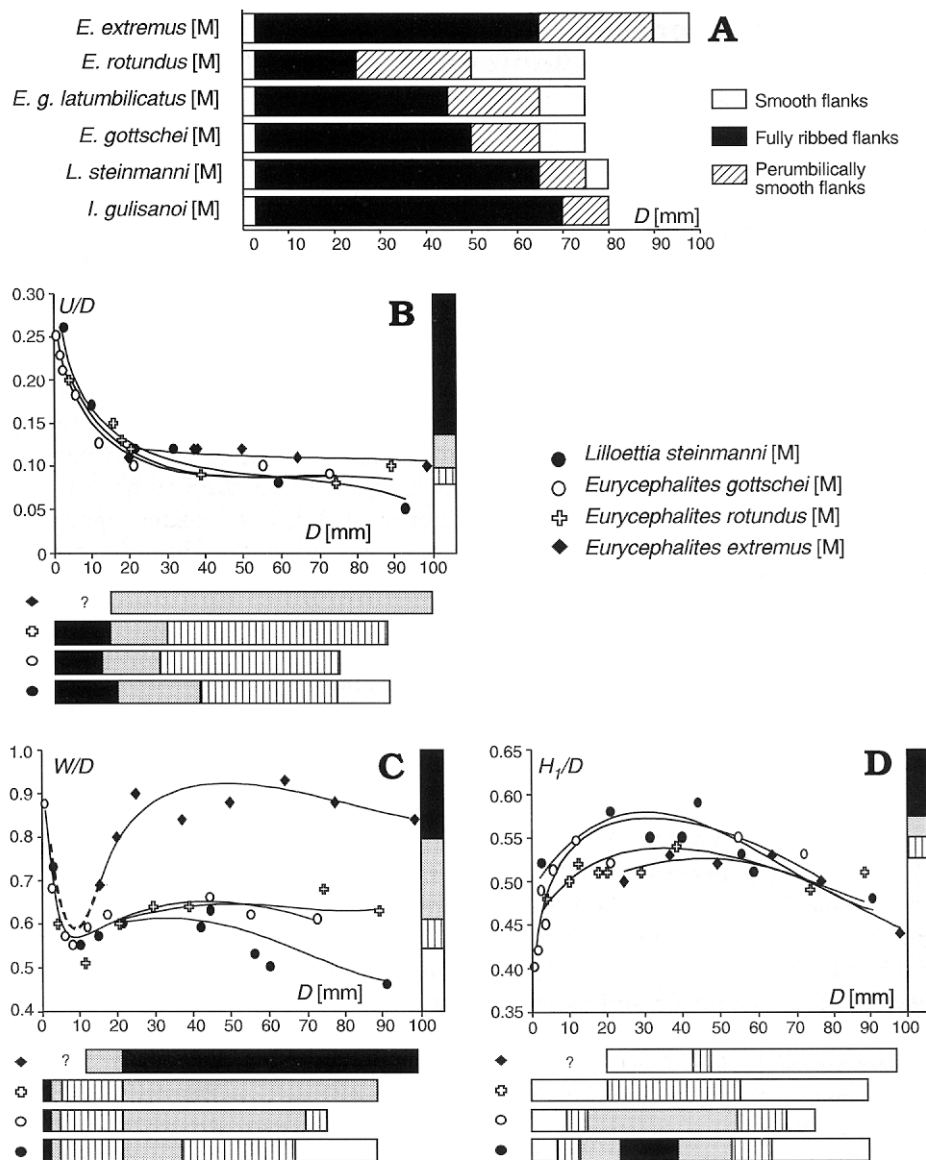


Fig. 33. Variation of adult size, costulation and relative morphology of selected modal specimens to show changes through the phyletic clade *Lilloettia steinmanni* [M] → *Eurycephalites gottschei* [M] → *E. rotundus* [M] → *E. extremus* [M]. **A**. Cartridges for ornamental stages and adult size. **B–D**. Ontogenetic trajectories for  $U/D$ - $D$ ,  $W/D$ - $D$ , and  $H_1/D$ - $D$ . Explanation in text.

ontogeny, so that all the developmental paths converge at the size of the adult body chamber (Fig. 33D).

The inner whorls of *Eurycephalites involutus* [M] are poorly known but the whorl section and involution of the adult body chamber and last whorl of the phragmocone strongly resemble those of *E. rotundus* [M]; the ribbing is strong and dense like in *E.*



*extremus* [M]. Thus it seems to fit into the phyletic morphocline as an intermediate form between *E. rotundus* and *E. extremus*.

These patterns of evolution within the morphocline may be described as a paedomorphocline (*sensu* McNamara 1982) for whorl section and coiling, but a peramorphocline for lateral ribbing. Following David (1989) and McNamara (1992) this combination of different heterochronic clinal patterns, within a single clade, is considered a mosaic heterochronocline.

The microconch of *L. steinmanni* has not been recognized yet. *E. gottschei* [m] and *E. rotundus* [m] (as described above) are progenetic when compared to their corresponding macroconchs (see Parent 1997); the same should be the case for *X. stipanicici* [m] when regarded as the corresponding microconch of *E. extremus* [M]. The evolutionary trend of the last three microconchs shows an increase in adult size towards *X. stipanicici*, the latter thus being a peramorph by hypermorphosis (like its macroconch). Ribbing is strong throughout the adult body chambers of these 3 microconchs, thus they do not reflect the peramorphic pattern seen in the macroconchs – a consequence of the progenetic truncation of the ontogeny in combination with epigenetic outgrowth (*sensu* Landman *et al.* 1991; Parent 1997). Whorl sections cannot be compared closely, but similar patterns to those described for the macroconchs seem to occur.

These complex patterns arising from combination of sexual differentiation between dimorphs and ontogenetic changes in rates of development through phylogenesis, result in microconchs being much less variable between successive species than their respective associated macroconchs, which are richer in characters, and thus more 'time-sensitive'.

A continuous abundant record of successive monospecific assemblages evolving by gradual transformation into a relatively restricted area is thought to imply eudemism (Callomon 1985). The segment of the Eurycephalitinae here analyzed covers these features, showing that the centre of evolution and the locus of phylogenesis, lay within the Neuquén-Mendoza Basin. In the upper middle Callovian to the lower Oxfordian there is no record of the Eurycephalitinae from the Neuquén-Mendoza Basin. From North Antofagasta, in the Tarapacá basin, some upper Callovian–lower Oxfordian ammonites of the Eurycephalitinae have been described by Hillebrandt & Groschke (1995). Some of these forms (casts kindly loaned to me by A.v. Hillebrandt) are globose macroconchs (Hillebrandt & Groschke 1995: pl. 5: 3a, b, 4), very close to *E. extremus* [M]; another macroconch (Hillebrandt & Groschke 1995: pl. 6: 1), more compressed and involute with smooth flanks, could be included in *Araucanites* Riccardi & Westermann (in Stipanovic *et al.* 1975). These Chilean forms seem to conform to the ancestral stock of the Oxfordian genus *Araucanites*, which was originally defined from material coming from beds at south-Mendoza that were correlated with the Cordatum and Plicatilis Zones (Stipanovic *et al.* 1975). Thus, from late populations of *E. extremus*, established in northern Chile after the Callovian regression in the Neuquén-Mendoza basin (see Introduction), *Araucanites* could have arisen through intermediate forms such as those cited above.

*Iniskinites crassus* evolved by gradual transformation, through transients  $\alpha$  and  $\beta$ , towards the highly variable *S. gerthi*. These changes may be analyzed from the innermost whorls, but it must be taken into account that the following conclusions come from small samples of inner whorls of *I. crassus*, so they could be somewhat biased. Mean adult size increases gradually (Tables 2 and 3), a peramorphic modal pattern by hypermorphosis, associated with parallel increase in the ranges of variability for this character, here

measured by means of the CV. Hypermorphosis is a process that affects the whole organism; the morphogenetic changes that differentiate *S. gerthi* from its ancestor, *I. crassus*, through the preadult whorls of the phragmocone ( $D > 30$  mm) and, especially, the adult body chamber, seem to be the consequence of this single heterochronic process. The umbilical ontogeny shows a widening trend throughout the body chamber, from *I. crassus* towards *S. gerthi*. In both species an inflection at  $D = 20$ – $30$  mm is followed by a stabilization phase up to the end of the phragmocone (Figs 12B, 18C). The whorl section becomes wider and more depressed at the level of the adult body chamber (Figs 12A, 18A) after a common inflection of  $W/D$  for both species at  $D = 5$ – $12$  mm followed by a stabilization phase up to the end of the phragmocone. These ontogenetic paths for whorl section with juvenile inflections are homologous to those of the clade *Lilloettia-Eurycephalites* described above, strongly supporting the hypothesis of direct phyletic relationships between all these forms. Lateral and ventral ribbing follow homologous developments in both species, being indistinguishable up to about diameter of 30 mm, then diverging to give more densely ribbed adults in *S. gerthi* [M].

Morphologic changes through evolution of the Eurycephalitinae here studied may be accounted for by heterochronic processes; innovations (as defined above), are not evident in the investigated material, nor have they been described previously.

## Acknowledgements

Laboratory research was partially financed by Facultad de Ciencias Exactas e Ingeniería (Universidad Nacional de Rosario). I am very grateful to the late P. Pasotti and F. Lattuca (Rosario), J.H. Callomon (London), K.J. McNamara (Western Australia), J.-L. Dommergues (Dijon), B. Joly (Beaugeancy), and C. Meister (Genève) for good advice and long fruitful discussions; and to the following friends and colleges for support, facilities and/or bibliography: D.T. Donovan (London), G. Meléndez (Zaragoza), D. Marchand and J. Thierry (Bourgogne), S. Elmi (Lyon), E. Cariou (Poitiers), J. Guex (Lausanne), G.E.G. Westermann (Ontario), B.M. Cox (Nottingham), R.L. Hall (Vancouver), T.P. Poulton (Ontario), A. v. Hillebrandt and M. Gröschke (Berlin), J. Sandoval (Granada), S. Fernandez-López (Madrid), A. Galacz (Budapest), N.H. Landman (New York), R.A. Raff (Michigan), S.C. Stearns (Basle), O.A. Albert and H. Fraga (Rosario), and to G. Cornero (Rosario) who have collected with me and have shown me some localities. V. Bochini (Rosario) is acknowledged for the photography. The following institutions have supported my work with their collaboration and/or facilities: Museo de La Plata, Museo Olsacher (J. Garate, Zapala), Geological Survey of Canada, British Geological Survey, Université Claude-Bernard et Institut des Sciences de la Terre (Lyon), and Geological Survey of Hungary, Université de Bourgogne.

## References

- Alberch, P., Gould, S.J., Oster, G.F., & Wake, D.B. 1979. Size and shape in ontogeny and phylogeny. — *Paleobiology* **5**, 296–317.
- Arkell, W.J. 1959. A monograph of English Bathonian ammonites. — *Monograph of the Palaeontographical Society*, Part 8, 209–264.
- Atrops, F. & Meléndez G. 1993. Current trends in systematics of Jurassic Ammonoidea: the case of Oxfordian–Kimmeridgian perisphinctids from southern Europe. — *Geobios, Mémoire Spécial* **15**, 19–31.
- Bonnot, A. 1993. Les Peltoceratinae (Ammonoidea) de la Sous-Zone à Trezeense (Zone à Athleta, Callovien Supérieur) en Côte d'Or (France). — *Geobios* **26**, 135–160.
- Burckhardt, C. 1903. Beiträge zur Kenntnis der Jura- und Kreideformation der Cordillere. — *Palaeontographica* **50**, 1–144.

- Burckhardt, C. 1927. Cefalópodos del Jurásico Medio de Oaxaca y Guerrero. — *Boletín del Instituto Geológico de México* **47**, 1–108.
- Callomon, J.H. 1984. A review of the biostratigraphy of the post-Lower Bajocian Jurassic ammonites of western and northern North America. In: G.E.G. Westermann (ed.), *Jurassic–Cretaceous Biochronology and Paleontology of North America*. — *Geological Association of Canada, Special Paper* **27**, 143–174.
- Callomon, J.H. 1985. The evolution of the Jurassic ammonite family Cardioceratidae. — *Special Papers in Palaeontology* **33**, 49–90.
- Callomon, J.H. 1988. The ammonite successions and Subzones of the Transversarium Zone in the Submediterranean Middle Oxfordian. — *Proceedings of the 2-nd International Symposium on Jurassic Stratigraphy, Lisbon 1987*, 433–444.
- Callomon, J.H., Dietl, G., & Niederhöfer, H.J. 1992. On the true stratigraphic position of *Macrocephalites macrocephalus* (Schlotheim, 1813) and the nomenclature of the standard Middle Jurassic 'Macrocephalus Zone'. — *Stuttgarter Beiträge zur Naturkunde B* **185**, 1–65.
- Cariou, E. 1984a. Les Reineckeiidés (Ammonitina, Callovien) de la Téthys occidentale. Dimorphisme et évolution. — *Documents des Laboratoires de Géologie de la Faculté des Sciences de Lyon, Hors Série* **8**, 1–460.
- Cariou, E. 1984b. Biostratigraphic subdivision of the Callovian Stage in the Subtethyan Province of ammonites, correlations with the subboreal zonal scheme. — *Proceedings of the International Symposium on Jurassic Stratigraphy, Erlangen 1984*, **2**, 315–326.
- Cepek, P. & Kemper, E. 1981. Der Blättertonstein des nordwestdeutschen Barrême und die Bedeutung des Nannoplanktons für die fein laminierten, anoxisch entstandenen Gesteine. — *Geologisches Jahrbuch A* **58**, 3–13.
- Cox, B.M. 1988. English Callovian (Middle Jurassic) Perisphinctid Ammonites. Part 1. *Monograph of the Palaeontographical Society*, 54 pp.
- David, B. 1989. Jeu en mosaïque des heterochronies: variation et diversité chez les Pourtalesiidae. — *Geobios, Mémoire Spécial* **12**, 115–131.
- Dayczak-Calikowska, K. & Kopik, J. 1976. Middle Jurassic. In: S. Sokołowski (ed.), *Geology of Poland, Volume 1: Stratigraphy, Part 2: Mesozoic*, 241–333. Instytut Geologiczny, Warszawa.
- Dietl, G. 1994. Der hochstetteri-Horizont- ein Ammonitenfaunen-Horizont (Discus-Zone, Ober-Bathonium, Dogger) aus dem Schwäbischen Jura. — *Stuttgarter Beiträge zur Naturkunde B* **202**, 1–39.
- Dígregorio, R.E., Gulisano, C.A., Gutierrez Pleimling, A.R., & Minitti, S.A. 1984. Esquema de la evolución geodinámica de la cuenca neuquina y sus implicancias paleogeográficas. — *Actas 9<sup>no</sup> Congreso Geológico Argentino* **1**, 236–259.
- Dommergues, J.-L. 1987. L'évolution chez les Ammonitina du Lias moyen (Carixien, Domerien basal) en Europe occidentale. — *Documents des Laboratoires de Géologie de la Faculté des Sciences de Lyon* **98**, 1–297.
- Dommergues, J.-L., Cariou, E., Contini, D., Hantzpergue, P., Marchand, D., Meister, C., & Thierry, J. 1989. Homéomorphies et canalisations; évolutives: le rôle de l'ontogénèse. Quelques exemples pris chez les ammonites du Jurassique. — *Geobios* **22**, 5–48.
- Donovan, D.T. 1987. Evolution of the Arietitidae and their descendants. — *Cahiers de Université Catholique Lyon, Série des Sciences* **1**, 123–138.
- Fernández-López, S., Chong, G., Quinzio, L.A., & Wilk, H.-G. 1994. The Upper Bajocian and Bathonian in the Cordillera de Domeyko, North-Chilean Precordillera: sedimentological and biostratigraphical results. — *Geobios, Mémoire Spécial* **17**, 187–201.
- Frebold, H. 1978. Ammonites from the Late Bathonian 'Iniskinites Fauna' of Central British Columbia. — *Bulletin of the Geological Survey of Canada* **307**, 1–27.
- Galacz, A. 1980. Bajocian and Bathonian ammonites of Gyenespuszta. — *Geologica Hungarica, Sèrie Palaeontologie* **39**, 3–227.
- Gould, S.J. 1977. *Ontogeny and Phylogeny*. 501 pp. Belknap Press of Harvard, Cambridge, Massachusetts.
- Gulisano, C.A., Gutierrez Pleimling, A.R., & Digregorio, R.E. 1984. Esquema estratigráfico de la secuencia jurásica del oeste de la provincia de Neuquén. — *Actas 9<sup>no</sup> Congreso Geológico Argentino* **1**, 236–259.
- Hahn, W. 1969. Die Perisphinctidae Steinmann (Ammonoidea) des Bathoniums im südwestdeutschen Jura. — *Jahreshefte des Geologischen Landesamtes Baden-Württemberg* **11**, 29–86.
- Hillebrandt, A. v. & Gröschke, M. 1995. Ammoniten aus dem Callovium/Oxfordium Grenzbereich von Nordchile. — *Berliner geowissenschaftliche Abhandlungen A* **169**, 1–40.



- Hillebrandt, A. v. & Westermann, G.E.G. 1985. Aalenian (Jurassic) Ammonite faunas and zones of the Southern Andes. — *Zitteliana* **12**, 3–55.
- Imlay, R.W. 1953. Callovian (Jurassic) Ammonites from the United States and Alaska. Part 2: Alaska Peninsula and Cook Inlet Regions. — *United States Geological Survey Professional Paper B* **249**, 1–107.
- Joly, B. 1976. Les Phylloceratidae malgaches au Jurassique. Généralités sur les Phylloceratidae et quelques Juraphyllitidae. — *Documents des Laboratoires de Géologie de la Faculté des Sciences de Lyon* **67**, 1–471.
- Kopik, J., Dayczak-Calikowska, K., & Myczyński, R.A. 1980. Order Ammonitida Zittel, 1884. In: L. Malinowska (ed.), *Budowa Geologiczna Polski, tom III, Atlas skamieniałości przewodnich i charakterystycznych, Część 2b, Mezozoik, Jura*, 174–217. Instytut Geologiczny, Warszawa.
- Krystin, L. 1972. Die Oberbajocium- und Bathonium-Ammoniten der Klaus-Schichten des Steinbruchs Neumühle bei Wien (Österreich). — *Annalen des Naturhistorischen Museum in Wien* **76**, 195–310.
- Landman, N.H. 1987. Ontogeny of Upper Cretaceous (Turonian–Santonian) scaphitid ammonites from the Western Interior of North America: systematics, developmental patterns, and life history. — *Bulletin of the American Museum of Natural History* **185**, 117–241.
- Landman, N.H., Dommergues, J.-L., & Marchand, D. 1991. On the complex nature of progenetic species – examples from Mesozoic ammonites. — *Lethaia* **24**, 409–421.
- Lóczy, v. L. 1915. Monographie der Villányer Callovien-Ammoniten. — *Geologica Hungarica* **1**, 255–507.
- Mangold, C. 1970. Les Perisphinctidae (Ammonitina) du Jura méridional au Bathonien et au Callovien. — *Documents du Laboratoire Géologique, Faculté des Sciences de Lyon* **41**, 1–246.
- McNamara, K.J. 1982. Heterochrony and phylogenetic trends. — *Paleobiology* **8**, 130–142.
- McNamara, K.J. 1986. A guide of nomenclature of heterochrony. — *Journal of Paleontology* **60**, 4–13.
- McNamara, K.J. 1992. The role of heterochrony in evolutionary trends. In: K.J. McNamara (ed.), *Evolutionary Trends*, 59–74. Belhaven Press, London.
- Parent, H. 1997. Ontogeny and sexual dimorphism of *Eurycephalites gotschei* (Tornquist) [M&M] of the Andean Lower Callovian (Ammonoidea, Middle Jurassic, Argentina-Chile). — *Geobios* **30**, 407–419.
- Raff, R.A. & Kaufman, T.C. 1983. *Embryos, Genes and Evolution*. 395 pp. Macmillan Publishers, New York.
- Raileanu, G. & Nastaseanu A. 1960. Contributii la cunoasterea faunei de ammoniti din Jurasicul Superior de la Svinita (Banat). — *Studii cercetari Geologie* **5**, 7–38.
- Riccardi, A.C. 1984. Las asociaciones de amonitas del Jurásico y Cretácico de la Argentina. — *Actas 9<sup>no</sup> Congreso Geológico Argentino* **4**, 559–595.
- Riccardi, A.C. 1985. Los Eurycephalitinae andinos (Ammonitina, Jurásico medio): Modelos evolutivos y resolución paleontológica. — *Boletín de Genética del Insitituto de Fitogenética* **13**, 1–27.
- Riccardi, A.C. 1993. Paleogeografía. Introducción. In: A.C. Riccardi & S.E. Damborenea (eds), *Léxico Estratigráfico de la Argentina*, vol. 9: Jurásico. — *Revista Asociación Geológica Argentina B* **21**, 19–20.
- Riccardi, A.C. & Gulisano, C.A. 1990. Unidades limitadas por discontinuidades. Su aplicación al Jurásico andino. — *Revista Asociación Geológica Argentina* **45**, 346–364.
- Riccardi, A.C., Gulisano, C.A., Mujica, J., Palacios, O., Schubert, C., & Thompson, M.R.A. 1992. 6. Western South America and Antarctica. In: G.E.G. Westermann (ed.), *The Jurassic of the Circum-Pacific*, 122–161. Cambridge University Press.
- Riccardi, A.C., Westermann, G.E.G., & Elmi, S. 1988. The Bathonian–Callovian ammonite Zones of the Argentine-Chilean Andes. — *Proceedings of the 2-nd International Symposium on Jurassic Stratigraphy, Lisbon 1987*, 347–358.
- Riccardi, A.C., Westermann, G.E.G., & Elmi, S. 1989. The Middle Jurassic Bathonian–Callovian ammonite Zones of the Argentine-Chilean Andes. — *Geobios* **22**, 553–597.
- Riccardi, A.C. & Westermann, G.E.G. 1991. Middle Jurassic ammonoid fauna and biochronology of the Argentine-Chilean Andes. Part III: Bajocian–Callovian Eurycephalitinae, Stephanocerataceae. Part IV: Bathonian–Callovian Reineckeidae. — *Palaeontographica A* **216**, 1–145.
- Sandoval, J. 1983. Bioestratigrafía y paleontología (Stephanocerataceae y Perisphinctaceae) del Bajoceno y Bathonense en las cordilleras Béticas. — *Tesis doctoral Universidad Granada*, I–XIV + 1–613.
- Sandoval, J., Westermann, G.E.G., & Marshall, M.C. 1990. Ammonite fauna, stratigraphy and ecology of the Bathonian–Callovian (Jurassic) Tecocoyunca Group, South Mexico. — *Palaeontographica A* **210**, 93–149.
- Siemiradzki, J. 1898–99. Monographische Beschreibung der Ammonitengattung Perisphinctes. — *Palaeontographica* **45**, 69–296 (1898), 297–352 (1899).

- Spath, L.F. 1927–33. Revision of the Jurassic cephalopod fauna of Kachh (Cutch). — *Palaeontologia Indica*, n.s. **9**, 1–945.
- Stearns, S.C. 1989. The evolutionary significance of the phenotypic plasticity. — *Bioscience* **39**, 436–445.
- Steinmann, G. 1881. Zur Kenntnis der Jura und Kreidenformation von Caracoles (Bolivia). — *Neues Jahrbuch für Mineralogie, Geologie und Paläontologie B* **49**, 239–301.
- Stipanovic, P.N., Westermann, G.E.G., & Riccardi, A.C. 1975. The Indo-Pacific ammonites *Mayaites* in the Oxfordian of the Southern Andes. — *Ameghiniana* **12**, 281–305.
- Thierry, J. 1978. Le genre *Macrocephalites* au Callovien Inférieur (ammonites Jurassique Moyen). — *Mémoires Géologiques Université Dijon* **4**, 1–490.
- Tintant, H. 1957. Principes de la Systématique. In: J. Piveteau (ed.), *Traité de Paléontologie* **1**, 41–64. Masson edit., Paris.
- Tornquist, A. 1898. Der Dogger am Espinazito Pass. — *Paläontologische Abhandlungen, N.F.* **3(2)**, 3(135)–69(201).
- Westermann, G.E.G., Corona, R., & Carrasco, R. 1984. The Andean Mid-Jurassic *Neuquenicer* Ammonite Assemblage of Cualac, Mexico. In: G.E.G. Westermann (ed.), *Jurassic–Cretaceous Biochronology and Paleogeography of North America*. — *Geological Association of Canada, Special Paper* **27**, 99–112.
- Westermann, G.E.G. & Riccardi, A.C. 1972. Middle Jurassic ammonoid fauna and biochronology of the Argentine-Chilean Andes. Part I: Hildocerataceae. — *Palaeontographica A* **140**, 1–116.
- Westermann, G.E.G. & Riccardi, A.C. 1979. Middle Jurassic ammonoid fauna and biochronology of the Argentine-Chilean Andes. Part II: Bajocian Stephanocerataceae. — *Palaeontographica A* **164**, 85–188.
- Westermann, G.E.G. & Riccardi, A.C. 1985. Middle Jurassic ammonite evolution in the Andean Province and emigration to Tethys. — *Lecture Notes in Earth Sciences* **1**, 6–34.
- Wray, G.A. & Raff, R.A. 1990. Pattern and process heterochronies in the early development of sea urchins. — *Developmental Biology* **1**, 245–251.
- Zakharov, V.M. 1992. Population phenogenetics: analysis of developmental stability in natural populations. In: V.M. Zakharov & J.H. Graham (eds), *Developmental Stability in Natural Populations*. — *Acta Zoologica Fennica* **191**, 7–30.

## Amonity górnego batonu i dolnego keloweju z Chacay Melehué (Argentyna)

HORACIO PARENT

### Streszczenie

W pracy opisano amonity górnego batonu i dolnego keloweju zebrane warstwa po warstwie z nowych odsłoneń w rejonie Chacay Melehué w Argentynie. Wyróżniono dwa nowe horyzonty: *Iniskinites gulisanoi* oraz *Iniskinites crassus*, pierwszy z dolnej, a drugi ze środkowej części poziomu Steinmanni. Zebrana fauna amonitowa zawiera nie opisane dotąd gatunki: *Choffatia* aff. *neumayri* (Siemiradzki, 1899) [M&m], *Iniskinites evolutus* sp. n. [M], *Iniskinites* sp. A [M], *Eurycephalites* aff. *gottschei* (Tornquist, 1898) [M], *Xenocephalites* aff. *neuquensis* (Stehn, 1923) [m] i *Xenocephalites* sp. A [m]. Gatunek *Oxycerites tenuistriatus* (de Grossouvre, 1888) jest nowy dla regionu andyjskiego. Wiele gatunków jest reprezentowanych przez duże próbki okazów o różnym stopniu rozwoju ontogenetycznego, co zezwala na dokładne prześledzenie ontogenezy, podanie charakterystyki głównych morfotypów w obrębie każdego gatunku oraz zaproponowanie relacji dymorficznych między niektórymi nominalnymi morfogatunkami. Następujące po sobie gatunki *Lilloettia steinmanni* (Spath, 1928), *Eurycephalites gottschei* (Tornquist, 1898), *E. rotundus* (Tornquist, 1898) i *E. extremus* (Tornquist, 1898) tworzą filetyczną morfoklinę, zinterpretowaną przez autora jako mozaikowa heterochronoklina.

## Appendix 1

Individual measurements of the specimens not described statistically. For abbreviations see pp. 74–75.

Specimen	BC/Ph	D	U(U/D)	W(W/D)	H <sub>1</sub> (H <sub>1</sub> /D)	H <sub>2</sub> (H <sub>2</sub> /D)	WH <sub>1</sub>	H <sub>2</sub> /H <sub>1</sub>	P	V
<b><i>Oxyerites (Alcidellus) tenuistriatus</i> (Grossouvre, 1888) [M]</b>										
LPB 293	BC	83.30	12.71 (0.15)	23.72 (0.28)	42.17 (0.51)	28.78 (0.35)	0.56	0.62	10	0
	Ph	61.11	-	18.17 (0.30)	36.55 (0.60)	-	0.60	-	-	-
<b><i>Choffatia subbackeriae</i> (d'Orbigny, 1850) [M]</b>										
LPB 033	BC	145.55	68.99 (0.47)	45.12 (0.31)	39.28 (0.27)	36.74 (0.25)	1.15	0.94	18	54
LPB 035	BC	136.22	67 (0.49)	36.41 (0.27)	36.33 (0.27)	31.56 (0.23)	1.00	0.87	20	53
<b><i>Choffatia suborion</i> (Burckhardt, 1927) [M]</b>										
LPB 032	BC	130.10	73.45 (0.56)	34.76 (0.27)	33.71 (0.26)	25.26 (0.19)	1.03	0.75	17	30
LPB 036	BC	87.17	44.53 (0.51)	27.20 (0.31)	24.90 (0.29)	18.70 (0.21)	1.09	0.75	14	37
	Ph	64.97	30.49 (0.47)	24.20 (0.37)	19.59 (0.30)	14.46 (0.22)	1.24	0.74	-	-
LPB 281	BC	108.75	50.74 (0.47)	31.56 (0.29)	30.85 (0.28)	-	1.02	-	13	40
<b><i>Choffatia jupiter</i> (Steinmann, 1881) [M]</b>										
LPB 091	BC	208.00	126.00 (0.60)	-	55.70 (0.27)	-	-	-	18	-
LPB 371	BC	161.00	72.20 (0.45)	-	49.90 (0.31)	-	-	-	14	-
	Ph	91.00	42.10(0.46)	-	32.00 (0.35)	-	-	-	17	-
<b><i>Iniskinites evolutus</i> nov. sp. [M] - Holotype</b>										
LPB 229	BC	94.00	21.12 (0.22)	46.80 (0.50)	41.35(0.44)	21.90 (0.23)	1.13	0.53	13	32
	BC/Ph	69.71	16.36 (0.23)	37.90 (0.54)	32.50 (0.47)	17.90 (0.26)	1.17	0.55	13	-
	Ph	52.38	11.3 <sup>e</sup> (0.22 <sup>e</sup> )	26.70 (0.51)	25.50 (0.49)	-	1.05	-	-	-
<b><i>Stehnocephalites crassicostatus</i> Riccardi &amp; Westermann, 1991 [M]</b>										
LPB 004	BC	83.30	25.00 (0.30)	40.00 (0.48)	27.50 (0.33)	22.70 (0.27)	1.45	0.83	11	30
LPB 006	BC	60.70	16.70 (0.28)	28.60 (0.47)	27.20 (0.45)	15 <sup>e</sup> (0.25 <sup>e</sup> )	1.05	0.55 <sup>e</sup>	12	29
	BC/Ph	43.60	12.10 (0.28)	24.80 (0.57)	18.00 (0.41)	10.60 (0.24)	1.38	0.59	11	24
LPB 007	BC	106.90	28.90 (0.27)	45.90 (0.43)	45.80 (0.43)	26.00 (0.24)	1.00	0.57	9	35
	BC/Ph	74.90	-	40.90 (0.55)	34.10 (0.46)	-	1.20	-	13 <sup>e</sup>	33
LPB 331	BC	78.12	20.00 (0.26)	37.73 (0.48)	33.60 (0.43)	19.80 (0.25)	1.12	0.59	12	34
LPB 333/1	BC	66.04	16.20 (0.25)	31.64 (0.48)	29.34 (0.44)	16.00 (0.24)	1.08	0.55	12	31
	BC/Ph	46.26	-	27.56 (0.60)	21.00 (0.45)	11.50 (0.25)	1.31	0.55	-	-
	Ph	35.20	-	21.23 (0.60)	-	-	-	-	-	-
LPB 333/2	BC juv.	40.00	9.00 (0.23)	21.00 (0.53)	18 <sup>e</sup> (0.45 <sup>e</sup> )	12.6 <sup>e</sup> (0.32 <sup>e</sup> )	1.17	0.70	13	27
<b><i>Lilloettia steinmanni</i> (Spath, 1928) [M]</b>										
LPB 040	BC	59.03	4.51 (0.08)	-	30.39 (0.51)	-	-	-	12	37
	Ph	44.34	-	27.90 (0.63)	26.24 (0.59)	14.18 (0.32)	1.06	0.54	-	-
	Ph	31.55	3.78 (0.12)	19.24 (0.60)	17.26 (0.55)	10.50 (0.33)	1.11	0.61	-	32
	Ph	21.21	2.50 (0.12)	14.60 (0.69)	12.31 (0.58)	7.11 (0.34)	1.19	0.58	-	-
LPB 082	BC	60.50	6.12 (0.10)	44.40 (0.73)	29.16 (0.48)	17.24 (0.28)	1.52	0.59	-	34
	Ph	32.90	-	20.30 (0.62)	-	-	-	-	-	31
LPB 084	BC	53.33	4.8 <sup>e</sup> (0.1 <sup>e</sup> )	28.00 (0.52)	28.70 (0.53)	14.53 (0.27)	0.97	0.51	-	29 <sup>e</sup>
LPB 220	BC	70.65	4.58 (0.06)	38.72 (0.55)	-	-	-	-	-	-
LPB 085	Ph juv.	32.03	-	21.24 (0.66)	16.93 (0.53)	10.19 (0.32)	1.25	0.60	13	33
LPB 085/1	Ph juv.	2.90	0.75 (0.26)	2.11 (0.73)	1.50 (0.52)	1.20 (0.41)	1.41	0.80	0	0
LPB 074	BC	60.00	-	30.00 (0.50)	29.03 (0.43)	-	1.03	-	10	31
	BC	41.80	-	24.82 (0.59)	21.60 (0.52)	11.50 (0.28)	1.15	0.53	10	-
	BC/Ph	31.10	-	-	-	-	-	-	-	-
	Ph	21.00	-	12.50 (0.60)	11.00 (0.52)	5.80 (0.28)	1.14	0.53	-	-
	Ph	14.80	-	8.50 (0.57)	9.20 (0.62)	-	0.92	-	-	-
	Ph	10.00	1.70 (0.17)	5.00 (0.50)	4.60 (0.46)	3.40 (0.34)	1.08	0.73	-	-
	Ph	6.30	-	4.07 (0.64)	3.00 (0.48)	2.00 (0.32)	1.36	0.67	-	-
	Ph	4.55	-	2.50 (0.55)	2.17 (0.48)	1.7 <sup>e</sup> (0.38 <sup>e</sup> )	1.15	0.8 <sup>e</sup>	-	-
<b><i>Eurycephalites aff. gottschei</i> (Tornquist, 1898) [M]</b>										
LPB 260	BC	77.62	7.00 (0.09)	38.96 (0.50)	40.41 (0.52)	-	0.96	-	14	33
LPB 261	BC	93.52	7.00 (0.07)	44 <sup>e</sup> (0.56 <sup>e</sup> )	47 <sup>e</sup> (0.60 <sup>e</sup> )	27 <sup>e</sup> (0.34 <sup>e</sup> )	0.93 <sup>e</sup>	0.57 <sup>e</sup>	-	-
	Ph	54.50	-	35.10 (0.64)	32.60 (0.60)	-	1.08	-	-	-
LPB 284/2	BC (juv.)	8.80	1.26 (0.14)	5.40 (0.61)	4.60 (0.52)	2.80 (0.32)	1.17	0.61	10	25
<b><i>Eurycephalites involutus</i> (Riccardi &amp; Westermann, 1991) [M]</b>										
LPB 049	BC	62.50	7.80 (0.12)	41.00 (0.66)	31.50 (0.50)	16.50 (0.26)	1.30	0.52	10	29
	BC/Ph	37.00	4.50 (0.12)	25.00 (0.68)	18.00 (0.49)	-	1.39	-	10	28



Specimen	BC/Ph	D	U(U/D)	W(W/D)	H <sub>1</sub> (H <sub>1</sub> /D)	H <sub>2</sub> (H <sub>2</sub> /D)	W/H <sub>1</sub>	H <sub>2</sub> /H <sub>1</sub>	P	V
<b><i>Eurycephalites extremus</i> (Tornquist, 1898) [M]</b>										
LPB 098	BC	99.87	9.03 (0.10)	83.76 (0.84)	44.13 (0.44)	23.25 (0.23)	1.89	0.52	-	-
	BC/Ph	77.00	-	68.5 <sup>u</sup> (0.88 <sup>u</sup> )	38.5 <sup>u</sup> (0.50 <sup>u</sup> )	18 <sup>u</sup> (0.23 <sup>u</sup> )	1.78 <sup>u</sup>	0.47 <sup>u</sup>	12	34
LPB 297	BC	36.70	4.62 (0.12)	30.93 (0.84)	17.99 (0.49)	-	1.72	-	10	24
	Ph	24.52	-	24.77 (1.01)	12.32 (0.50)	7.48 (0.30)	2.01	0.60	11	24
	Ph	19.50	2.12 (0.11)	15.60 (0.8)	-	5.73 (0.29)	-	-	-	28
	Ph	14.88	-	10.26 (0.69)	-	-	-	-	-	23
<b><i>Xenocephalites neuquensis</i> (Stehn, 1923) [m] morph α</b>										
LPB 081	BC	44.00	8.30 (0.19)	29.30 (0.67)	18.00 (0.41)	9.80 (0.22)	1.63	0.54	8	16
	BC/Ph	35.50	6.00 (0.17)	25.70 (0.72)	17.00 (0.48)	7.00 (0.20)	1.51	0.41	9	-
	Ph	29.50	4.50 (0.15)	21.00 (0.71)	14.00 (0.47)	-	1.50	-	-	30
<b><i>Xenocephalites aff. neuquensis</i> (Stehn, 1923) [m]</b>										
LPB 078	BC	44.00	5.50 (0.13)	26.00 (0.59)	26.00 (0.52)	9.40 (0.21)	1.00	0.36	8	20
	BC/Ph	34.00	4.00 (0.12)	22.70 (0.67)	17.00 (0.50)	6.80 (0.20)	1.34	0.40	9	23
	Ph	21.00	2.00 (0.10)	14.50 (0.69)	11.50 (0.55)	-	1.26	-	-	-
<b><i>Xenocephalites</i> sp. A [m]</b>										
LPB 077	BC	48.35	10.80 (0.22)	26.03 (0.54)	21.54 (0.44)	12.02 (0.25)	1.21	0.56	11	24
	Ph	35.55	8.02 (0.22)	18.50 (0.52)	15.60 (0.44)	9.31 (0.26)	1.18	0.60	10	26
	Ph	26.07	5.97 (0.23)	14.50 (0.56)	13.02 (0.50)	7.4 <sup>u</sup> (0.28 <sup>u</sup> )	1.11	0.57 <sup>u</sup>	11	-
	Ph	7.50	1.5 <sup>u</sup> (0.20 <sup>u</sup> )	1.07 (0.51)	3.35 (0.45)	-	1.21	-	17	17
	Ph	5.00	-	2.73 (0.55)	2.56 (0.51)	-	1.07	-	-	-